A NOVEL STEP-UP/STEP-DOWN FULL-BRIDGE DC-DC CONVERTER FOR DISTRIBUTED SOLAR POWER APPLICATIONS

by

Yu Cao

B.Sc., Hohai University, 2012

A THESIS SUBMITTED IN PARTIAL FULFILLMENT OF

THE REQUIREMENTS FOR THE DEGREE OF

MASTER OF APPLIED SCIENCE

in

THE COLLEGE OF GRADUATE STUDIES

(Electrical Engineering)

THE UNIVERSITY OF BRITISH COLUMBIA

(Okanagan)

September 2015

Abstract

Among the many renewable energy sources, solar power is becoming one of the quickest to be adopted due to continuous technological progress and reductions in cost. Today's typical photovoltaic system includes many photovoltaic modules that are connected together in series and parallel to form strings and sub-arrays. Various distributed photovoltaic architectures are introduced in this thesis and DC-DC converters with maximum power point tracking are also introduced.

Partial power processing is a technique to allow only a fraction of the power to be processed by the DC-DC converter, thereby reducing losses and improving efficiency. A new partial power isolated DC-DC converter is proposed in this thesis. The converter features maximum power point tracking and its controller selectively engages the buck portion or the boost portion or both in response to the maximum power point tracking input signal to achieve the desired output voltage and maximum power. With series connected DC-DC converters, each DC-DC converter carries an equal string current and adjusts its output voltage proportional to the available power of the connected photovoltaic module. The proposed topology allows each photovoltaic module to operate at its own maximum power point under varying or mismatched solar irradiance conditions, yet keep the total DC string voltage constant.

The proposed circuit is verified using PLECS simulation software. In comparison to the existing circuit with partial power processing method, the proposed circuit overcomes the disadvantage that the output voltage can only be greater than the input voltage. With the two

metal oxide semi-conductor field effect transistors added in series with the diodes in the secondary side of the transformer, the new circuit operates at a 100kHZ switching frequency and is able to perform both step up and step down modes with a properly designed control block. As a result, the circuit can convert a voltage from a PV panel that is higher or lower than the output to a regulated DC output voltage.

Table of Contents

List of Tables

List of Figures

List of Symbols

C_{in}	Primary dc link
D_1, D_2	Rectifier diodes
D_{S1} - D_{S4}	Antiparallel diode
i_c	Current across secondary dc link
i_{con}	Current goes into the converter
i_{in}	Input current
i_L	Current through output inductor
I_m	Rated current at maximum power point (MPP)
i_o	Output current
i_P	Transformer primary side current
I_{ph}	Light-generated current or photocurrent
I_{sc}	Cell's short circuit current
i_{s1}, i_{s2}	Transformer secondary side currents
I_o	Cells reverse saturation current at reference temperature and a solar radiation
k	Boltzmann's constant (1.38 x 10-23J/K)
L_o	Output filter inductor
n	Diode characteristic factor
q	Electron charge (1.6 x 10-19C)
R_{sh}	Shunt resistance
R_s	Series Resistance
S_1 - S_4	MOSEFTs
T	Cell's working temperature
T_{ref}	Cell's reference temperature
U_{oc}	Cell's open circuit voltage
V_{in}	Input voltage
V_N	Rectifier voltage
V_p	Transformer voltage on primary side
V_c	Voltage across the output capacitor
V_{s1}, V_{s2}	Transformer voltages on secondary side

V_o	Output voltage
V_m	Rated voltage at MPP

List of Abbreviations and SI Units

A	Amperes
AC	Alternating Current
C	Coulombs
CCM	Continues Conduction Mode
CMPPT	Central Maximum Power Point Tracking
DC	Direct Current
DCM	Discontinues Conduction Mode
F	Farads
FB	Full-bridge
H	Henries
Hz	Hertz
k	Kilo (10^3)
M	Mega (10^6)
m	Milli (10^{-3})
MPP	Maximum Power Point
MPPT	Maximum Power Point Tracking
MOSFET	Metal Oxide Silicon Field Effect Transistor
n	Nano (10^{-9})
PI	Proportion-integral
PLECS	Piece Wise Linear Electronic Circuit System
PV	Photovoltaic
PWM	Pulse Width Modulation
V	Volts
W	Watts
ZCS	Zero Current Switching
ZVS	Zero Voltage Switching
μ	Micro (10^{-6})

Acknowledgements

I would like to express my heartfelt gratitude towards all the faculty members, staff and my fellow students at UBC Okanagan Campus, who have constantly supported my ideas and work in the field of electrical engineering. And I owe special gratitude towards Dr. W. Eberle, my supervisor. I am reflecting, with enormous respect and admiration, on your immeasurable guidance, wisdom, inspiration and motivation that has influenced me so greatly. I thank you for your generosity with your time, your energy and your valuable supervision during my studies in the University of British Columbia (Okanagan).

I also want to thank Dr. M. Agamy, my co-professor, who supportively raised in-depth questions which enabled me to probe deeply into this field during my research project period. His clear thinking style, professional research capabilities, and integral industrial experiences will influence me continuously.

It is an honor for me to have Dr. Klukas and Dr. Wang as my internal advisory committee members. I am thankful for their encouraging words, thoughtful criticism, valuable time and attention.

I would like to offer my thanks to all the people who generously supported me and provided me constructive academic and industrial experience during my life in Kelowna, including Hansen Lu, Raed Mohsen Saasaa, Hamid Reza Hafezi Nasab, Mohammed Yafia, Changle Zhu, Tim Giesbrecht and Haibo Feng.

Finally, I would like to extend my sincerest appreciation to the School of Engineering for providing the support and material I needed for my research thesis.

Dedication

To my parents who have supported me throughout my years of education financially and spiritually. To my husband who have encouraged to study for the master degree.

Chapter 1: Introduction

1.1 Introduction of DC-DC Converter for Distributed Solar Power Application

Solar (Photovoltaic) power is a very effective, clean and renewable energy sources. A maximum power point tracking (MPPT) algorithm [1, 2] is usually required in PV systems due to the non-linear characteristics of the Photovoltaic (PV) panel. Distributed maximum power point tracking (DMPPT), which is based on the use of module dedicated DC-DC converters realizing MPPT for each module and central inverters, provide several benefits compared with standard central inverter MPPT systems, including higher energy yield, design flexibility, and improved monitoring and diagnostic capabilities [3, 4].

A grid-connected inverters' input voltage typically ranges from 180 to 500 V. Therefore, a number of PV modules are usually connected in series to supply the inverter with an input voltage within its operating range, and identical strings are then connected in parallel to achieve the desired output power. For these reasons, a system composed of parallel strings of a number of PV modules with its own distributed DC-DC converter connected in series will be considered in this thesis (Figure 1.1).

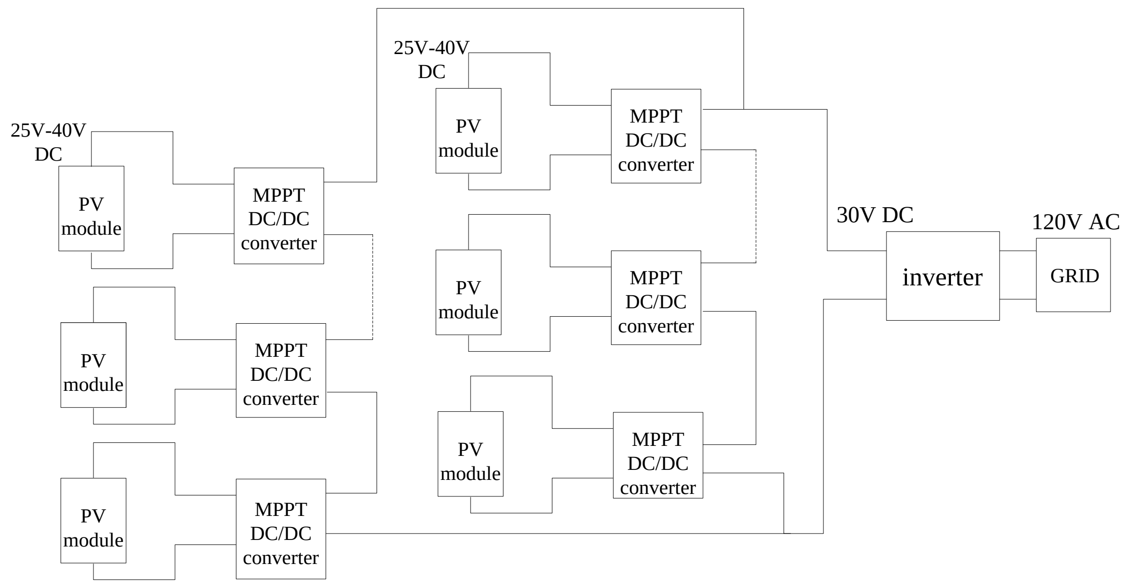

Figure 1.1 Grid connected PV system with distributed DC-DC converter with maximum power point tracking (MPPT)

In order to get the maximum utilization efficiency of a PV module, it is necessary to match the PV module to the load. This matching includes searching for an equilibrium operating point that coincides with the maximum power point (MPP) of the PV module. Therefore, a DC-DC converter, which acts as the matching load to the PV source, continuously tracks the maximum power point of solar module(s) connected to it and either increases (boost) or decreases (buck) the output voltage to match the optimum voltage requested by the central inverter [5]. These distributed DC-DC converters also work in conjunction with a central inverter, which is still required to convert DC power to AC grid power.

In recent years, DC-DC converters have become smaller in size, lighter in weight, and higher in efficiency, and are therefore more suitable for use in photovoltaic systems [6]. The design of DC-DC converters is one of the key factors that affects the system designs on large scale distributed solar power systems. The use of smaller power rating converters, compared to large centralized converters, will lead to a cost increase in per unit power and a decrease in conversion efficiency. Thus, in a PV plant, this issue has to be taken into account to ensure that the benefits of distributing DC-DC converters are not offset by the drop in conversion efficiency.

1.2 Research Motivation and Objectives

Two main obstacles for using solar energy are the high initial capital costs and the low conversion efficiency. Thus, a variety of research work intensely focused on how to reduce the cost and increase the conversion efficiency of the converter is ongoing. The partial power processing method is a very simple method that can improve the efficiency for DC-DC converters without added components and increasing the complexity of the circuit. Their ability to achieve very high efficiency (e.g. typically > 98%) is one of the reasons that this method is so widely used in PV power applications. Furthermore, the use of high-frequency DC-DC converters greatly reduces the size and control simplicity of the PV systems while still achieving high power density and a fast response rate [7].

One problem with using the partial power processing method in the series connected distributed PV panel system is that the DC-DC converters are all boost converters, thus less flexible in voltage ranges. When shade or mismatch occurs only on a few PV panels in the series connection, the buck mode DC-DC converter should be installed only on those PV panels experiencing shade [8]. However, the adoption of buck converters on all the PV modules of the string is impractical, because of the associated step-down voltage conversion ratio, which leads, of course, to a more or less consistent increase in the number of self-controlled PV modules for each string to obtain a string voltage compatible with the input voltage range of the inverter.

The objective of this thesis is to summarize and propose a high efficiency DC-DC converter to apply in distributed solar power systems. Thus, a partial power buck-boost DC-DC converter unit with MPPT optimization algorithm is first proposed. The revised full-bridge converter can perform both step-up and step-down modes according the operation state of the PV panel, which can be used to connect in series with each other to reach the desired dc-link input voltage to the inverter. Unlike the traditional boosting full-bridge partial power converter, the newly proposed converter is quite useful with an increased operating range and the ability to correct for a greater amount of system mismatch. Since the device includes two conversion stages rather than one, the increased flexibility may come at the cost of a slight efficiency reduction as well as possible size and cost increases relative to single-stage devices.

Chapter 2: Literature Review

2.1 Overview

This review chapter includes the basic information on PV-cell behavior, and the concepts of classical central and newly distributed architecture of solar power systems are introduced. An overview of various distributed architecture options and a comparison of their performance is presented. After that, the existing topologies that have been proposed to increase the efficiency of a DC-DC converter for PV application are presented, followed by a comparison of candidate DC-DC converter topologies to be used in distributed PV applications. The chapter concludes by establishing the technical knowledge for the work presented in the remainder of the thesis.

2.2 Solar Power Development and Generation Model Introduction

Currently, the energy crunch is becoming worse due to continuously decaying fossil fuels, such as oil, coal, and gas, and continuous growth in energy consumption [9], [10]. As a consequence, exploration and research for renewable power supplies is increasing around the world in order to avoid the situation of energy depletion.

The Solar Photovoltaic system with the following advantages [11, 12, 13, 14, 15, and 16] is attracting international attention and interest [17]:

1. It is a real, non-polluting (both air and noise), renewable green energy and is of great significance to the ecological environment and to the coordinated development of economic and social stability;

2. Due to the broad and flexible application venues, it is not restricted to geographical locations, and also it does not need a large number of electricity networks;

3. It can greatly improve the reliability of power quality;

4. Because it can be located closer to load centers, it can reduce power losses during transmission, and reduce construction and updates of transmission and distribution lines.

Solar power transfers the irradiation produced by the sun directly into electrical power via the PV effect [12], [13], shown in Figure 2.1. This simple principle involves sophisticated technology that is used to build efficient devices, namely solar cells, which are the key components of a PV system. Solar cells are made out of a semiconductor material where the following main phenomena occur when exposed to light: photon reflection, photon absorption, generation of free carrier charge in the semiconductor bulk, migration of the charge, and finally charge separation by means of an electric field [18], [19].

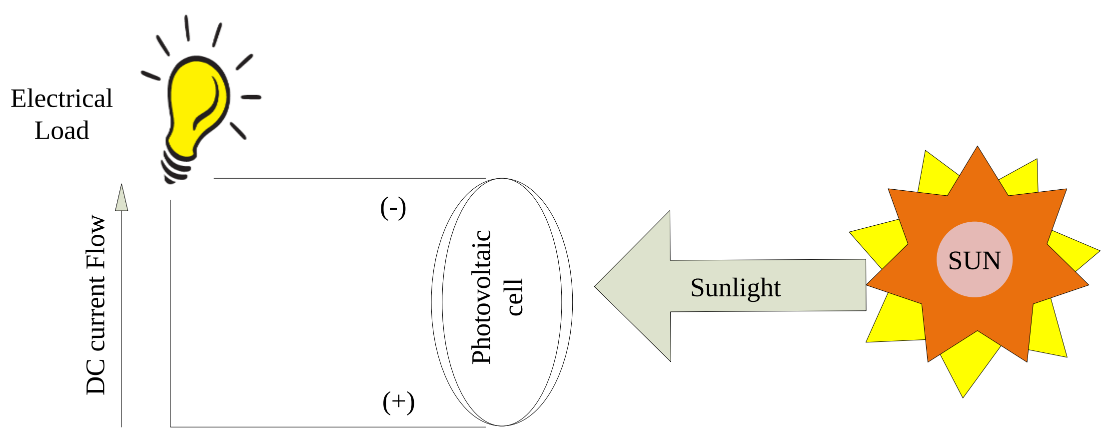

Figure 2.1 The basic principle of the photovoltaic system

The most frequently used equivalent circuit of a simplified PV model is a single diode model [20], shown in Figure 2.2. More complex models, such as the two diode model, also exist. However, the single diode model serves well in understanding the basic properties of a PV cell.

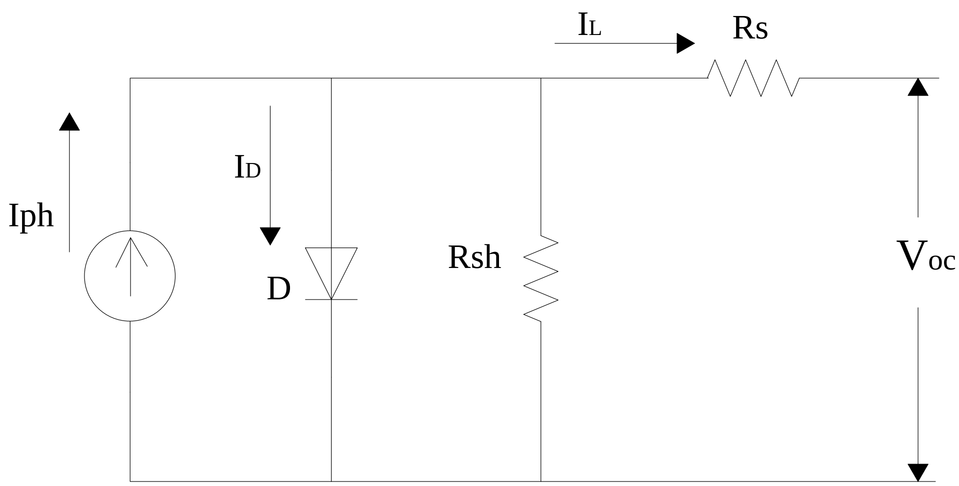

Figure 2.2 Equivalent circuit of a single photovoltaic cell

According to the physical structure and output characteristics of a solar cell, we have easy access to the mathematical model. The PV cell itself behaves as a highly nonlinear current source with limited output voltage. The current source generates the photocurrent I_{ph}, which is proportional to the solar irradiation, and this model shows good agreement with theoretical characteristics of PV modules [20].

In Figure 2.2, the equivalent circuit models the general form of the equation (2.1) that relates current in a photovoltaic cell [21]:

$$I_L = I_{ph} - I_d - I_{sh} \tag{2.1}$$

Currents through these components are generated by the voltage across them:

$$V = V_{oc} + I_L R_s \tag{2.2}$$

Based on the equation of a Schottky diode, the current through the diode can be written as [21]:

$$I_D = I_o[\exp\left(\frac{qV + I_L Rs}{nKT}\right) - 1] \tag{2.3}$$

According to Ohm's law, current through the shunt resistor is [4]:

$$I_{sh} = \frac{V}{R_{sh}} \tag{2.4}$$

Combining the equation (2.2), (2.3), (2.4) into equation (2.1), generates the IV characteristic equation of photovoltaic cell:

$$I = I_{ph} - I_o\left[\exp\left(\frac{qV - I_L R_s}{nkT}\right) - 1\right] - \frac{V + I_L R_s}{R_{sh}} \tag{2.5}$$

The output characteristics of photovoltaic cells are susceptible to external factors. In order to make the output power of photovoltaic cells maximum, a maximum power tracking device is needed [18]. The maximum power point of a photovoltaic array is a variation over time, so search algorithms are given according to the current-voltage (I-V) and power-voltage (P-V) characteristic of the solar cell. Currently, the proposed tracking methods at home and abroad are mainly the disturbance observer method, incremental conductance method, the adaptive algorithm based on disturbance observer improvement, fuzzy control techniques, the neural network control algorithm, and so on [19]. All of them have the function of maximum power point tracking and can improve the use of solar energy to improve system efficiency.

2.3 Classical Central Maximum Power Point Tracking Architecture

When a single DC-AC inverter is directly connected to strings of parallel-linked PV modules, and tracks the MPP for the whole PV field, this system is often referred to as Central Maximum Power Point Tracking (CMPPT) [22]. In another kind of architecture that also performs CMPPT, all PV modules first connect to a high power central DC-DC converter with MPPT operation and then to a DC-AC inverter to feed into the utility [23]. In this two-stage central inverter architecture, 98% or even higher efficiencies for DC-DC converters should be guaranteed to match the conversion efficiency.

The system, shown in Figure 2.3, is simple and low-cost, but the main drawback is the fact that the complete array is operated at one overall MPP. Thus, neither of these CMPPT architectures can extract the maximum power produced by the solar array because one global MPP is usually not the maximum power point for each individual module [24]. In case of mismatch (due to clouds, shadows, dirt, manufacturing tolerances, aging, different orientation of parts of the PV field, etc.), the P–V characteristic of the PV field may exhibit more than one peak, because of the adoption of bypass diodes, and MPPT algorithms can fail. Even when CMPPT can perform the tracking of the maximum power from the mismatched PV modules (due to shadows, clouds, manufacturing tolerances, dirtiness, aging, different orientation of parts of the PV array, etc.), this power is still less than the total power of the mismatched PV fields with available maximum powers [23].

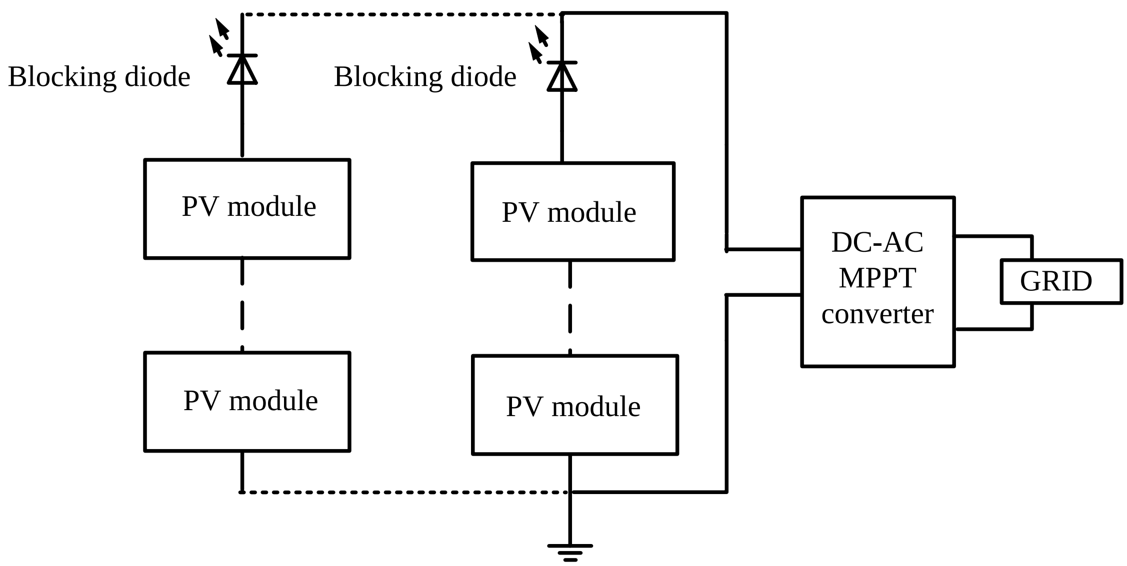

Figure 2.3 PV systems with central maximum power point tracking (CMPPT)

2.4 Distributed Converter Architecture for Solar Power Application

To deal with the failure of tracking MPP for each PV module, two-stage distributed maximum power point tracking systems have been investigated to secure individual and more accurate panel maximum power point tracking [25]–[27].

2.4.1 Advantages and Problems of Distributed Maximum Power Point Tracking

DMPPT, also referred to as self-controlled PV modules (SCPVM), is based on the use of a module dedicated DC-DC converters, each with its own MPPT, ensuring that each PV array operates at its MPP [28-36]. Thus, this kind of architecture can greatly alleviate the drawbacks associated with mismatching power losses and the failure to track MPP for each module [4, 26, 37, 38].

In [25, 26, 27], although the acronym of DMPPT is not mentioned, these papers all address the problem of DMPPT for PV systems. For example, in [25], a DC-DC module integrated converters (MIC) topology is proposed for application in PV systems, and a comparison of four basic, non-isolated DC-DC converters in terms of efficiency is presented. However, an AC or DC analysis for a string of SCPVMs or a single SCPVM is not presented in these papers.

In this DMPPT architecture, PV panels can be installed in different orientations, as solar panels do not have to be matched and partial shading degrades the performance only on the shaded panel. In [39], a soft switching resonant buck converter with highly efficient MPPT topology of low-power, low-cost was investigated to be connected with each PV panel, and an efficiency higher than 98% was achieved for almost its entire operating time. In an otherwise ideal installation for small solar power applications, if each converter performs an independent MPPT for its PV panel, this will compensate for almost 2.5% of mismatches [40].

The inverter, which is connected to the grid and takes care of the grid current control, ensures the string at a certain DC voltage and as MPPT is applied per module in DMPPT architecture, this DC voltage can be kept fixed. This optimizes the efficiency of DC-AC inversion regardless of the string length or the environmental conditions, since an input boost stage is no longer needed. Hence, high conversion efficiency of PV arrays and increased energy yield can be ensured [22, 40–43].

Furthermore, the distributed architecture of PV plants offers some other advantages over the centralized photovoltaic plants. This architecture makes the installation of distributed supplied PV systems easy since the only task for each DC-DC converter is MPPT (and perhaps voltage amplification). Better control and protection of each PV string/module is achieved, while redundancy when the source or converter fails and insensitivity to shading can also be guaranteed [44]. Great flexibility and modularity in the panel design and layout, the ability to have a controlled high dc voltage with lower cable losses, higher energy yield, better data gathering, improved diagnostics, and monitoring capabilities can all be ensured by this DMPPT architecture [23, 24].

However, compared to large centralized converters, using distributed converters with smaller power per converter will lead to an increase of cost per unit power and a decrease in conversion efficiency. This problem has to be taken into consideration to ensure that the advantages of distributed solar architectures will not be canceled out by the decrease in power conversion efficiency [44]. Therefore, for large scale systems, module level distributed systems are not suitable because the gains in energy are always offset by a significant increase in system cost [45]. In the case of large scale utilities, Petrone [46] introduced string level or multi-string level distribution of DC-DC converters with a small number of panels connected in series to each DC-DC converter, instead of having a separate MPPT circuit in each converter for each solar panel. This multi-string distribution, which has a different number of strings or modules per DC-DC converter, increases energy yield significantly for large power rating plants or utility scale plants (MW range and up).

2.4.2 Series Configuration to Implement Distributed Architecture

According to the connection of output terminals of converters, the following concepts are used to install DMMPT systems: series configurations and parallel configurations [47]. In the series configuration (see Figure 2.4), the output of each converter is connected in series with the next to connect to a common inverter, and each solar panel is connected to its own DC-DC converter. Therefore, the current carried by each PV module is equal and it has been frequently shown that the operating points of several modules may be forced away from the MPP [48], [49], [50].

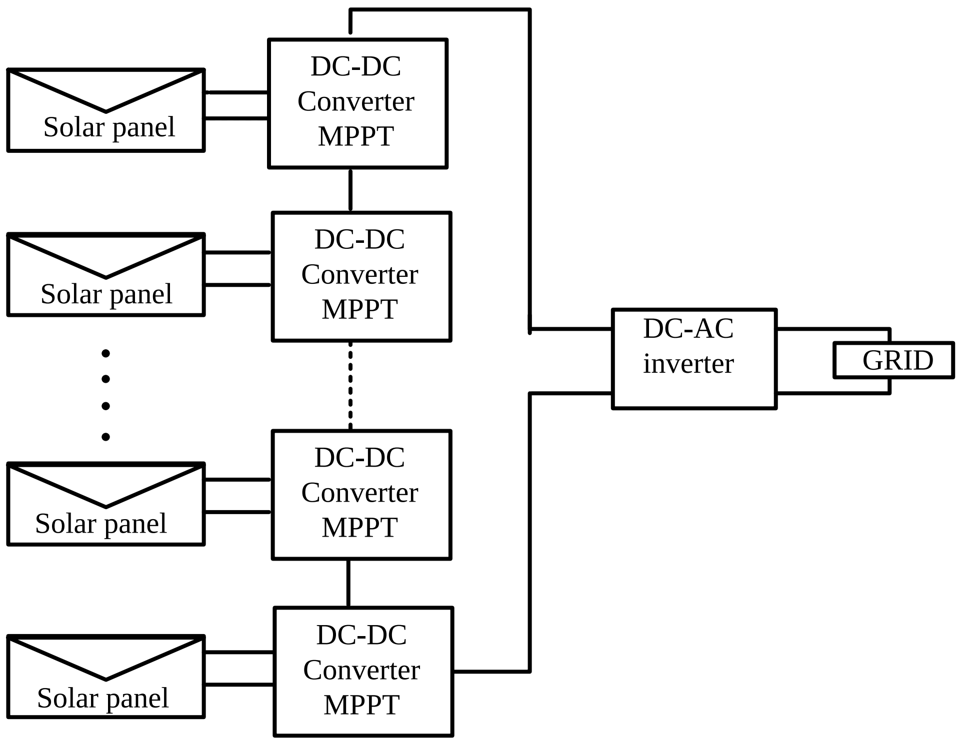

Figure 2.4 Grid-connected DMPPT PV systems with the output ports of MPPT DC-DC converters connected in series

Due to the relatively low output voltage of PV arrays, the PV series-connected configuration is proven to be a good solution to satisfy the requirements of high voltage transfer ratios for half-bridge, full-bridge, or multilevel grid inverters [49]. Usually, in order to achieve the desired constant string DC input voltage to the inverter, 10–20 PV modules are connected in series with each, equipped with their own boost converters [32]. In this way, a much lower voltage conversion ratio can be achieved and the increase of voltage for each converter is greatly reduced [25]. Converter components will operate under much less stress, possibly resulting in improved efficiency and durability [32]. Also, the distribution of the total dc-link voltage needed to generate the grid AC voltage between the converter output terminals is based on the power levels [51]. As a result, the voltage command for each module only depends on generated power within the circuit as opposed to being performed on a centralized collection of the power from the entire circuit.

2.4.3 Parallel Configuration to Implement Distributed Architecture

Operating converters in parallel is another option for PV power conditioning systems. In the parallel configuration (see Figure 2.5), the converter output terminals are connected to the dc-link - the input of an inverter. In this configuration, each converter has to withstand the entire dc-link voltage at the output terminal. Thus, the need for high conversion ratio has to be satisfied by specific solutions.

The advantages of converter paralleling are as follows [52, 53]:

1. It is reliable, due to the independence between the DC-DC converter modules and DC-AC inverter modules. They are connected independently of one another without communication;

2. Flexible design (for example: Plug-in and hot swap) and further extension can be achieved, since it is easy to plug a new PV panel with its own DC-DC converter into the existing system.

However, there exist many drawbacks for this parallel configuration. The first is that the system itself and the control system are both very complex [54]. The second one is a performance versus cost disadvantage because converters connected in parallel require fast recovery diodes and MOSFETs to withstand high voltage stress. Another obvious drawback is that parallel-connected DC-DC converters in this kind of distributed architecture are required to characterize two contrasting requirements: a high voltage transfer ratio [from 40 to 300V, a great difference between the input (low) and output (high) voltage of a converter], and a high conversion efficiency. This required high voltage conversion ratio will greatly decrease the efficiency of the whole PV system.

Another disadvantage of this configuration, shown in Figure 2.5, is the differences among the parallel modules resulting from finite tolerances in control parameters and the power stage. Therefore, special previsions should be taken to distribute the load current equally and stably to avoid an excessive load current. Excessive load current decreases the system reliability and increases thermal stress on power electronic devices [53]. In order to deal with this problem, some load-sharing topologies have already been proposed [55]–[58]. In PV systems, the control problem of load-sharing is included within the problem of MPPT for the solar array. In the literature [59]–[61], several solutions can be found.

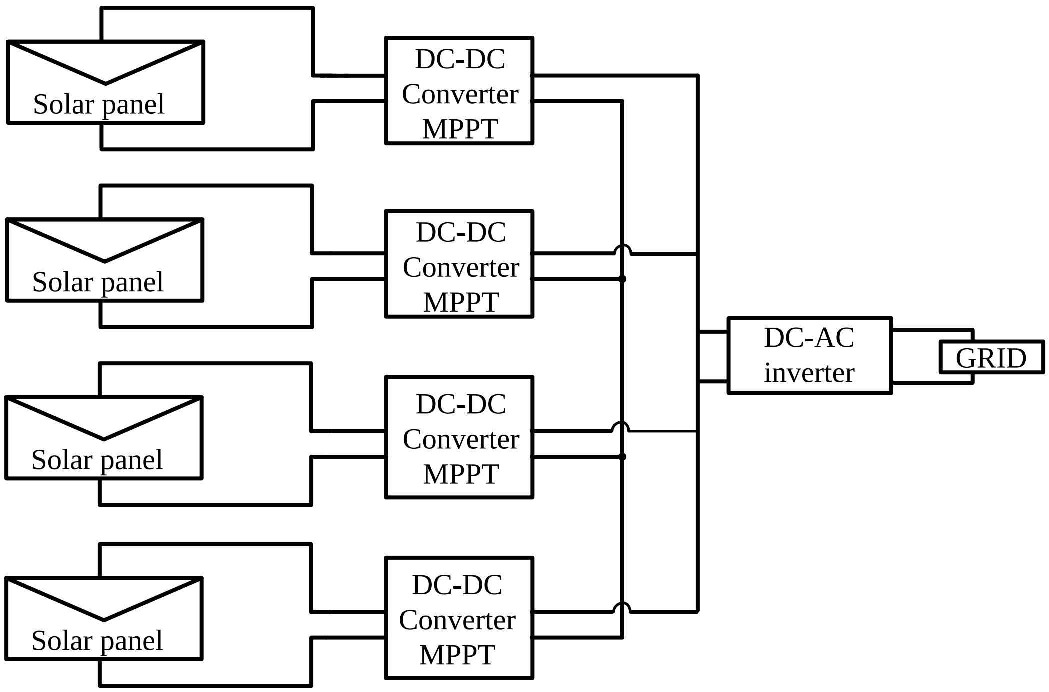

Figure 2.5 Grid-connected DMPPT PV systems with the output ports of MPPT DC-DC converters connected in parallel

2.4.4 Comparison between Series and Parallel Configurations to Implement DMPPT Solar System

It is now evident that series-connected converters have multiple advantages over parallel-connected ones [51]:

1) Flexible design — A number of modules are series connected to achieve the required voltage level. The output voltage of one PV module is independent of the others in the series connection, therefore ensuring a wide, flexible range of voltage. And it is more suitable for use in mismatch conditions.

2) High reliability and efficiency — Serial topology leads to efficiency improvement in the power electronics stage. A series-connected converter allows the

conversion ratio of input-output voltage to be close to unity, and therefore, higher switch utilization can be achieved. It also allows each converter to use a comparatively small step-up ratio (usually 3 to 4), which increases efficiency and allows converters to be light, small, and low cost. Near 100% efficiencies are possible with this serial connection.

3) Reduced installation cost — A decreased size of PV-system elements due to energy savings can result in a cost reduction. With strings being longer for the serial configuration, the cost of Balance of System (BOS) element count, installation, and labor will be much lower. In addition, the series configuration costs less than the parallel one by using fewer power electronics devices and a cheaper digital structure to support the supervisor implementation.

On the basis of the aforementioned considerations, in the following thesis, PV systems adopting the distributed architecture with the output ports of DC-DC converters connected in series, as shown in Figure 2.4, will be discussed and analyzed in detail.

2.5 Partial Power Processing Circuit

In the previous subsection, it was noted that the distributed solar panel architecture with the output DC-DC converters connected in series provides better maximum power point tracking and more control flexibility. However, it can be quite challenging to maintain very high efficiency for such small distributed power converters. Generally, converter losses can be broken down into load dependent losses and constant losses [62]. A drop in the system efficiency and a decrease in energy yield are expected when using low power converters. In order to increase the PV energy yield by distributing the DC-DC converters with individual

MPPT controllers, the DC-DC converter composite efficiency has to be very high (> 98%) to avoid a tremendous negative impact on the annual energy yield.

Therefore, in such distributed PV application, the DC-DC converter topology should have design simplicity, high efficiency, and high reliability. The partial power processing method is one of the simplest methods to improve the efficiency of the converter.

The introduced concept of partial power processing converter is shown in Figure 2.6. These converters process only a part of the input PV power to generate the voltage differential between the PV string and the output dc-link, while the rest of the power is directly fed forward to the output at almost 100% efficiency. Usually, only 20% or less power of the total PV system power is processed by DC-DC converters in this method. The percentage of power processed by the converter depends on the voltage difference between the PV side and the dc-link voltage; Figure 2.7 shows what percentage of power is being processed by the DC-DC converter for a given input/output voltage gain.

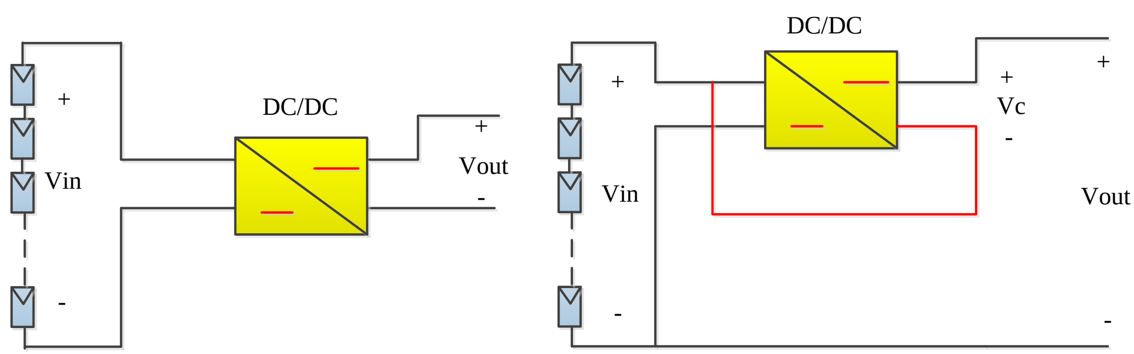

Figure 2.6 Full power structure VS partial power processing structure

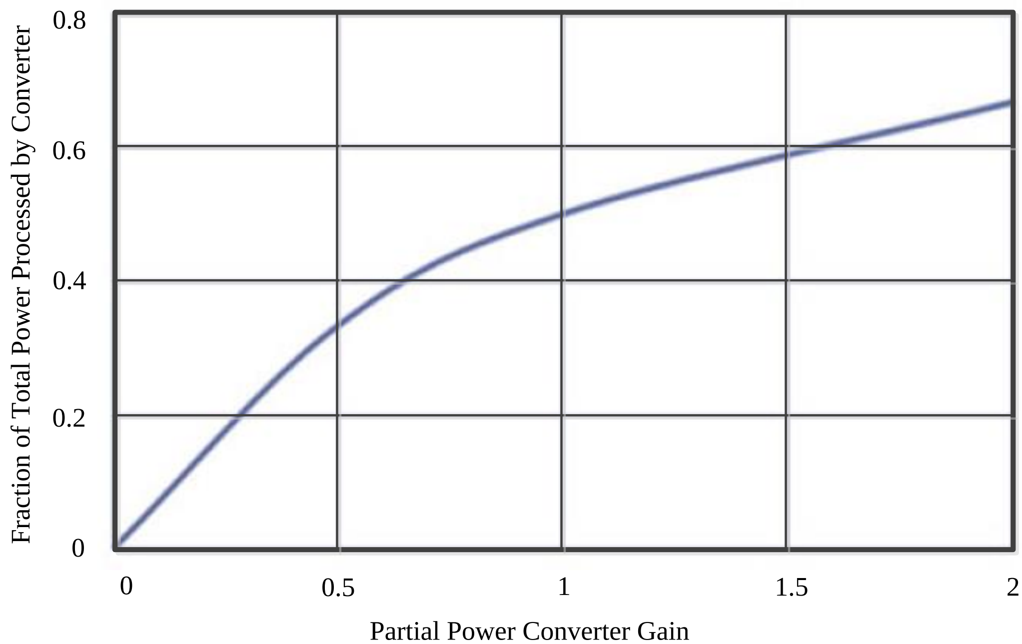

Figure 2.7 Fraction of total power processed versus voltage gain (Vs / Vin) for a partial power converter (cited from [68])

Therefore, with a proper design, the pressure on the converter block can be greatly reduced without compromising the overall conversion efficiency, which helps to reduce the system cost [63-66]. Figure 2.8 shows an example of this application. One DC-DC converter with an assumed efficiency of 95% is used in a partial power conversion connection; the overall efficiency is expected to be above 98% when the input voltages are equal to 60% or even higher of the output dc-link voltage. And when the ratio is 1, it means that zero partial power is processed, thus zero converter losses.

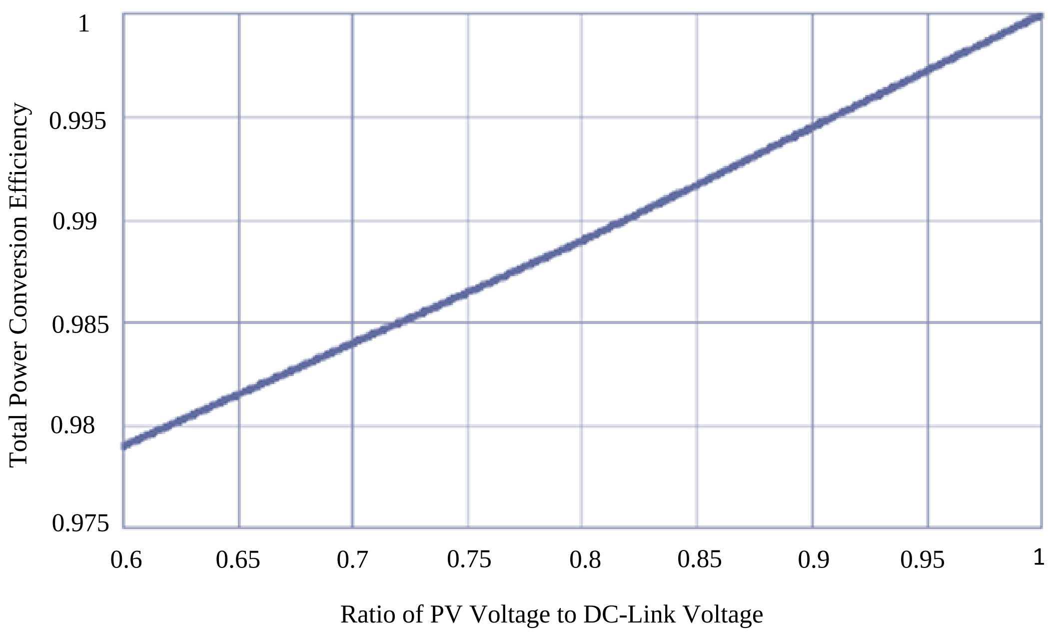

Figure 2.8 An example of overall efficiency increased by partial power conversion topology assuming an original DC-DC converter efficiency of 95% (cited from [68])

The DC-DC converter usually acts as an interface between the load and the PV module. The suitability of different basic converter topologies for application in distributed solar panel architecture is assessed in the following sub-sections.

2.5.1 Transformer-less Design Topologies

For this kind of application, the boost converter with a low device number and a simple design is the simplest solution. However, the boost converter in this operational range has the following disadvantages: a switching voltage in the (800V-1200V) range is required, which leads to using a relatively low switching frequency and consequently a large input inductor. On the other hand, the efficiency requirement for the boost converter cannot be met without adding auxiliary circuits for soft switching.

A buck-boost converter with partial power processing is one solution proposed in paper [66], as shown in Figure 2.9 (a). Since a large portion of the input voltage is directly feeding forward, the converter just needs to process a very small part of the input power, and the overall conversion efficiency of the system is quite high, as shown in Figure 2.9 (b). The topology is very simple; however, the use of high voltage rating devices still cannot be avoided. And the output voltage is always the input PV string voltage plus the voltage across the output capacitor in this topology.

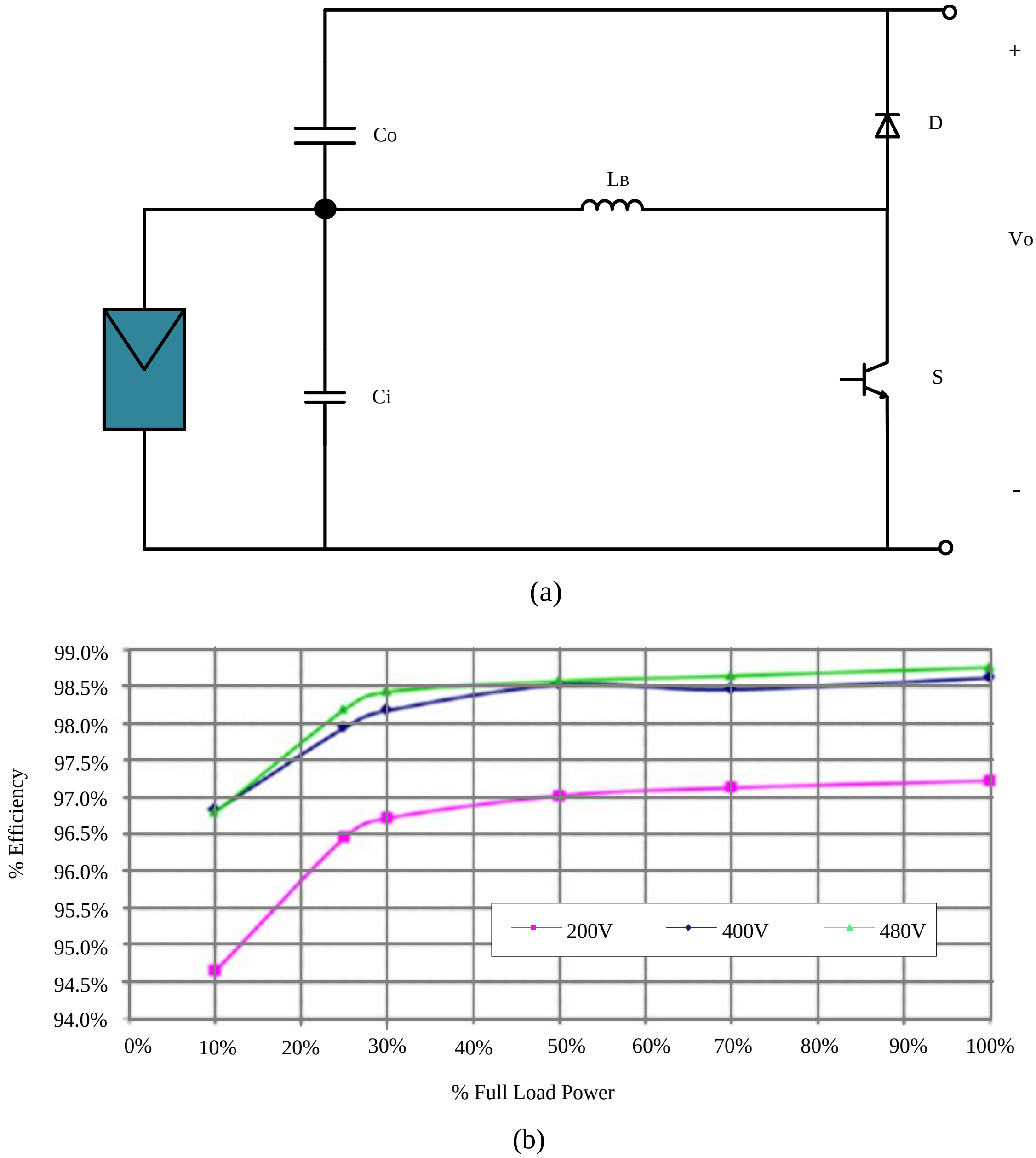

Figure 2.9 Buck-boost topology with partial power processing: (a) Circuit topology, (b) Efficiency for different input power and input voltages (cited from [68])

2.5.2 High Frequency Transformer Design Topologies

One of the most frequently used isolated converter topologies in this operational power range is the full-bridge (FB) converter, whether it is a voltage-fed converter or a current–fed converter, as shown in Figure 2.10 (a) and (b). The isolation of the input and output side is not necessary; however, it will be easy to parallel multiple DC-AC inverter stages to the same transformer, since for non-isolated topology designs, the inverters are required to be isolated in order for them to operate in parallel, resulting in use of large power line, medium voltage transformers. DC-DC converter topologies with an isolation feature, on the other hand, provide the advantage of size reduction and cost savings by allowing the inverters to be tied to a multi-winding power transformer. However, this type of converter has more components than an isolation transformer, four switches, and an output rectifier, which lead to lower power density, reduced reliability, and higher cost. Furthermore, it may be much more challenging for full-bridge converters to achieve efficiencies higher than 98% at low cost.

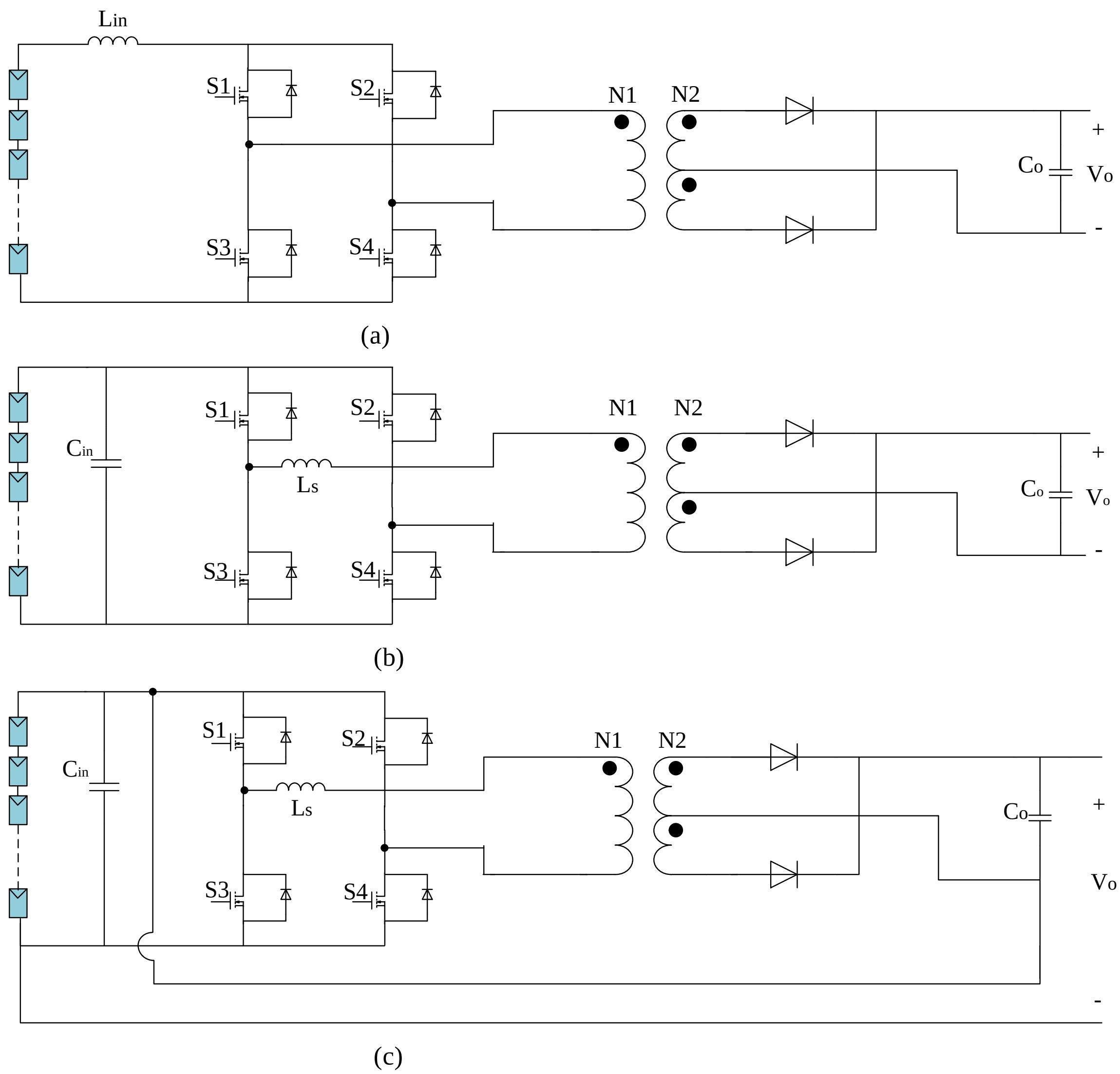

Figure 2.10 Topologies based on full bridge converter (a) current-fed, (b) voltage-fed, (c) combine with partial power processing

To solve the problem of low efficiency, a full-bridge converter combined with the partial power processing method can be used [67], as shown in Figure 2.10 (c). Lee et al. [68] introduced a full bridge photovoltaic DC-DC converter with partial power processing. Dramatically improved and flat energy efficiency was achieved by reducing the generated power flowing through the converter at all load ranges [68]. Subsequently, Agamy [69] achieved a higher composite weighted efficiency of 98.22% by directly feeding forward a fraction of the generated PV power to the output DC bus. However, this mode of operation results in losing the benefit of the converter being an isolated topology.

Resonant converters can also be one way to improve the efficiency for high power density converters [70], similar to the full-bridge with input feed forward as shown in Figure 2.11. These types of converters, utilizing a resonant L-C circuit to achieve zero voltage switching (ZVS) and/or zero current switching (ZCS), are defined as the combination of converter topologies and switching strategies [71]. They can be operated at very high switching frequencies with nearly zero switching losses; however the resulting converter becomes very complex in control implementation and topology design, and also very expensive.

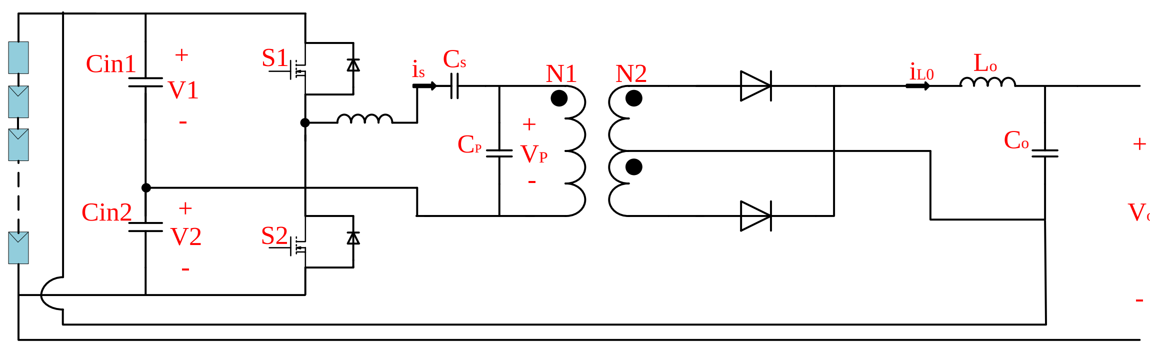

Figure 2.11 Half-bridge resonant converters with partial power processing

The key factors influencing DC-DC converter selection when designing a solar power converter are efficiency, design complexity, reliability, power density, and cost. Based on the two basic topologies mentioned above, it follows that half-bridge topologies with partial power processing are the strongest candidates for this type of application. This transformer topology has the characteristic of easy step-up and step-down, which is needed to regulate the output voltage. Moreover, storing the input solar energy temporarily in the transformer inductance and then releasing that energy to the output side at a different voltage can greatly help to regulate the output voltage from the PV panel. Furthermore, the transformer can improve overall safety of the system when the converter's output is cascade connected to a grid-tie inverter [72, 73]. Thanks to this topology, the size of the transformer can be reduced because it concerns with high switching frequency.

2.6 Summary

The architecture of PV systems and the partial power processing method used to improve the efficiency have been reviewed in this chapter. The work is summarized as follows: Solar power has become a promising renewable energy source for various reasons, such as its zero pollution in both noise and air, easy maintenance, and the flexibility to operate with much less restriction on location [16]. Photovoltaic power plants with distributed power electronic converters provide several advantages over the standard central inverter systems, including higher energy yield, more flexibility in plant design, and improved monitoring and diagnostics capabilities [3, 4]. Then, a comparison study was done on different distributed architectures of the PV system. The grid-connected distributed PV systems with the output ports of DC-DC converters connected in series is better suited than the parallel one due to the reduced installation cost, high reliability and efficiency, and flexible design. Efficiency over a wide input power and input voltage range is a key factor in DC-DC converter topology selection and thus circuits operating with partial power processing provide a very good solution for this distributed application.

The concept of partial power processing was introduced to increase the efficiency by directly feeding forward a fraction of the generated power, thus achieving close to 100% efficiency. A comparative evaluation of some basic DC-DC converter topologies to be applied in distributed PV plant architectures was performed. The high frequency transformer topology was investigated in detail and chosen for the distributed PV system application. Resonant converters can also increase the efficiency by reducing the switching losses in the conversion process. However, this method results in cost increase and more design complexity for the whole circuit.

The remaining of the thesis is organized as follows: The design and theoretical operation of the proposed step-up/step-down full-bridge partial power converter are given in Chapter 3. Further, the closed loop control circuit is also presented to regulate the output DC voltage. In Chapter 4, the PLECS simulation results of the proposed circuit are presented to verify the theoretical analysis and to benchmark the contributions. Finally Chapter 5 contains concluding remarks.

Chapter 3: Proposed FB Partial Power Step-up / Step-down DC-DC Converter

3.1 Overview

In a distributed solar power system, DC-DC converters function as downstream load connections and energy storage. Individual controllers are implemented to control the DC-DC converters in the most optimum way. As such, the total PV system becomes interconnected and a wide variety of dynamic interactions are possible.

The voltage and current output of a PV module is affected by various factors, such as dissimilarities of panel production, different temperatures and irradiations due to the orientation of the panels, and different aging and shading of each panel. In Chapter 2, the distributed solar panel architecture with the output ports of DC-DC converters connected in series with each other was chosen. Because of the series connection, the output voltage of a given PV module is related to the ratio between its output power and the total output power:

$$V_{outk} = \frac{P_{pank}}{I_{outl}} = \frac{V_b}{\sum_{k=1}^{N} P_{pank}} P_{pank} \tag{3.1}$$

where P_{pank} is the power extracted from the k^{th} PV module, V_{outk} and I_{outk}, respectively, are the output voltage and current of the k^{th} module, and V_b is the inverter DC input voltage. According to (3-1), the output voltage of a PV module can vary widely because of possible imbalances among powers delivered by modules. When shade or limited mismatches occur on only a few PV modules, the DC-DC converter connected to such modules should be able to operate in buck mode to reduce the current mismatch between shaded and unshaded modules. Also, if the PV system includes modules of different size, power rating, or orientation, a buck-boost DC-DC converter can be placed on every module in the series string, allowing for differences in the various module power outputs. In this case, the DC-DC converter should be able to convert voltage from PV cells to a regulated DC output voltage that is not only higher but also lower than the input PV voltage. Therefore, a DC-DC converter with both step-up/step-down function is preferred in the series connected distributed PV application [74].

The output voltage of the standard boosting partial-power, full-bridge circuit is always equal to the input voltage plus the voltage across the capacitor, which is always higher than the input PV voltage. However, in practical conditions, the buck mode operation is needed for some panels experiencing shade in the series connection. Thus, this existing converter design is not suitable anymore. In this chapter, a novel buck-boost full-bridge DC-DC converter circuit with partial power processing is proposed, which has both step-up and step-down characteristics.

This chapter is organized in the following manner: The model of a PV panel with MPPT control for system use in the thesis is simulated in PLECS in Section 3.2. The design of the novel full-bridge step-up/step-down DC-DC converter with partial power processing circuit and its two operation mode is first presented in Section 3.3, followed by the designed control circuit for the proposed topology presented in Section 3.4. A design procedure with circuit parameters used and a design example is then presented in Section 3.5. Conclusions are presented in Section 3.6.

3.2 Solar Panel Modeling with Maximum Power Point Tracking

It is known on the basis of the PV-cell voltage-current characteristics that the generated power reaches its maximum only under specific loading. This maximum power point separates the constant current region (CC), where the PV-cell current stays relatively constant, from the constant voltage region (CV), where the PV-cell voltage remains relatively constant. Because the PV-cell terminal voltage and current are both proportional to ambient operating conditions, the loading must be adjusted to provide maximum power under all operating conditions [75]. This is known as MPP tracking. The DC-DC MPPT modules track the MPPs of photovoltaic modules and deliver power to the DC bus [76]. The control variable that represents the MPP can be either the photovoltaic voltage or the photovoltaic current [76]. An analysis shows that regulating the photovoltaic voltage has advantages to improve the performance of MPPT [27, 39, and 77].

Due to the nonlinearity of the solar cells with temperature and radiation, MPPT [27], [78]-[80] in the design of the PV system aims to maximize the extracted energy irrespective of the irradiance conditions. The MPPT of an SCPVM can be achieved by means of several standard MPPT techniques. An important research effort has been devoted to finding simple, efficient, and minimal-knowledge-demanding methods of MPPT and a wide variety of them have been proposed in the literature, some of the most recent being described in [40, 81-86].

Generally, MPPT algorithms can be classified into two categories: Perturb and Observe (PO), which are based on injecting high frequency, small-amplitude (usually harmonic) perturbations in the system in order to detect the sign of the power gradient [87], [88]; and Incremental Conductance (IncCond), which perturbs the voltage in one direction and evaluates the sign of the derivative of the power dP/dV [89]. By comparison of the two algorithms, for digital implementation, the PO algorithm is less complicated and more feasible than IncCond. But the dynamic and tracking characteristics of IncCond are better than PO during rapid changes of solar radiation, and it is also simple and can be implemented using lower cost microcontrollers [90, 91]. In this thesis, the Incremental Conductance technique is adopted due to its good performance under quick changing circumstances [92].

3.2.1 The Topology of Incremental Conductance

IncCond [93], [94], [95] is one of the commonly used methods to achieve MPPT for solar panels. It is based on the following criterion: the slope of the PV array power curve is zero at the MPP, positive to the left of the MPP, and negative to the right (see in Figure 3.1), as given by:

$$\begin{cases} \mathrm{dP/dV} = 0 & \text{at MPP} \\ \mathrm{dP/dV} > 0 & \text{left of MPP} \\ \mathrm{dP/dV} < 0 & \text{right of MPP} \end{cases} \tag{3.2}$$

If the sign is negative, the algorithm will decrease the voltage, otherwise it will increase the voltage. Since the algorithm attempts to maximize the power by driving the derivative to zero, $\frac{dP}{dV} = \frac{d(IV)}{dV} = I + V\frac{dI}{dV} \approx I + V\frac{\Delta I}{\Delta V}$, (3.2) can be simplified and rewritten as:

$$\begin{cases} \Delta\mathrm{I}/\Delta\mathrm{V} = -\,\mathrm{I/V} & \text{at MPP} \\ \Delta\mathrm{I}/\Delta\mathrm{V} > -\,\mathrm{I/V} & \text{at left of MPP} \\ \Delta\mathrm{I}\,/\Delta\mathrm{V} < -\,\mathrm{I/V} & \text{at right of MPP} \end{cases} \tag{3.3}$$

Therefore, the MPP can be tracked by comparing the incremental conductance ($\Delta I/\Delta V$) to the instantaneous conductance (I/V), shown in the flowchart in Figure 3.2. The

PV array is forced to operate at a reference voltage, identified in the figure as V_{ref}. At MPP, V_{ref} is equal to VMPP. Once the MPP is reached, the operation of the PV array will be maintained at this point unless a change occurs in ΔI, which indicates changes in MPP and the atmospheric conditions. This algorithm works by decrementing or incrementing the value of V_{ref} to track the new MPP. The increment step size determines steady tracking accuracy and dynamic response. Fast tracking can be achieved with bigger incremental step size but the system might not operate exactly at the MPP and oscillate about it instead, so this is a trade-off.

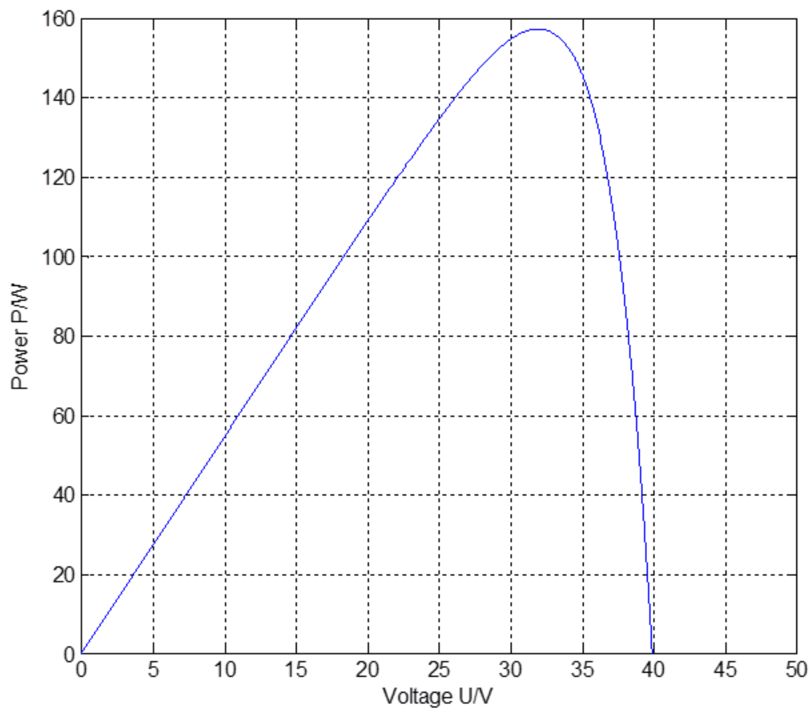

Figure 3.1 Characteristic PV array power curve

Measurements of the instantaneous PV array voltage and current require two sensors. The IncCond method lends itself well to DSP and microcontroller control, which can easily keep track of previous values of voltage and current and make all the decisions as per Figure 3.2.

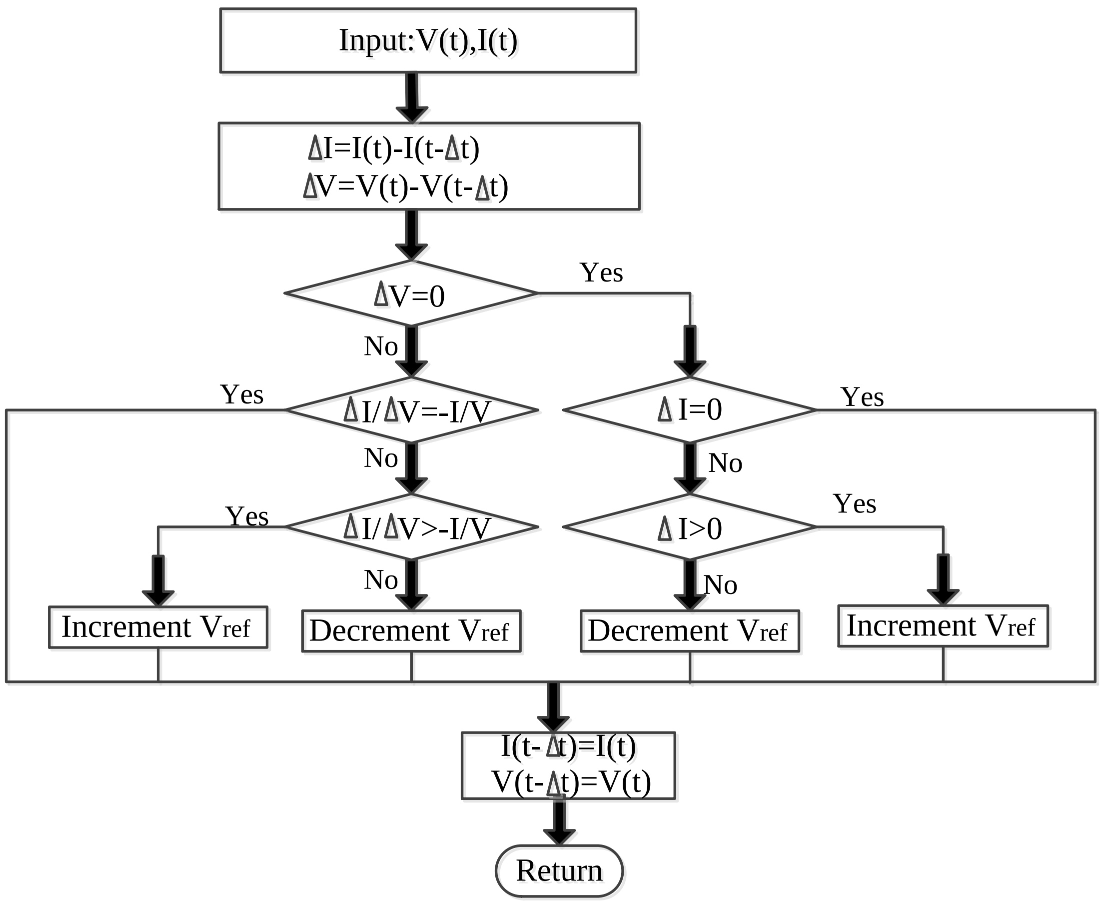

Figure 3.2 IncCond algorithms as shown in [89], [93], [94], and [95]

3.2.2 The Simulation Results of IncCond Method

The diagram of the PV system and the code-based MPPT designed in PLECS is presented in Figure 3.3. The PV module is modeled using electrical characteristics to provide output current and voltage of the PV module. The provided current and voltage are fed to the converter and the controller simultaneously. The PI control loop is eliminated.

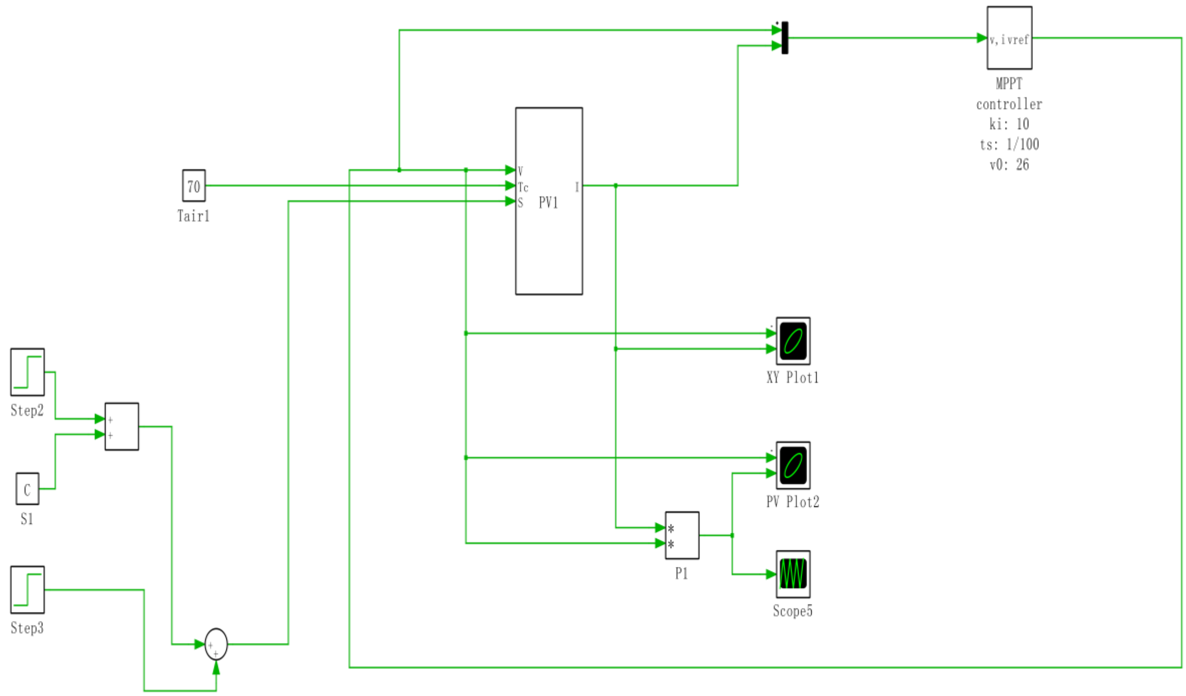

Figure 3.3 Simulation model of incremental conductance MPPT

The proposed work is validated with the help of Table.3.1, where system responses for different solar insolation levels are given. The simulation is run for 0.8 sec and insolation is varied at each 0.2 sec between four levels, such that insolation is set at 600w/m^2 initially from 0-0.2s and after that insolation is set at 800w/m^2 from 0.2-0.4s, and then insolation remains at 1000w/m^2 for the remaining interval.

Table3.1 Maximum power points at various irradiation levels

Simulation Time(sec)	MPP's according to Irradiation levels		
	Irradiation level(W/m^2)	PV Current at max. power(Imp)	PV Voltage at max. power(Vmp)
0.0-0.2	600	3.21	26.42
0.2-0.4	800	4.28	27.02
0.4-0.8	1000	5.46	27.48

The original voltage (V_o) is chosen to be 26V so that the controller can quickly track the MPP. Figure 3.4 shows the change in PV output voltage adjusted by MPPT control in order to extract maximum power from the module. The variation of irradiation or insolation level with simulation time is also shown in Figure 3.4. The change in PV output power and current by variation in irradiation are shown in Figures 3.5, and 3.6.

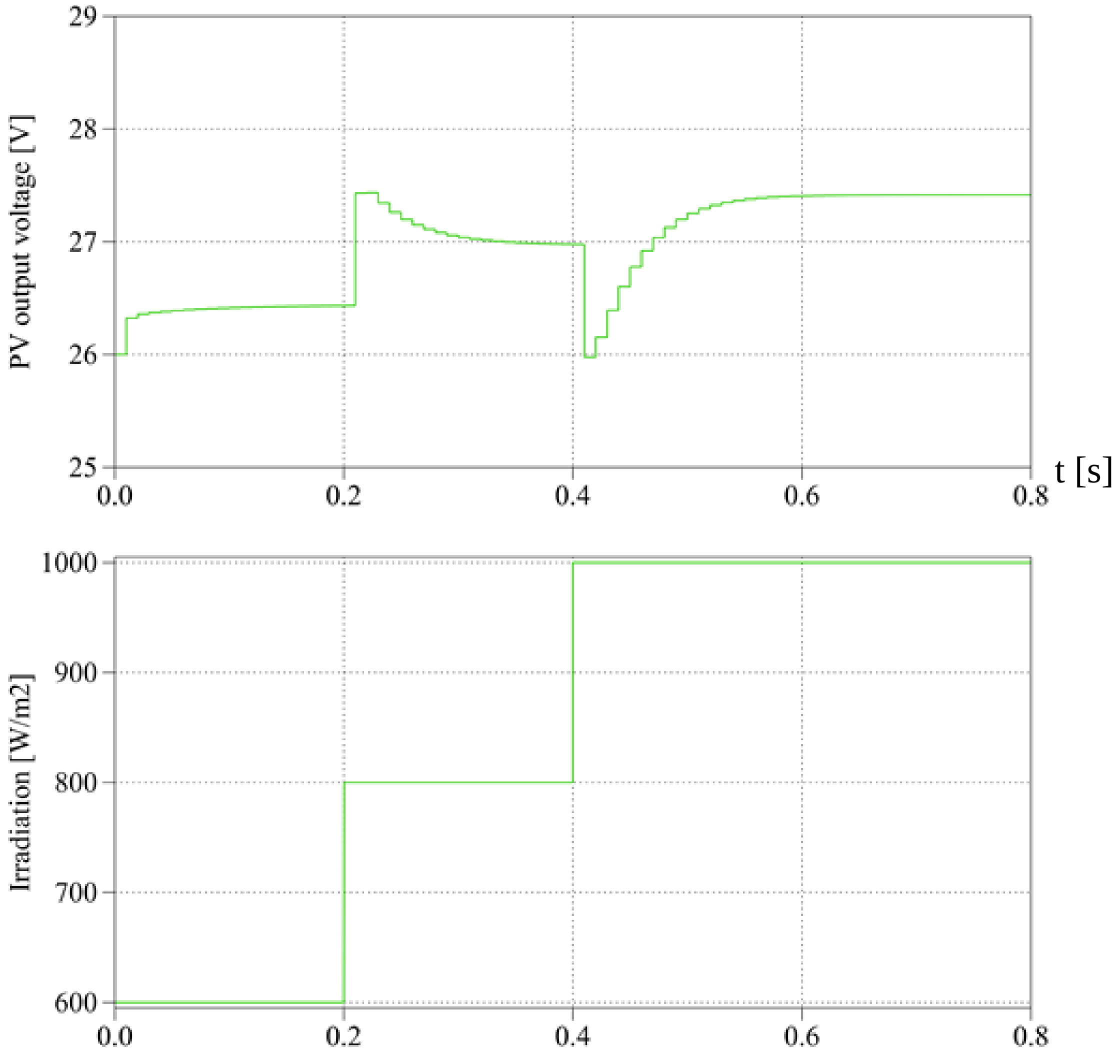

Figure 3.4 PV module output voltages and irradiation level changing with time (sec)

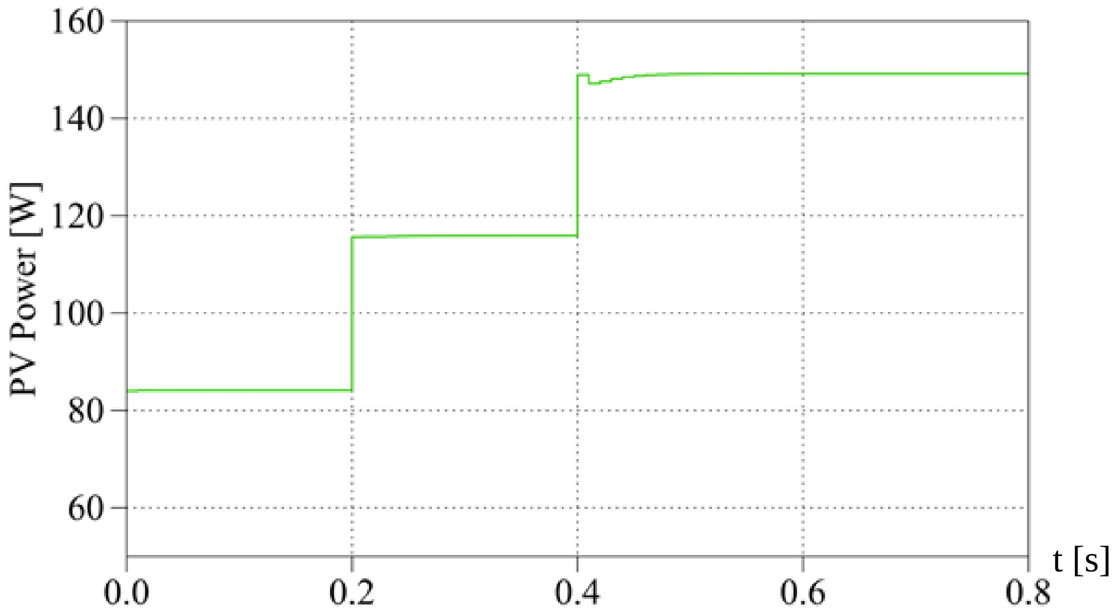

Figure 3.5 PV output power changing with irradiation

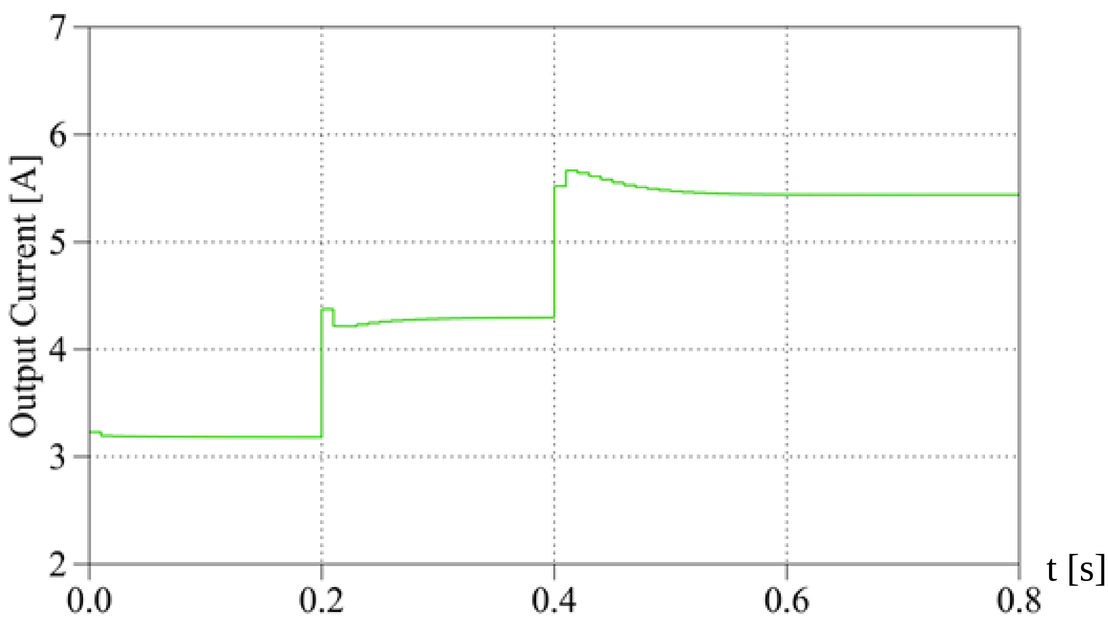

Figure 3.6 PV module output current changing with irradiation

MPPT algorithms used in PV systems are one of the most important factors for maximizing the electrical efficiency of a solar photovoltaic system. As a result of cost optimization, after the decision to use an MPPT system is made by the designer, it is important to decide which algorithm has to be used in the application. This section has presented a maximum power point tracking technique and its performance at different weather conditions. The proposed PV system and MPPT was simulated. From Figure 3.4, it can be easily understood that in order to track the MPP, the output voltages keep changing according to its corresponding MPP point. Figure 3.5 shows tracking performance of the PV's output power when the irradiance level G is varied and the ambient temperature T is fixed. Based on this condition, the simulation results using the INC algorithm verify the correctness of the proposed model. By the proposed system simulation, the MPP tracker takes less than 0.15 sec to track the MPPT. Through simulation, we can see that the system completes the maximum power point tracking successfully and accurately despite fluctuations. When the external environment changes suddenly, the system can track the maximum power point quickly (less than 0.15 sec). Although there is little deviation in the results, the overall trends and forms have good stability. The Incremental Conductance method, therefore, is a very efficient MPPT method because panel terminal voltage is changed according to its value relative to the MPP voltage. This method offers good performance under rapidly changing atmospheric conditions.

3.3 Proposed Full-bridge Step-up / Step-down DC-DC Converter with Partial Power Processing

The basic structure of the proposed FB step-up/step-down partial power processing converter is the standard full-bridge partial power processing circuit. This proposed converter consists of an input capacitor (Cin) to reduce ripple output voltage at the terminal of the PV array, six controllable switches (S1 - S6), two rectifier diodes (D1 and D2), and an isolated high frequency (HF) transformer. The two added MOSFET switches are each connected in series with a diode in each branch of the transformer center-tapped rectifier. The operation of the proposed circuit can be divided two ways with a proper control block: one for the step up function and the other for the step down function.

With a properly designed selection block, the circuit will be operated in the step up function when the input PV voltage is smaller than the desired output voltage and operated in the step down function when the input voltage is larger than the desired output voltage. The selection signal comes from the comparison of the input PV voltage and the referenced output voltage. In the mode of step up operation, the four MOSFETs on the primary side of the transformer will operate in sequence as the pulse width modulated (PWM) signals, and the two MOSFETs on the secondary side of the transformer will stay closed for the whole time the input is smaller than the set V_{ref} output. On the other hand, in the mode of step down operation, the four MOSFETs on the primary side will stay open for the whole time the input PV voltage is larger than the set V_{ref} output, and the two MOSFETs on the secondary side will conduct with a phase shift of 180 degrees with respect to the PWM signals.

The modes of converter operation that the proposed converter goes through when it is operating as a boost or as a buck converter are introduced in detail in subsections 3.3.1 and 3.3.2, respectively. A block diagram of the proposed full-bridge step-up/step-down circuit is shown in Figure 3.7.

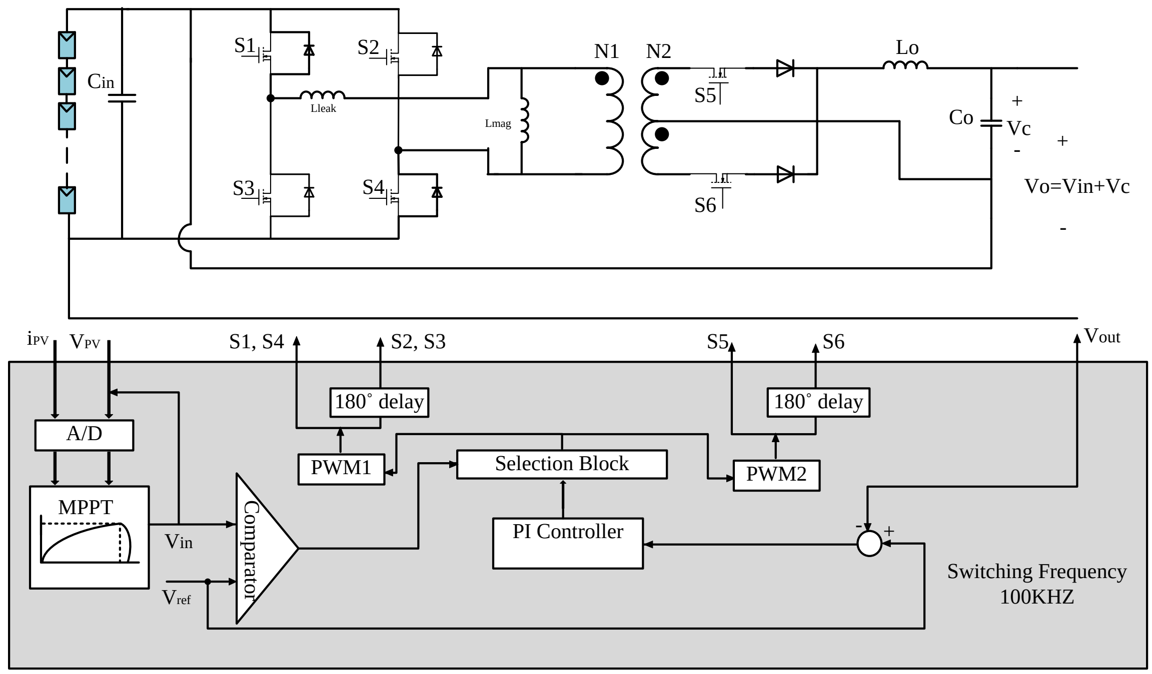

Figure 3.7 Block diagram of the proposed high efficiency step-up/step-down full-bridge circuit

3.3.1 The Operation of the Step-up Mode for the Circuit

The purpose of the step up function for the circuit is to convert the lower PV input voltage into the desired higher output voltage. When operating in this function, it will be exactly the same circuit as a standard boost partial power full-bridge converter.

In this topology, the output voltage equals the sum of the input PV module voltage and the voltage across the output capacitor. Since this partial power converter does not need to process all the input PV power, the total system conversion efficiency is very high. The converter is designed to be composed of two switching MOSFETs and one diode per channel, as illustrated in Figure 3.8, thus the MOSFETs and diodes do not need to withstand the total output voltage. These classical partial power processing converters include a high frequency transformer in their design, which helps to reduce the size of the system in PV power conditioning systems.

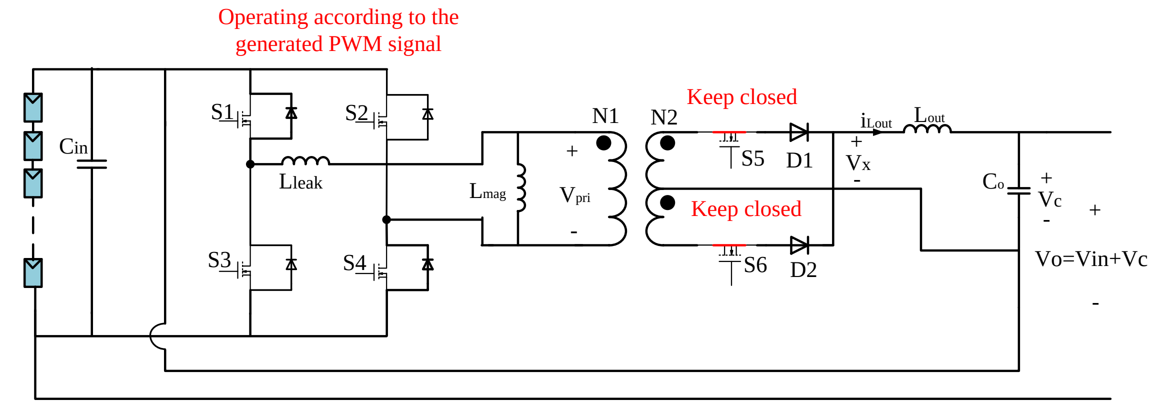

Figure 3.8 The circuit operation in the step up function

In this step-up mode of operation, switches in each leg of the FB inverter are driven by non-overlapping voltages that are out of phase by 180 degrees. The leg that conducts first is called the leading leg while the other leg is called the lagging leg. The two switches in the leading inverter leg conduct after the freewheeling interval in order to initiate the power delivery interval. The operation of the converter is similar to that of a simple full-bridge circuit. The stages of operation over a switching period T_s are shown in Figure 3.9 and can be summarized as follows:

Stage 1 ($0 < t < DT$): In this stage, the MOSFET S1 and S4 is turned ON as well as diode D1, and the inductor current builds up. The input PV voltage is transformed to the secondary side of the winding. Capacitor Co delivers energy to the output.

$$V_{L_{outf}} = V_{in}\left(\frac{Ns}{Np}\right) - Vc \tag{3.4}$$

$$\frac{\Delta i_{Lout}}{\Delta t} = \frac{\Delta i_{Lout}}{DTs} = \frac{Vs(Ns/Np) - Vc}{Lout} \tag{3.5}$$

Stage 2 (DT < t < T/2): All four MOSFETs are turned off; the current in the primary winding is zero. The current in the filter inductor L_{out} must maintain continuity, resulting in both diodes becoming forward-biased in this freewheeling stage. Assuming that the rectifier circuit is symmetrical and operated in continuous conduction mode, the inductor current is divided equally between the diodes.

$$V_{L_{outf}} = -Vc \tag{3.6}$$

$$\frac{\Delta i_{L_{out}}}{\Delta t} = \frac{\Delta i_{L_{out}}}{Ts/2 - DTs} = \frac{-Vc}{Lout} \tag{3.7}$$

Stage 3 (T/2 < t < T/2+DT): This stage occurs when the switches S1 and S4 as well as diode D1 are off, and the switches S2 and S3 as well as well as diode D2 are on.

Stage 4 (T/2+DTs < t < T): All switches are OFF and both diodes are ON during this time interval. The equivalent circuit of this stage is the same as that of stage 2.

Figure 3.10 shows the timing diagram and key idealized converter waveforms for the step up mode of operation. Since the net change in inductor current over one period must be zero for steady-state operation, solving for Vc,

$$V_c = 2V_{in}\left(\frac{Ns}{Np}\right)D \tag{3.8}$$

$$\text{Thus, } Vout = Vin + Vc = Vin + 2Vin(\frac{Ns}{Np})D \tag{3.9}$$

where D is the duty ratio of the four switches in the primary side, which is always less than 0.5 in this mode, as shown in Figure 3.10.

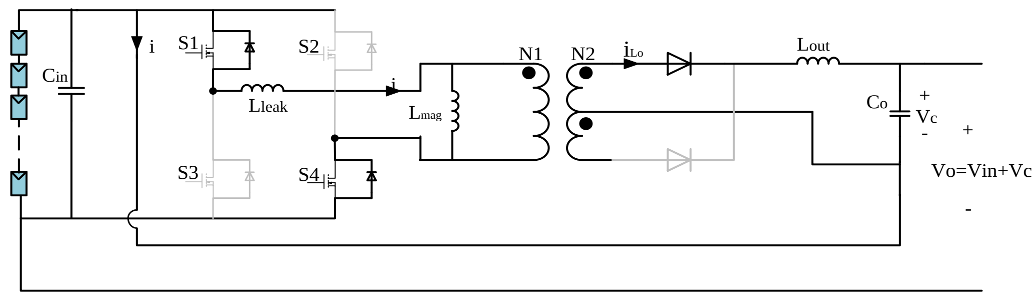

Stage 1

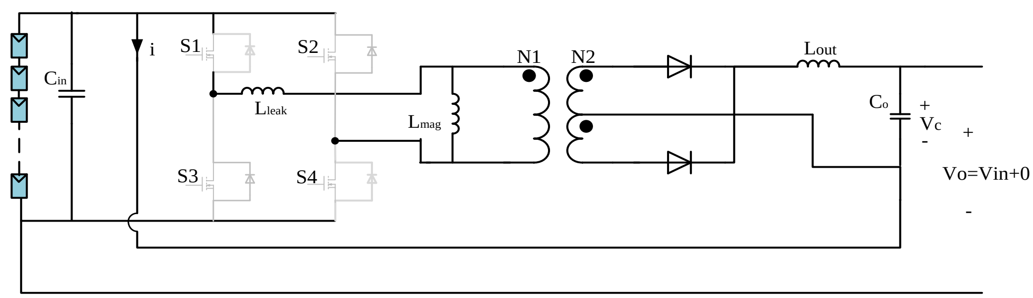

Stage 2

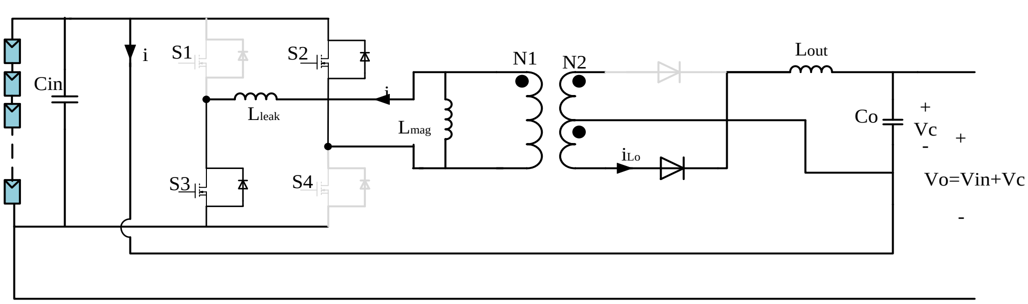

Stage 3

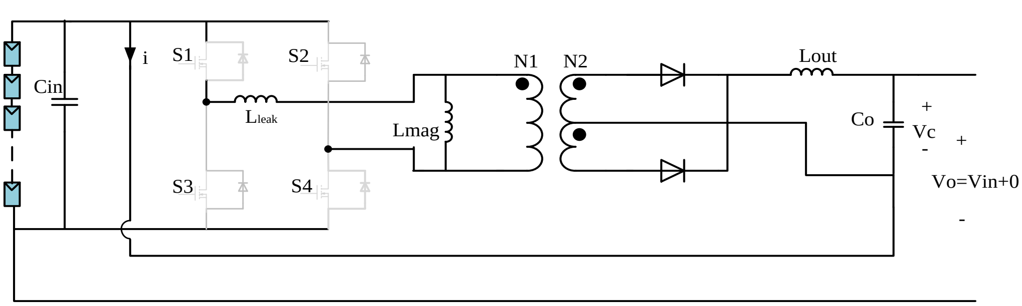

Stage 4

Figure 3.9 Stages of operation of partial power processing full-bridge DC-DC converter

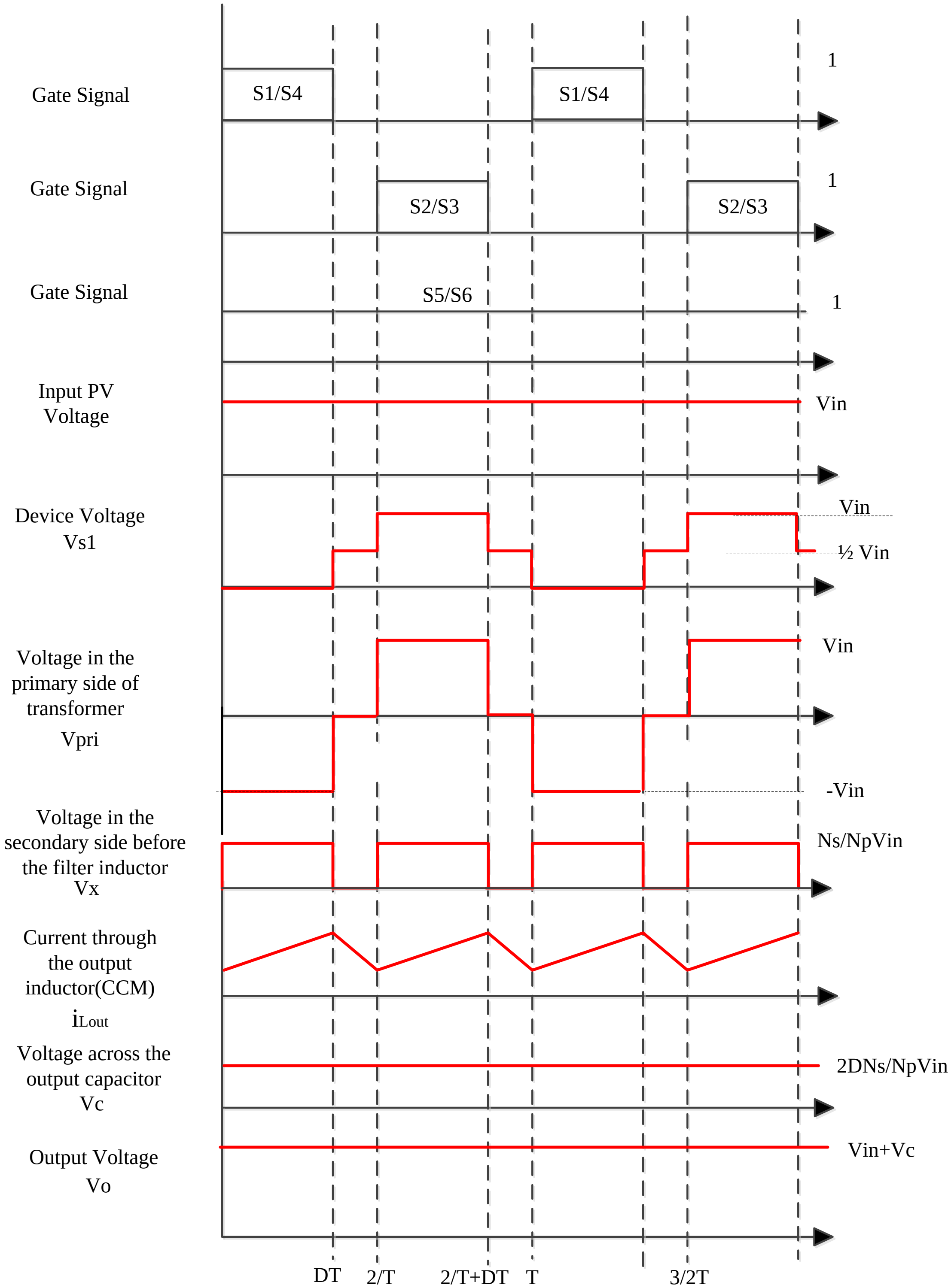

Figure 3.10 Timing diagram and idealized theoretical converter waveforms for the stages of operation shown in Figure 3.9

The source of energy that displaces the charge is different for the two legs. The transformer's leakage inductance is the source of energy for displacing the charge in the capacitance of the leading leg. The converter's output inductor is the energy source for the lagging leg. As the switching frequency increases for PWM power converters, switching losses dominate the total power dissipation. Due to the partial power processing method, the power flow through the converter section is quite small; the compared switching losses will not be a problem that needs to be taken care of. Therefore, high efficiency for the whole system can still be achieved without the need for the soft switching technique used for switching loss reduction.

3.3.2 The Operation of the Step-down Mode for the Circuit

The step down function is required when a shaded or limited mismatch condition happens. In this case, the PV input voltage is higher than the desired output voltage. The operating circuit is illustrated in Figure 3.11. The selection control block should generate a selection signal, which represents the choice of a PWM control block and the operation of the 6 MOSFETs.

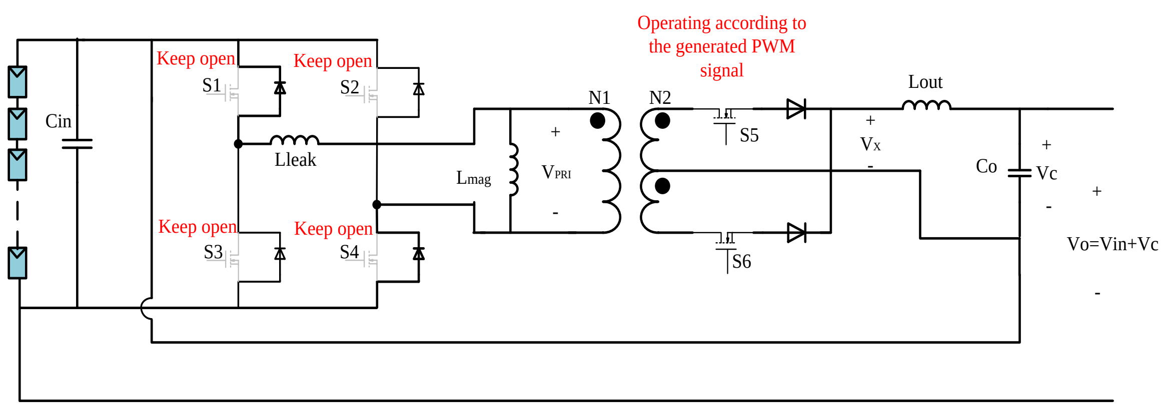

Figure 3.11 The circuit operation in the step-down function

The operation of this mode is similar to a reversed half-bridge circuit with full-bridge rectifier. The circuit operation is explained below.

Stage 1 (0< t < DTs-2/Ts): In this stage, both MOSFETs in the secondary side are turned on, and the inductor current builds up. Capacitor Cs delivers energy to the output. And there is no current flow through the primary side of the transformer.

$$V_{L_{out}} = -V_{in}\left(\frac{Ns}{Np}\right) - Vc \tag{3.10}$$

$$\frac{\Delta i_{Lout}}{\Delta t} = \frac{\Delta i_{Lout}}{Ts - DTs} = \frac{-Vin(Ns/Np) - Vc}{Lout} \tag{3.11}$$

Stage 2 (DTs-2/Ts < t < T2): Only MOSEFT S5 in turned on in this stage, and the inductor current is continuously decreased. The diodes D2, D3 on the primary side are also turned on by the reflecting current from the secondary side of the transformer. Thus, a negative value of the input PV voltage is connected to the primary side of the transformer. The inductor energy is consequently discharged into the capacitor Cs. For continuous conduction mode, T2 = 2/Ts.

$$V_{L_{out}} = Vc \tag{3.12}$$

$$\frac{\Delta i_{Lout}}{\Delta t} = \frac{\Delta i_{Lout}}{DTs - 1/2Ts} = \frac{Vc}{Lout} \tag{3.13}$$

Stage 3 (T2 < t < 2/Ts): This stage occurs when the circuit operates in discontinuous conduction mode (DCM). In this mode, the PV power is transferred from both the input and output capacitors to the output side. There is no current flowing through the inductor.

Furthermore, it is also worth noting that resonances can occur between the device capacitance and the input inductor in this mode of operation. The operation of DCM makes the MOSFET turn on under zero current situation, thus the turn-on losses are greatly reduced at light loads. However, in this thesis, we adjust the output resistance low enough and the output inductor high enough to avoid the stage of DCM.

Stage 4 (Ts-DTs < t < Ts): Only the MOSFET S6 is turned on in this stage, and the inductor current starts to decrease again and the inductor energy discharged. The diode D1, D4 in the primary side is turned on by the reflecting current from the secondary side of the transformer. Thus, in this case, the input PV voltage is connected to the primary side of the transformer.

The stages of operation over a switching period Ts are provided in Figure 3.12.

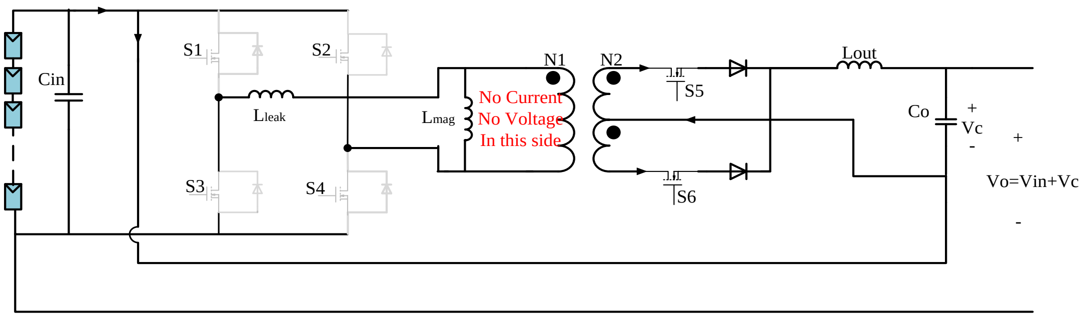

STAGE 1

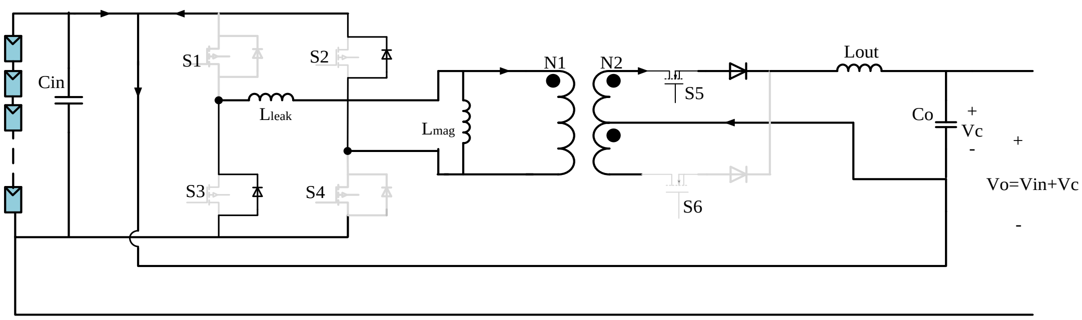

STAGE 2

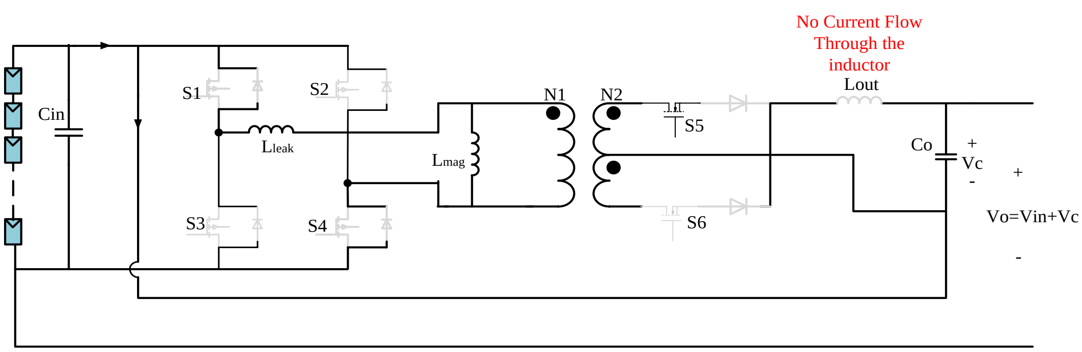

STAGE 3 (DCM)

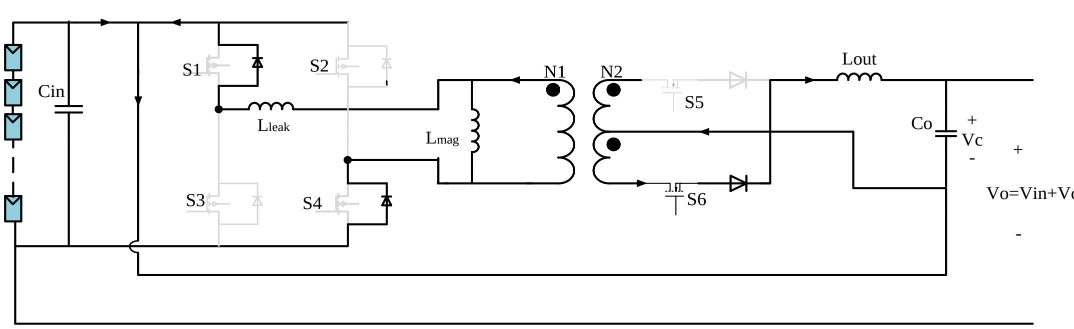

STAGE 4

Figure 3.12 Stages of operation of the step down mode of the proposed converter

The output of the converter can be regulated by modulating the operating duty ratios of the two switches in the bridge, which are conducting with a 180 degree delay. In this operation mode, the voltage across the capacitor will always be a negative value due to the reversed operation similar to a buck converter and the partial power processing branch. Figure 3.13 shows the timing diagram and key idealized converter waveforms for the step down mode of operation. Since the net change in the inductor current over one period must be zero for steady-state operation, solving for V_c,

$$\mathrm{V_c} = -2\mathrm{V_{in}}\left(\frac{\mathrm{Ns}}{\mathrm{Np}}\right)(1 - \mathrm{D}) \tag{3.14}$$

$$\text{Thus, } \mathrm{Vout} = \mathrm{Vin} + \mathrm{Vc} = \mathrm{Vin} - 2\mathrm{V_{in}}\left(\frac{\mathrm{Ns}}{\mathrm{Np}}\right)(1 - \mathrm{D}) \tag{3.15}$$

where D is the duty ratio of the two switches in the secondary side of the transformer, which is always larger than 0.5 in this mode ($0.5 < D \leq 1$), is shown in Figure 3.13.

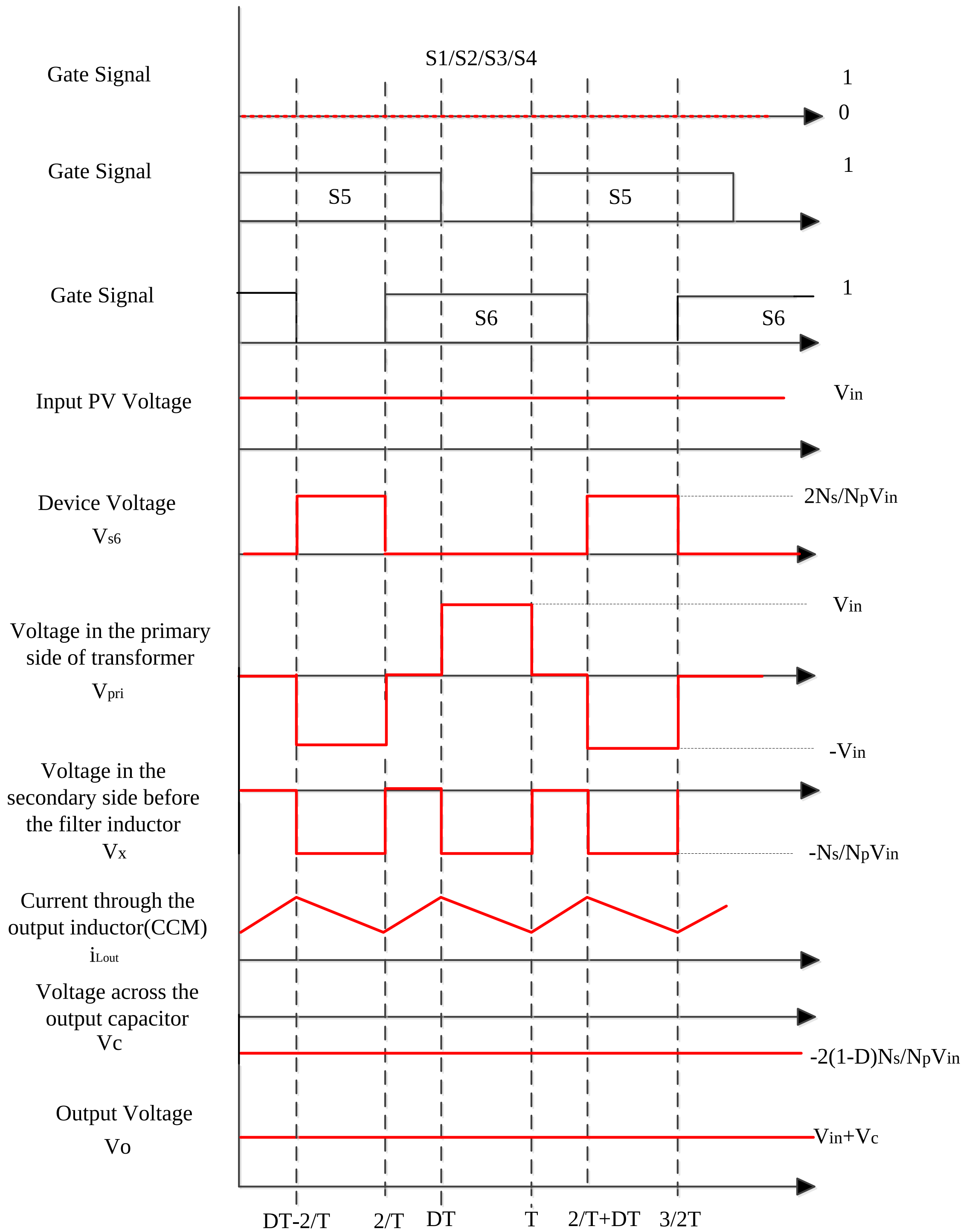

Figure 3.13 Timing diagram and idealized theoretical converter waveforms for the stages of operation shown in Figure 3.12

3.4 The Control Circuit for the Proposed Step-up / Step-down Circuit Operation

The proposed full-bridge step-up/step-down converter control is based on maintaining a defined value for the voltage across the dc-link. This voltage needs to be maintained at the referenced voltage value V_{ref}. In this thesis, a dual-loop control has been implemented. This control loop consists of an inner And&Or logical selection control loop, and an outer PWM voltage control loop, which is fulfilled by a proportional-integral (PI) controller. The duty cycle (D) is calculated to adjust the PV string voltage V_{in} such that the maximum power of the PV string/array can be tracked. In this case, V_c is determined in order to compensate for the difference between the PV input voltage Vin and the output dc-link voltage. The maximum input PV voltage is calculated by the MPPT controller. An IncCond MPPT algorithm is used for locating local maximum power points. The design of each controller will be described in detail in this section. The general scheme of the full-bridge DC-DC controller is shown in Figure 3.14. In this figure, D represents the duty cycle of the converter; V_{ref} is the reference output dc-link voltage.

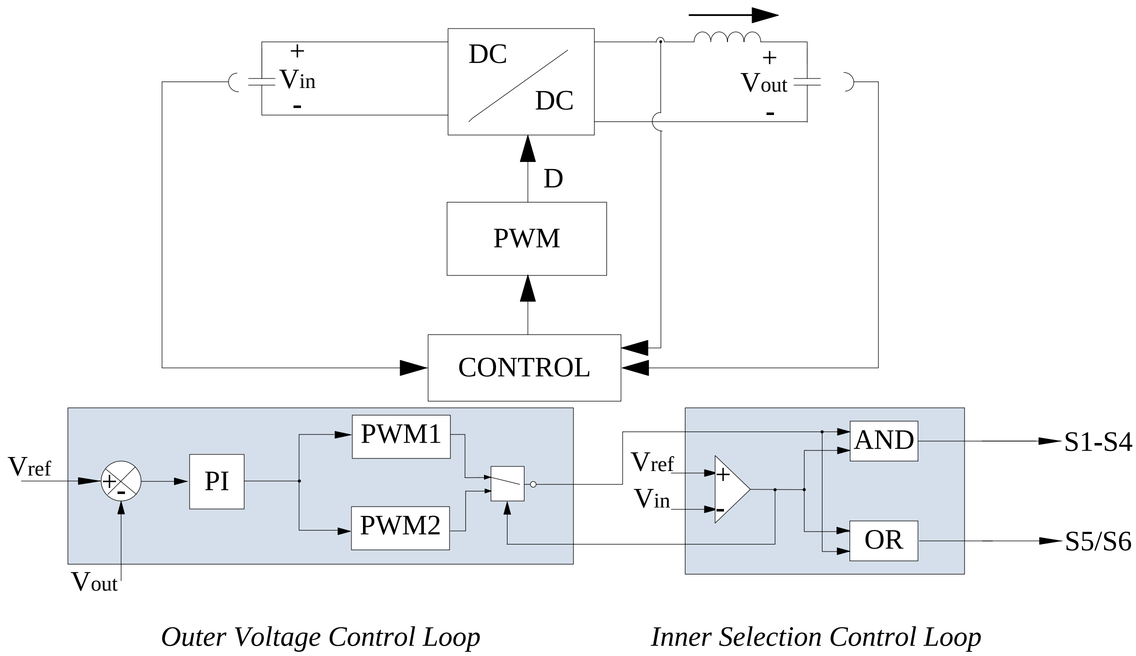

Figure 3.14 The control strategy diagram block

For the outer PI voltage control loop, the constant voltage control method is used in this thesis to guarantee voltage reference tracking. The MPPT controller for the PV panel section measures open circuit voltage and sets the maximum power point voltage (V_{max}) accordingly. The task of the MPPT algorithm introduced in section 3.2 is to set V_{max} only, and it is repeated periodically. Then, the voltage PI control loop is implemented to regulate the input voltage of the converter. Its task is to minimize the error between the measured output voltage V_{outm} and the referenced output voltage V_{ref} by adjusting the duty cycle continuously. The PI control loop operates at quite a fast rate to provide overall stability and fast response of the system.

The purpose of the inner selection block is to select the proper PWM block according to different operating modes. By comparing the input voltage from the PV panel with the referenced output voltage, the system will choose its corresponding PWM block.

The signal from the comparator and the PWM block will feed both the two logical blocks $(+ \, and \; \times)$, and the PWM block. On the one hand, the signal from the And block $(\times)$ will feed the four switches on the primary side of the transformer with a 180 degree phase delay. And on the other hand, the signal from the Or block (+) will go to the two switches on the secondary side of the transformer, also with a 180 degree phase delay.

It is known that any digital signal A anded $(\times)$ with 1 will give the signal itself, and ored (+) with 1 will always give 1, such that $A \times 1 = A,$ and $A + 1 = 1$. Furthermore, a digital signal A anded $(\times)$ with 0 will always give 0, and ored (+) with 0 will give the signal itself, such that $A \times 0 = 0, A + 0 = A$. Due to the logical operation of the $(\times)\&(+)$ block, when the circuit is operating in the boost mode, the comparator gives a signal 1 and the four switches on the primary side of the transformer will receive the PWM signal itself, while the two switches on the secondary side will always get 1 after it goes through the logical block. Thus, in this mode, the four switches on the primary side will operate in sequence according to the PWM signal while the other two switches on the secondary side will always stay closed in this whole operating mode.

Although it is the same as in the buck mode, the comparator this time will give out a signal 0. The four switches on the primary side of the transformer will always receive the signal 0 to stay turned off while the two switches in the secondary side will get the PWM signal itself from its corresponding PWM block after it goes through the logical block. Thus, in this mode, the four switches in the primary side will always stay off while the other two switches will operate in sequence in this whole operating mode.

With a proper coordination of the two control block, the proposed circuit can operate as the expected step up and step down full-bridge converter, depending on the input PV voltage.

3.5 Design Procedure and Example for the Proposed Circuit

3.5.1 Design Procedure

Given the input voltage range, Vin, output desired voltage, Vout, switching frequency, fs, load current, I_{load}, assuming 100% efficiency and continuous current in the inductor, the duty cycle, D, of the power MOSFET is given by (3.16), and the switching period T, is given by the inverse of frequency fs, as in (3.17).

$$\begin{cases} \text{For step} - \text{up mode: } \mathrm{D} = \dfrac{\mathrm{V_c}}{2\mathrm{V_{in}}\dfrac{\mathrm{Ns}}{\mathrm{Np}}} \\ \text{For step} - \text{down mode: } \mathrm{D} = 1 - \dfrac{|V_c|}{2\mathrm{V_{in}}\dfrac{\mathrm{Ns}}{\mathrm{Np}}} \end{cases} \tag{3.16}$$

$$\mathrm{T} = \frac{1}{\mathrm{f_s}} \tag{3.17}$$

In a design, the specifications for the six MOSFETs in the buck-boost full-bridge converter need to be decided using the above parameters. The switching speed for the six MOSFETs should be sufficient such that the turn-on and turn-off transient times are much smaller than T. In addition, the drain-source voltage rating of the power MOSFETs must be larger than V_{in}, and the drain current rating must be larger than I_{load}. The larger the ratings chosen, the more robust the design will be. However, high ratings require MOSFETs that are large and therefore more expensive. Typically, the V_{ds} voltage rating is chosen to be about twice as large as Vin, leaving some safety margin in the design. Another factor that may need to be considered when choosing the six power MOSFETs is the switching loss, which can be larger than the conduction loss. Thus MOSFETs with faster switching speeds, and therefore smaller die size, are preferred. However, due to the partial power processing method, the switching losses may not be a problem that affects overall efficiency of the proposed converter.

For the high frequency transformer design, assume the turns ratio of the transformer is Ns/Np=1/3.

After selecting the MOSFET switches and the transformer, the filter inductor value must be determined. The average current in L_{out} is the same as average current in the load since the average current in the capacitor is zero. Thus, the critical inductance value for continuous current mode is given by (3.18), where R_l in the equation represents the resistance of a resistive equivalent load, given by (3.19). In order to produce a smooth output current, the filter inductor is usually chosen to be twice as large as L_{cri}, or even larger if the volume and the cost of the inductor are tolerable.

$$L_{cri} = \frac{1 - 2D}{4} T_s R_l \tag{3.18}$$

$$R_l = \frac{V_{out}}{I_{load}} \tag{3.19}$$

The last component to be chosen for the power stage circuit is the capacitor. The minimal capacitance value, C_{min}, is given by (3.20), where L is the chosen inductance value and K_{rip}% is the allowed maximum output voltage ripple. A capacitance of 1.5 to 2 times C_{min} is typically selected.

$$C_{min} = \frac{1 - 2D}{32Lxf_s{}^2(K_{rip}\%)} \tag{3.20}$$

3.5.2 Design Example

Using the design procedure provided above, the power stage design for the full-bridge converter was completed. The proposed step-up/step-down full-bride converter is designed for solar power application, which converts a 25V-40V PV input voltage to a 33V constant output at a switching frequency of 100kHz and a load current of 10A. A list of circuit parameters are summarized in Table 3.2. Values of the inductor and capacitor are chosen according to the CCM operation and standard E24 values for circuit elements, as given in Appendix A. The PV panel model built in section 3.2 is chosen for the simulation of the proposed circuit. In this case, the input voltage of the PV panel changes from 25V to 40V according to different levels of irradiance. Therefore, the designed DC-DC converter need to continuously adjust the voltage levels and moves the operating point to match the load to PV source to get the desired constant output voltage.

Table 3.2 The parameters in the design of the full-bridge step-up/step-down circuit

Parameter	Value
Switching Frequency, f_s	100kHz
PV input Voltage, V_{in}	25V-40V
Desired output Voltage, V_{out}	33V
Output Load Current, I_{load}	10A
Input capacitor, C_{in}	1mF
Turns ratio, Ns:Np	3:1:1
Leakage inductance, L_{leak}	5uH
Magnetizing inductance, L_{Mag}	500uH
Output filter capacitor, C_{outf}	100uF
Output filter inductor, L_{outf}	2uH
Maximum output voltage ripple	54.3mV

The design parameters used in the PI control loop are given in Table 3.3. Once the control signal is obtained from the dual-control loop, two conventional PWM controls are implemented according to different operating ranges of the duty ratio for each operating mode (step-down mode: $0 \leq D < 0.5$, step-up mode: $0.5 \leq D \leq 1$). Thus, the operating duty cycle is determined by the operation mode of the converter and the proposed converter with PWM control can achieve a very high efficiency at high operating frequencies.

Table 3.3 The design parameters in the PI control loop

Parameter	Value
K_P	0.012
K_I	800

3.6 Summary

In this chapter a high efficiency FB step-up/step-down PWM DC-DC converter operated with a code-based MPPT algorithm has been proposed for the PV array system. In addition to the circuit, the steady-state operation of the converter has been analyzed to fully characterize its operation and the design equations. The design procedure and design example have also been presented.

This proposed converter topology is suitable for PV cells application, which is subject to its operating temperature and irradiation. This topology can convert voltage from PV cells to a regulated DC output voltage that is higher or lower than the input. The converter's operation modes in one switching period are described step by step. Furthermore, a dual-loop control scheme has been proposed to regulate the dc-link voltage at its reference output by means of tracking the selection signal. The conventional PWM control algorithm is fulfilled by a PI controller. Moreover, switching losses can be greatly reduced using the partial power processing method and high efficiency can be achieved. The proposed circuit and its control scheme have been implemented in software PLECS and several simulations have been performed under different input operating conditions in Chapter 4.

Chapter 4: Simulation Results of the FB Step-up / Step-down Converter Circuit

4.1 Overview

The proposed converter has the advantages of simplicity, high efficiency, accurate maximum power point tracking (MPPT), and low cost. High efficiency is achieved by having a portion of the input PV power directly fed forward to the output without being processed by the converter. The operation of this converter allows for a simplified maximum power point tracker design using fewer measurements. The 100kHz proposed circuit was built in PLECS to confirm the theoretical performance analyzed in detail in Chapter 3.

In this chapter, performance of the proposed closed-loop controller for the converter circuit is presented in Section 4.2. It is used to regulate the input PV voltage to get a constant output dc-link voltage when external factors are changing. Next, the performance for the two different modes of operation for the proposed circuit with its partial power processing method are analyzed in detail in Section 4.3 and Section 4.4, respectively. These sections include simulation waveforms using PLECS (Piece Wise Linear Electronic Circuit System) and power analysis of the distributed PV system comprised of the proposed DC-DC converters. The performance of three proposed distributed modules connected in series to achieve the desired input dc voltage to the inverter are investigated in Section 4.5.

4.2 Closed-loop Control

The proposed full-bridge step-up/step-down with partial power processing circuit for solar power application was simulated using PLECS. As shown in Figure 4.1, the simulated system consists of the PV array built in Chapter 3 and the converter operated with a MPPT algorithm at switching frequency of 100 kHz. The output of the PV panel module is partly fed to the isolated full-bridge partial power DC-DC converter while the rest is directly feeding to the output side. The current load used in the model is for simulation purposes. The MPPT controller is designed to track the maximum power output, while the closed-loop controller is used for output voltage regulation with variation of input PV power.

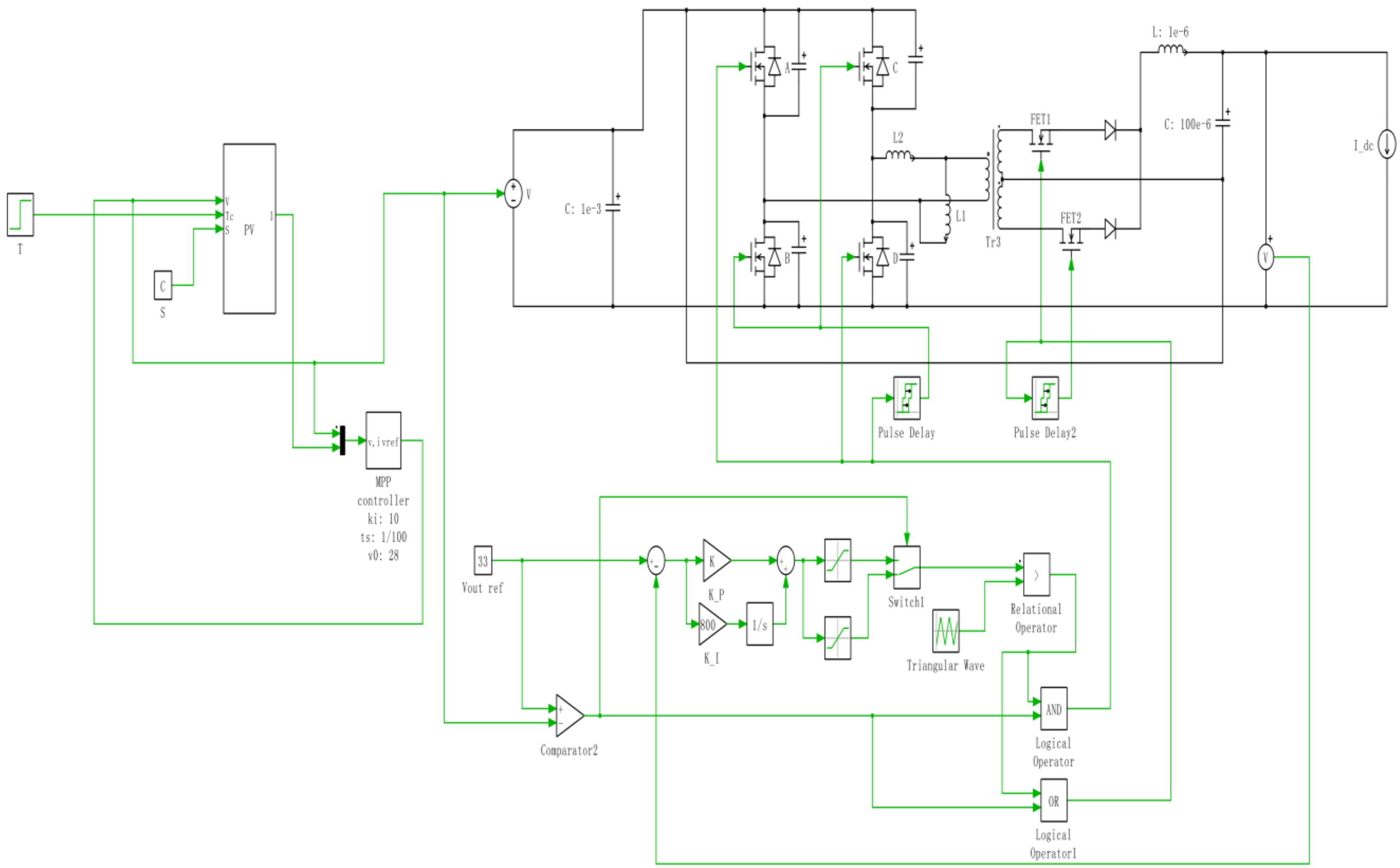

Figure 4.1 The full-bridge step-up/step-down with the partial power processing simulation circuit

A voltage mode PWM controller was designed to regulate the output voltage of the step-up/step-down full-bridge converter. The dual-loop controller and full-bridge converter are illustrated in Figure 4.1. Figure 4.2 shows the output voltage maintaining performance with the variation in ambient temperature T and the irradiance G is fixed at 1,600 W/m2. The MPPT control ensures that the PV panel always operates at its MPP with the external condition changes. With the designed control block, it is clear that the output voltage is maintained constant at 33V with the change in input PV panel voltage when the temperature varies, and also the relationship $Vout = Vin + Vc$ for partial power processing method can be easily verified from the simulation results. The average, value of the output at steady state is 33.000V.

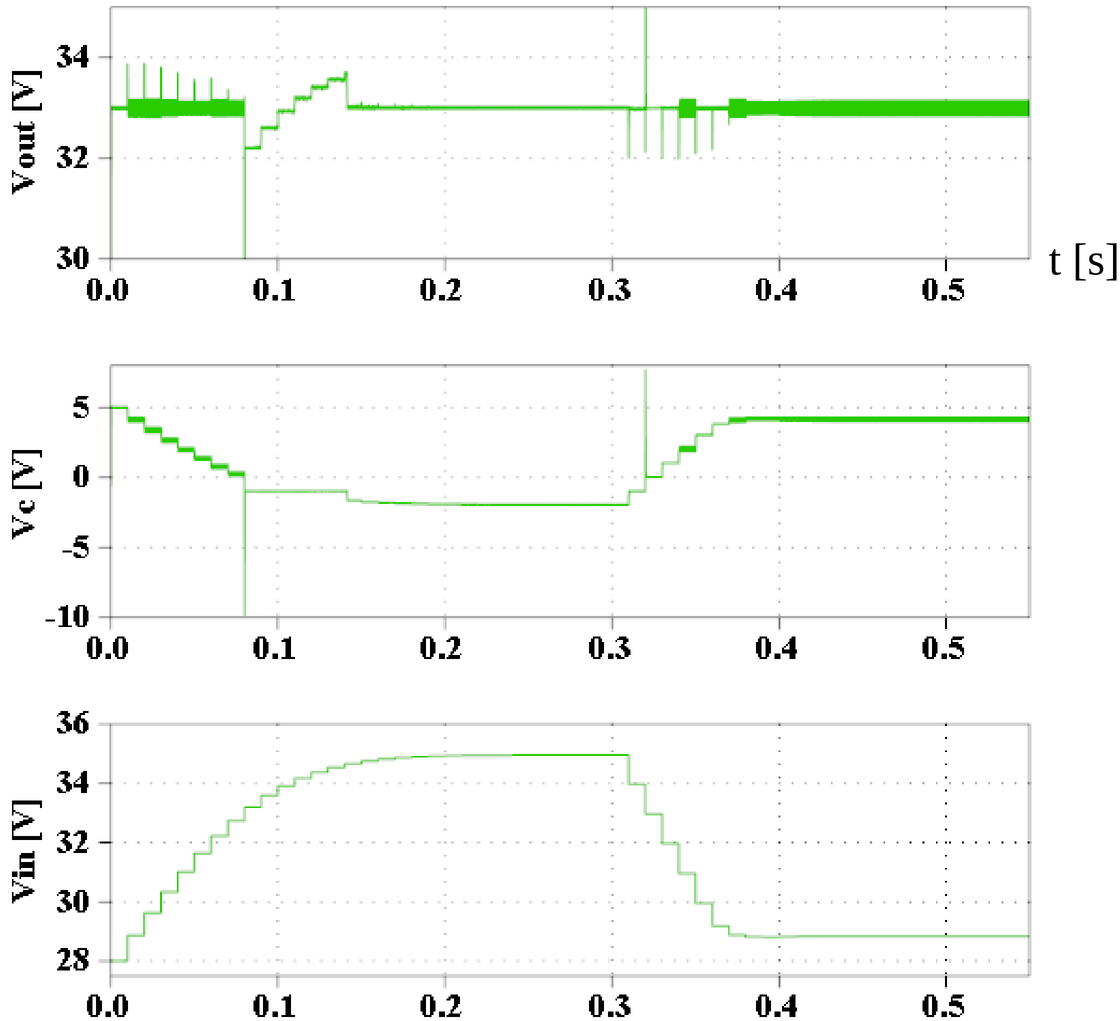

Figure 4.2 The simulation waveform of the output voltage, the voltage across the output capacitor with the change of input PV voltage

Figure 4.3 shows the control signal received from the selection control block, and the gating signal of the 6 MOSFET switches (S1-S6), which switch at a fixed frequency, e.g. 100kHz. Above 0.3 seconds, temperature varies from 10 F to 65 F. Immediately, the system gives control according to the signal from the selection block to reach the reference output voltage. Four switching cycles of the PWM signal for the 6 MOSFETs of the converter in two different operating modes are illustrated in Figure 4.4. It can be seen in Figure 4.4(a) that when the selection block gives a signal of 1, the four switches on the primary side will operate according to the PWM control signal, while the two switches in the secondary side will keep closed at the same time. In this case, the circuit operates in standard boost mode. Figure 4.4 (b) presents the buck mode operation with four switches in the primary side staying open and the two MOSFETs in the secondary side switching at 100kHZ frequency.

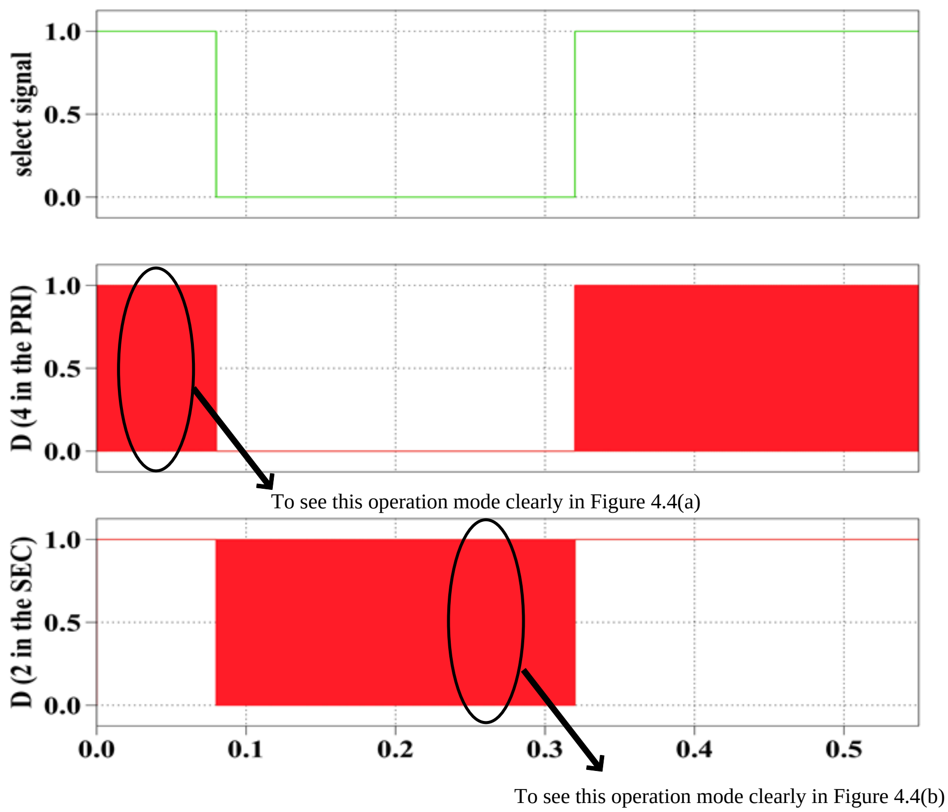

Figure 4.3 The waveform from the control block: the selection control signal, and the two PWM signals for the four MOSFETs on the primary side of the transformer and the two MOSFETs on the secondary side of the transformer separately

(a) PWM signal for boost mode operation

Figure 4.4 Four switching cycles of the PWM signal of the 6 MOSFETs in the converter

(b) PWM signal for buck mode operation

Figure 4.4 Four switching cycles of the PWM signal of the 6 MOSFETs in the converter

There are several advantages of voltage mode control. First, the circuit analysis is easier because the topology of regulator includes only a single-feedback loop, compared with current mode control, which includes two feedback loops in the regulator. Therefore, voltage mode control can make design and circuit analysis easier. Secondly, the use of a large-amplitude ramp waveform provides a good noise margin for a stable-modulation process, and a low-impedance power output provides better cross-regulation for multiple-output supplies.

4.3 Partial Power Processing in Step-up Operation Mode

When the circuit is in step-up operation mode, it is just a standard boost partial power full-bridge converter, simplified as shown in Figure 4.5.

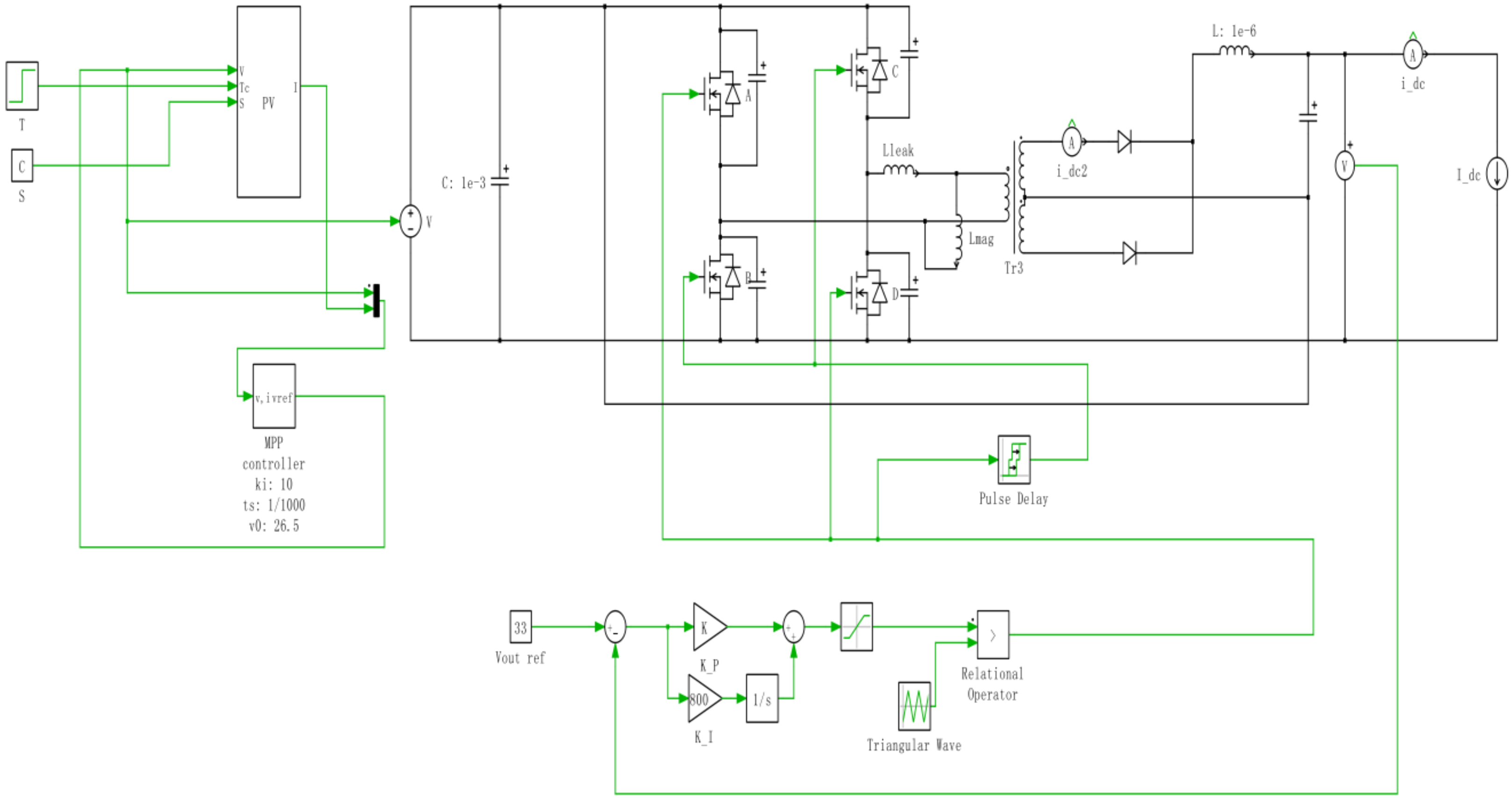

Figure 4.5 Simulation circuit of the step-up mode as a standard partial power full-bridge converter with PI controller for PV system

Figure 4.6 clearly depicts the corresponding values for the transformer primary voltage V_{pri} and the current through the output inductor i_{outL} with the operation of the 6 MOSFETs in the step up operation mode. From the inductor current waveform, it is easily noted that the circuit is operated in continuous conduction mode, and the average current in the output inductor is 10A, the same as the load current. Moreover, the output voltage equation from the theoretical analysis in Chapter 3, which predicts that V_{out} is always equal to the input PV voltage plus the voltage across the output capacitor, is verified by the simulation results.

For the partial power processed method, the efficiency of the whole circuit can be quite high since only a small portion of the generated power will flow through the converter section, while most of the input power directly feeds forward to the output side. This reduces the pressure on the converter block design without compromising the overall conversion efficiency, which helps to reduce system cost.

The average input power Pin over a switching cycle is given by (4.1). The input voltage over a small period of time can be considered as constant, regardless of the variations. Therefore it can be taken out of the integration operator, and the input power can be expressed as the product of the DC PV input voltage and the average input current. The same method to obtain the average power goes through the converter P_{con}, is given by (4.2).

$$P_{in} = \frac{\int_t^{t+T} p_{in} d\tau}{T} = \frac{\int_t^{t+T} v_{in} i_{in} d\tau}{T} = V_{in} \frac{\int_t^{t+T} i_{in} d\tau}{T} = V_{in} I_{in\_avr} \quad (4.1)$$

$$P_{con} = \frac{\int_t^{t+T} p_{con} d\tau}{T} = \frac{\int_t^{t+T} v_{in} i_{con} d\tau}{T} = V_{in} \frac{\int_t^{t+T} i_{con} d\tau}{T} = V_{in} I_{con\_avr} \quad (4.2)$$

The power processed by the converter is given by (4.3).

$$\text{Fraction of Power Processed} = \frac{P_{con}}{P_{in}} 100 \quad (4.3)$$

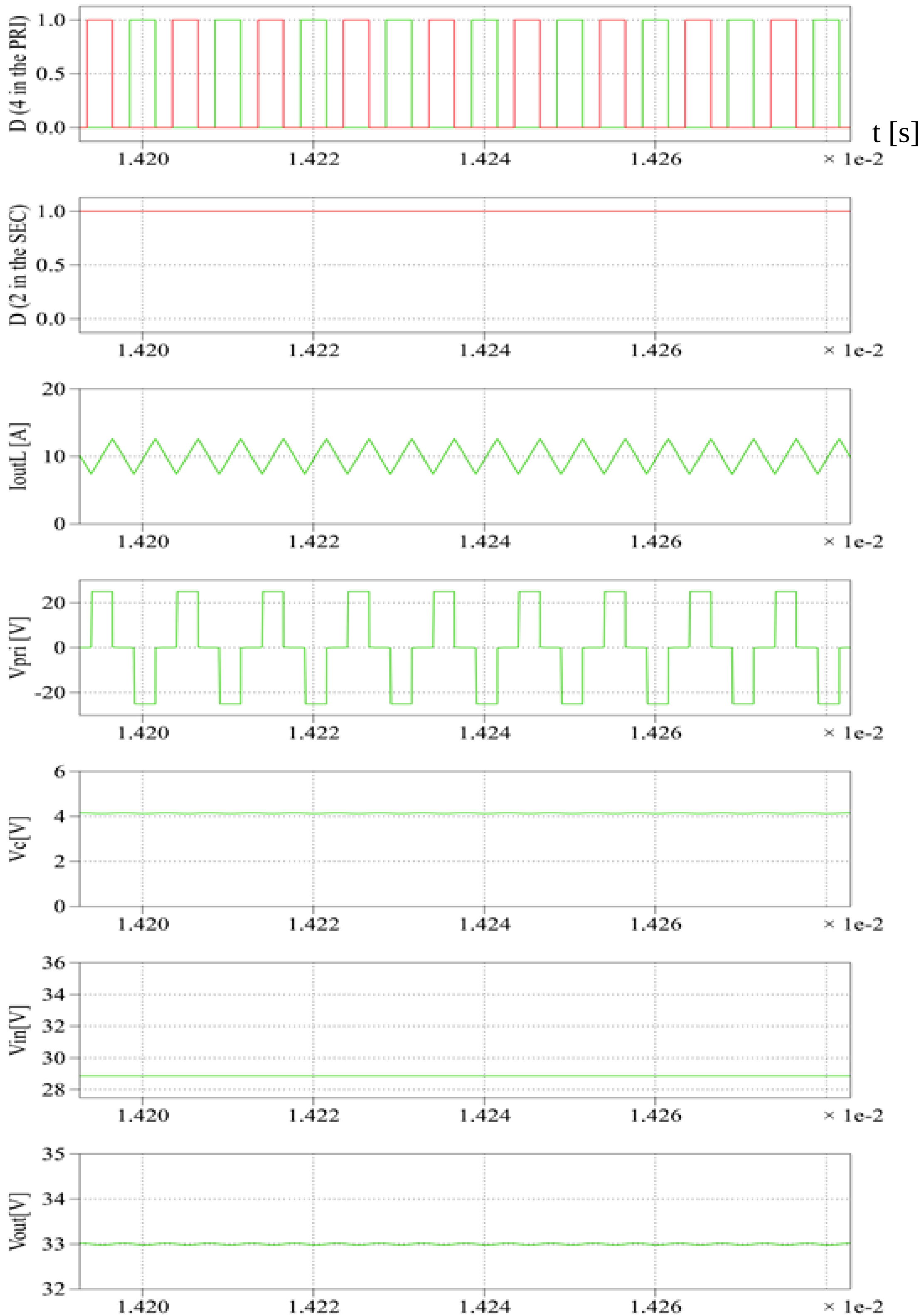

Figure 4.6 Simulation results of the key waveform for the converter in step-up operation mode

All parameters remained unchanged for the two example simulation results except the input PV voltage value (28V and 31V respectively in Figure 4.7 and Figure 4.9). At a 28V input voltage, the average input current of the proposed converter with closed-loop controller is 11.8025 A, and the average current going into the converter is 1.7898A. As a result, the average input power, the power processed by the converter, and the percentage of input power being processed by the converter at 28V input voltage are given by (4.4), (4.5) and (4.6) respectively. The voltage stress and current go through the switch as shown in Figure 4.8.

$$\mathrm{P_{in}} = \mathrm{V_{in}} \mathrm{I_{in\_avr}} = 28\mathrm{V} * 11.8025\mathrm{A} = 330.54\mathrm{W} \tag{4.4}$$

$$\mathrm{P_{con}} = \mathrm{V_{in}} \mathrm{I_{con\_avr}} = 28\mathrm{V} * 1.7898\mathrm{A} = 50.1144\mathrm{W} \tag{4.5}$$

$$\text{Fraction of Power Processed} = \frac{\mathrm{P_{con}}}{\mathrm{P_{in}}} * 100\% = \frac{50.1144}{330.54} * 100\% = 15.2\% \tag{4.6}$$

Similarly, at a 31V input voltage, the average input current of the proposed converter with closed-loop controller is 10.6619A, and the average current going into the converter is 0.657578 A. As a result, the percentage of input power being processed by the converter at 31V input voltage is 6.2%. Therefore, with the input PV voltage becoming larger, the power processing by the converter is smaller, which means that more power is directly feeding forward at almost 100% efficiency. With this configuration, higher power handling capability and higher conversion efficiency can all be achieved. Therefore, the proposed circuit functions as expected.

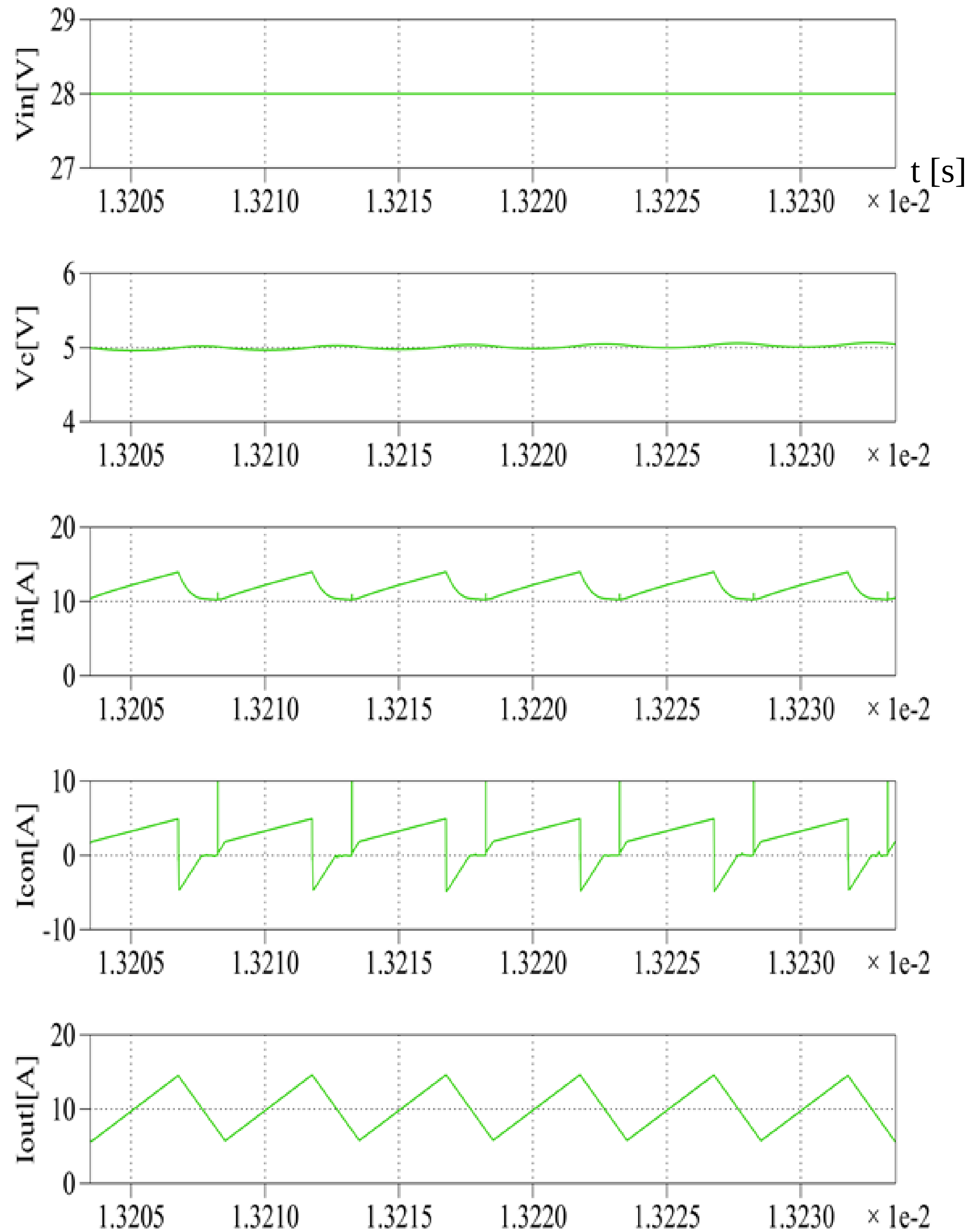

Figure 4.7 Current performance of the proposed circuit at a input voltage of 28V

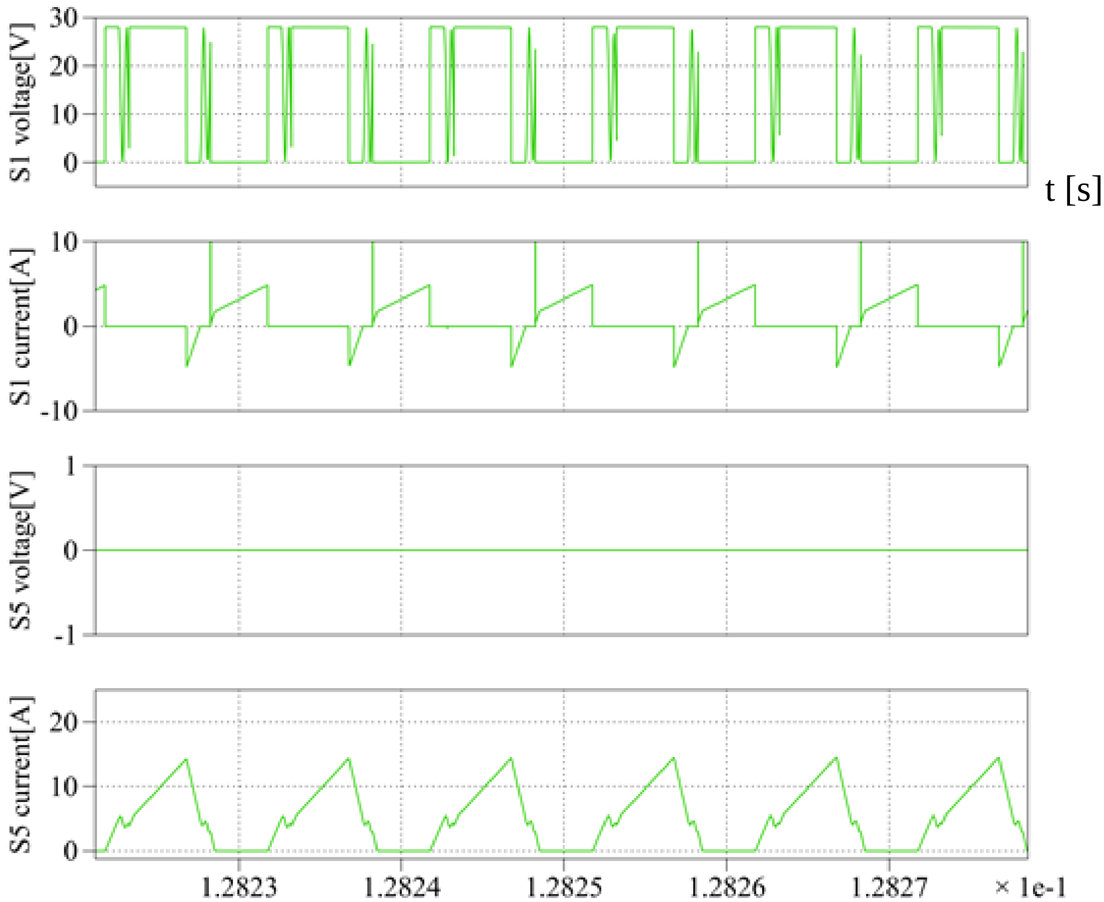

Figure 4.8 Device current and voltage stress (for 28V input voltage)

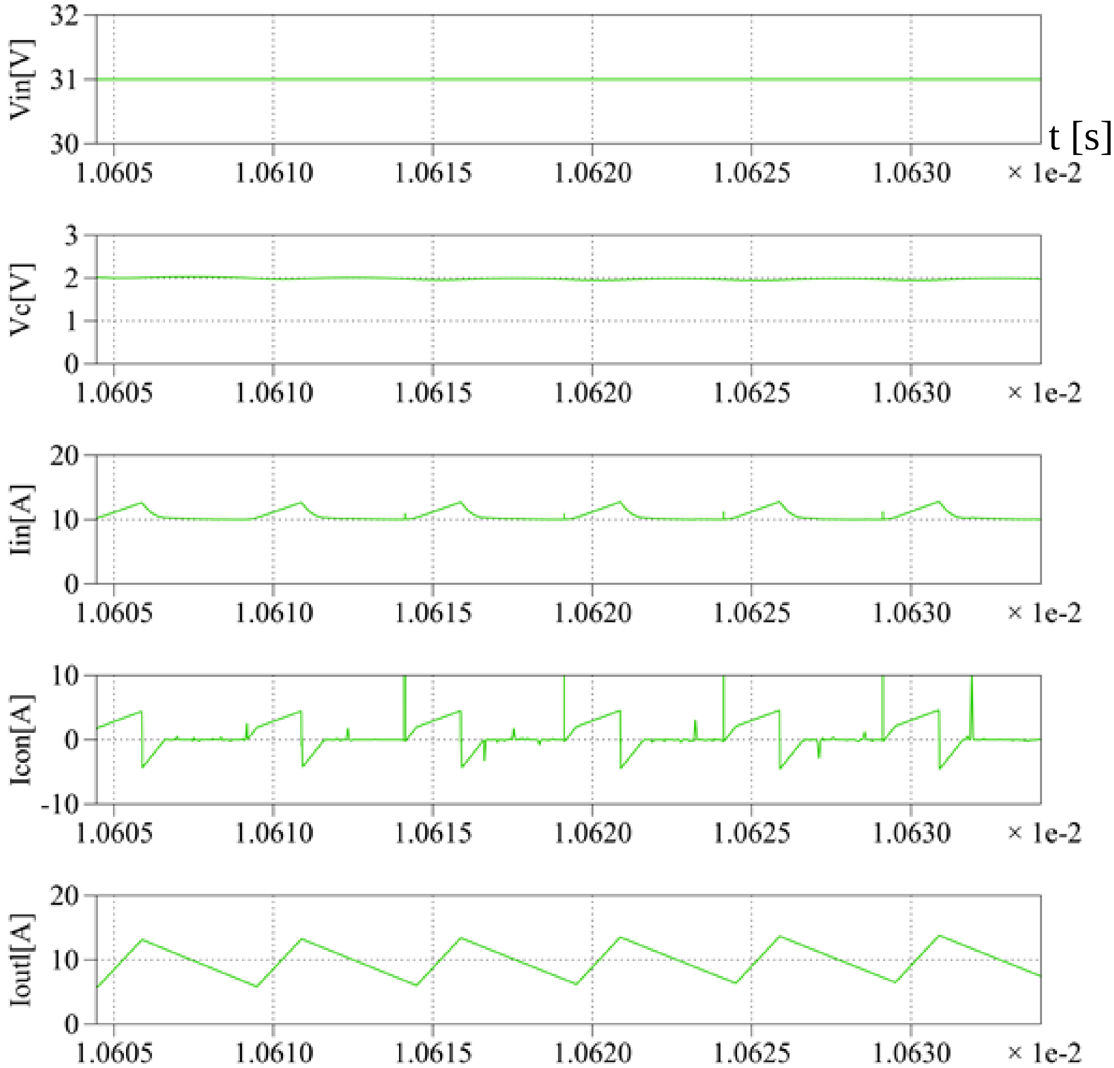

Figure 4.9 Current performance of the proposed circuit at an input voltage of 31V

4.4 Partial Power Processing in Step-down Operation Mode

When the circuit is in step-down operation mode, the four switches in the primary side are useless. In this case, the primary side is acting as a full-bridge rectifier, simplified as shown in Figure 4.10.

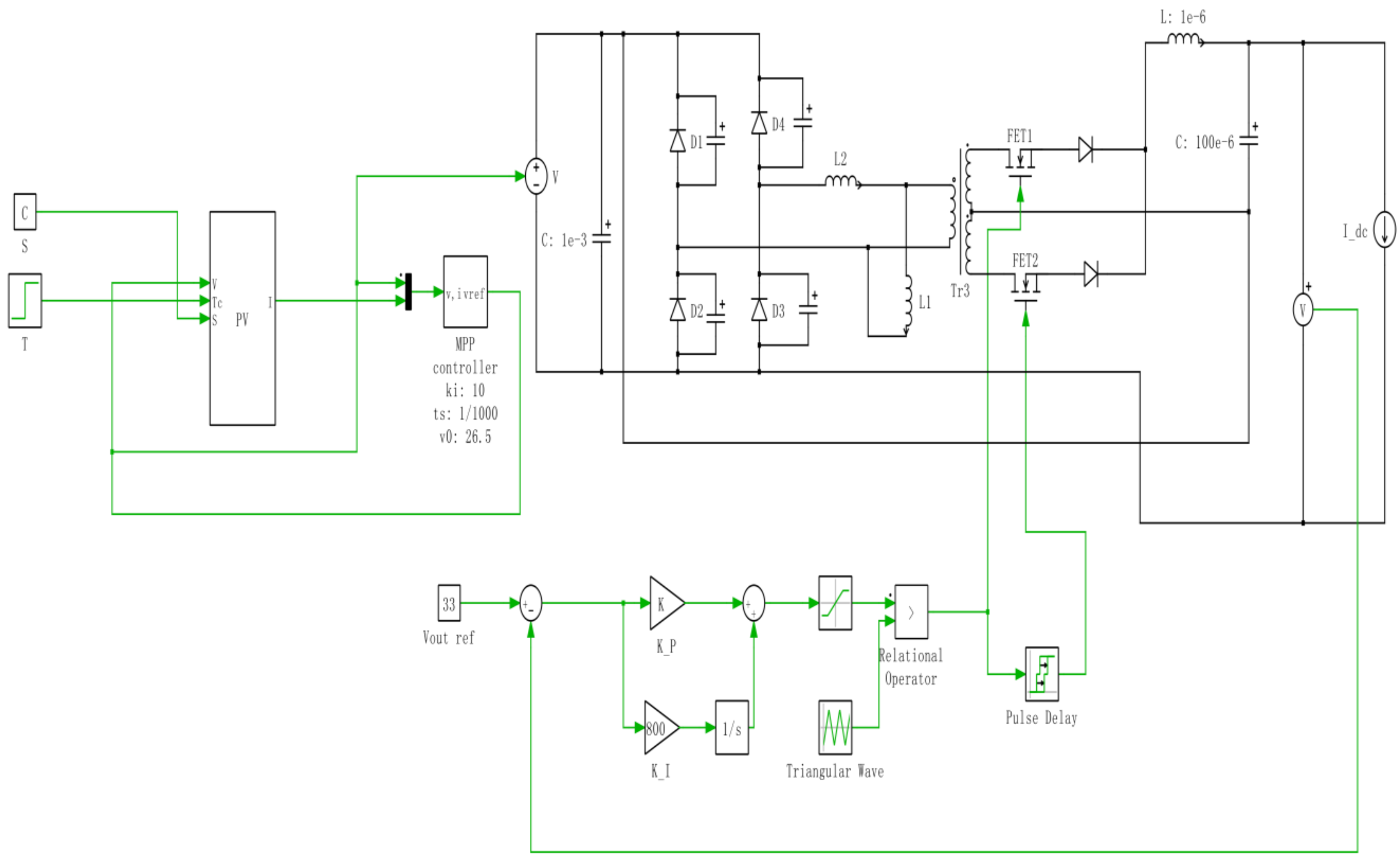

Figure 4.10 Simplified simulation circuit of the step-down mode with PI controller for PV system

In Figure 4.11, a detail of the output inductor current and the voltage on primary of the transformer in the step down mode is presented. The voltage gain of the regulated voltage Vc in this mode is always negative to give a step-down input PV voltage (in continuous inductor current conduction mode), given by equation (3.14), which is similar to the conversion ratio of an inverting full-bridge converter. The simulation results verify the theoretical analysis of the buck mode operation given in Chapter 3. For example, the output voltage is regulated at 33V as required.

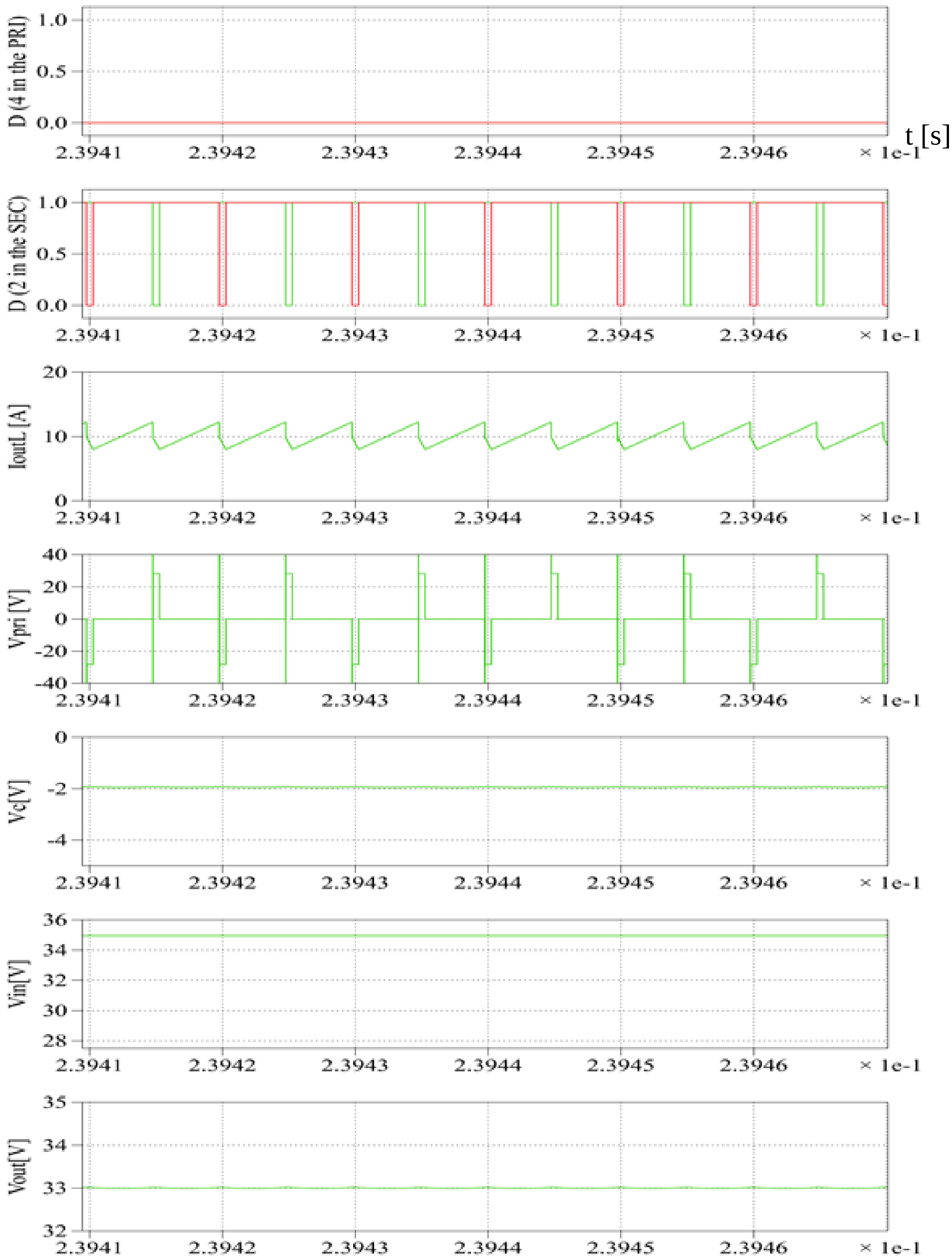

Figure 4.11 Simulation results of the key waveform for the converter in step-down operation mode

In the last subsection, it was noted that the power processed by the converter is smaller with an increase in PV input voltage, meaning an increased efficiency for the whole circuit in the boost operation mode. The waveforms of the converter power performance with a 40V input voltage are shown in Figure 4.12. The voltage stress and current stress waveforms are shown in Figure 4.13.

It is noted from the waveform that the output voltage of the converter can still be kept at 33V with the implemented control circuit. The average input current for the circuit is 8.2527A, and the average current going into the converter is -1.5818 A, which means a reversed direction of the current flow. As a result, the percentage of input power being processed by the converter at 40V input voltage is 19.16%. The converter can still achieve very high efficiency with only a small portion of power flow through the converter block.

The target converter design for this application is an input PV voltage range of (28V-40V) with an output dc-link voltage of 33V. For this range of operation, additional simulations were run for the proposed circuit at input PV voltage in 1V increments from 28V to 40V. The percentage of input power to be processed by the converter over the entire input voltage range, with a 33V output, can be calculated and these results are made into curves as a function of input PV voltage and provided in Figure 4.14.

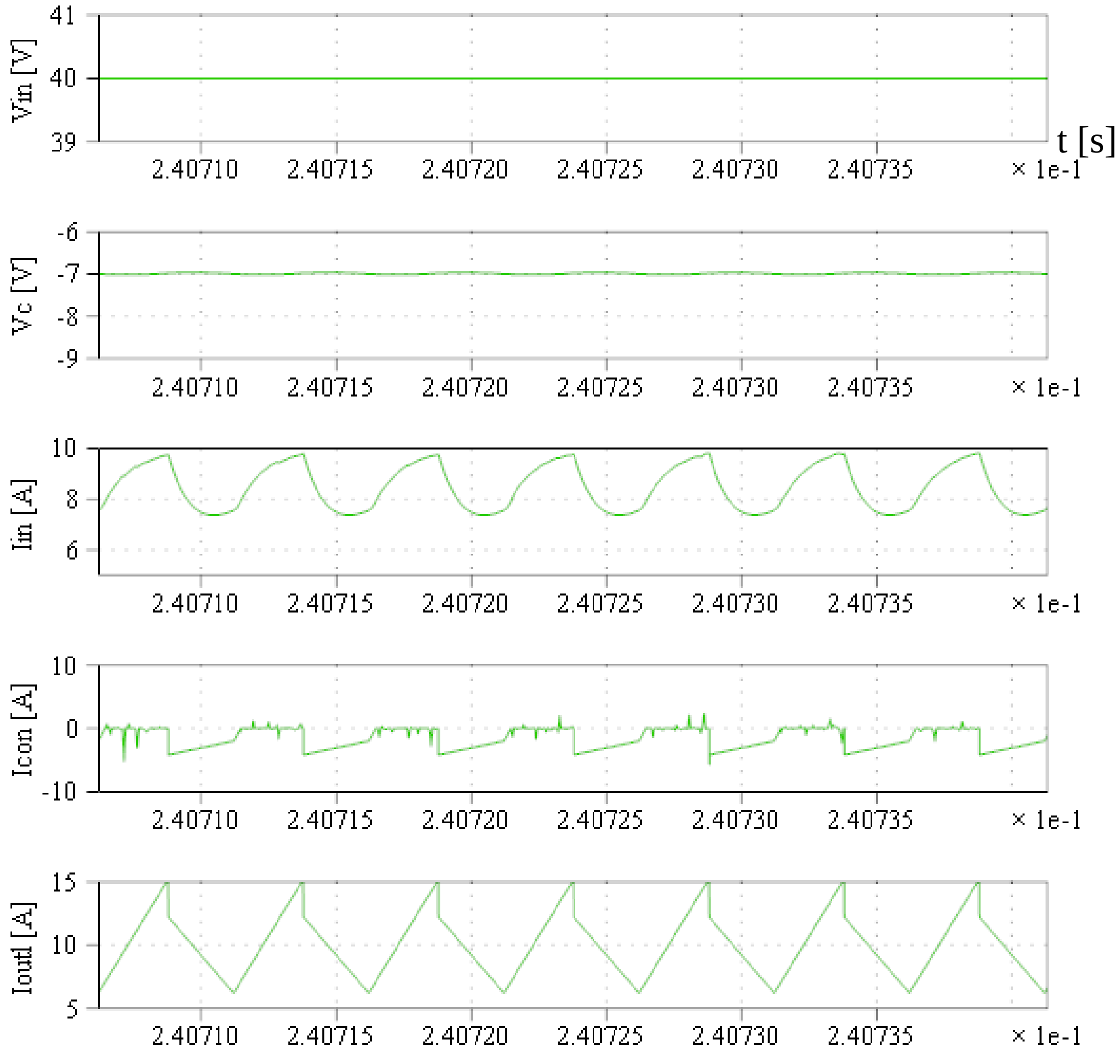

Figure 4.12 Current performance of the proposed circuit at a input voltage of 40V to keep a constant output voltage at 33V

Figure 4.13 Device current and voltage stress (for 40V input voltage)

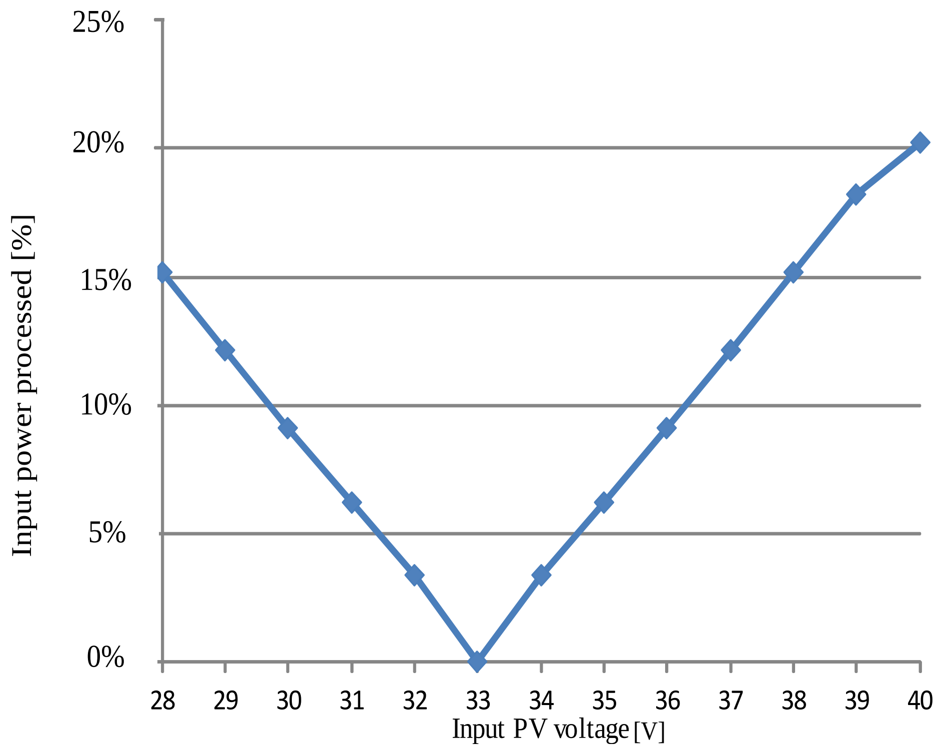

Figure 4.14 Percentage of input power processed by the converter vs. input voltage with a 33V output voltage

4.5 Operation Performance for Proposed Modules in Series Connection

The typical series-connected DMPPT for a PV power generation system used in this thesis is illustrated in Chapter 2, with a number of series-connected converters to obtain sufficient dc-link voltage. By using DMPPT converters, it is possible to regulate the PV string voltage to a fixed value, giving rise to the possibility of adding more strings or batteries to the system. A constant string voltage is also beneficial because it becomes possible to optimize the inverter design, size, and cost.

The exact configuration of the system depends on the current and voltage requirements of the load. Matching of the interconnected panels with respect to their outputs can maximize the efficiency of the array. Due to the self-controlled PV modules, there is no interconnection between PV modules, but there is interconnection between the associated DC-DC converters. Therefore, each PV module can operate at its own optimal power and current, and all the available energy in the PV array can be delivered.

Generally, it is preferred that a solar array is built with all the same panels and is kept away from any shading. However, it is not easy to avoid shading in residential installations because of the change in sunlight direction throughout the day. Furthermore, obstacles such as trees, birds, and other constructions can cause partial shading. In this configuration, losses from shading of a single PV module are limited to that module; the performance of any other nearby unshaded modules is unaffected. Therefore, the overall system is only impacted to the extent that the single degraded module affects it.

For this study, a 3-module PV series string was simulated under shaded conditions of the solar power. The same concept can be extended to a number of panels connected in series. Figure 4.15 shows the series connection of three self-controlled PV panels with the proposed DC-DC converter connected to each module.

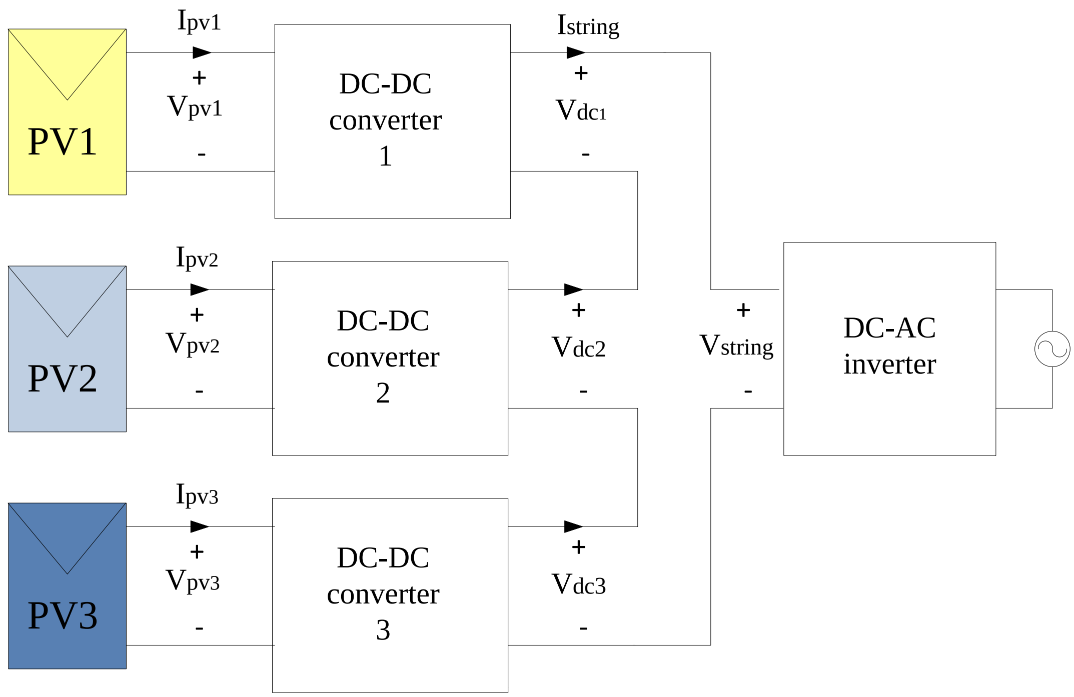

Figure 4.15 The series-connected 3-module DMPPT PV system under mismatched conditions

Because of the series connection, the output current of each module should be the same. Therefore, each converter output terminal voltage, Vdci, will share the string voltage according to the extracted maximum power from its individual PV module weighting by the global output power, given as:

$$V_{dci} = V_{string} \frac{P_{pvi}}{\sum_{i=1}^{n} P_{pvi}} \tag{4.7}$$

This means that the output voltage may have large variations when some panels are shaded. Therefore, the proposed DC-DC converter with the ability of both voltage step-up and step-down has the greatest flexibility for this application.

Using the proposed DC-DC converter in the above subsections for the power stage, the theory was confirmed with PLECS of a DMPPT 3-module series PV-string for mismatched solar insolation where the converter modules were integrated to individual solar panels, as in the setup shown in Figure 4.16. Each module block includes the buck-boost power stage and a solar panel model with MPPT. Inputs to this block are solar irradiance and referenced string voltage. The block output is each DMPPT module voltage.

The control algorithms include a main control loop for power point tracking that scans through all the allowed operating points of the PV panel and chooses the mode of operation that results in maximum output power. An inner loop within the control program adjusts the duty cycle of the switching converter in order to maintain the appropriate "string" PV conversion ratio.

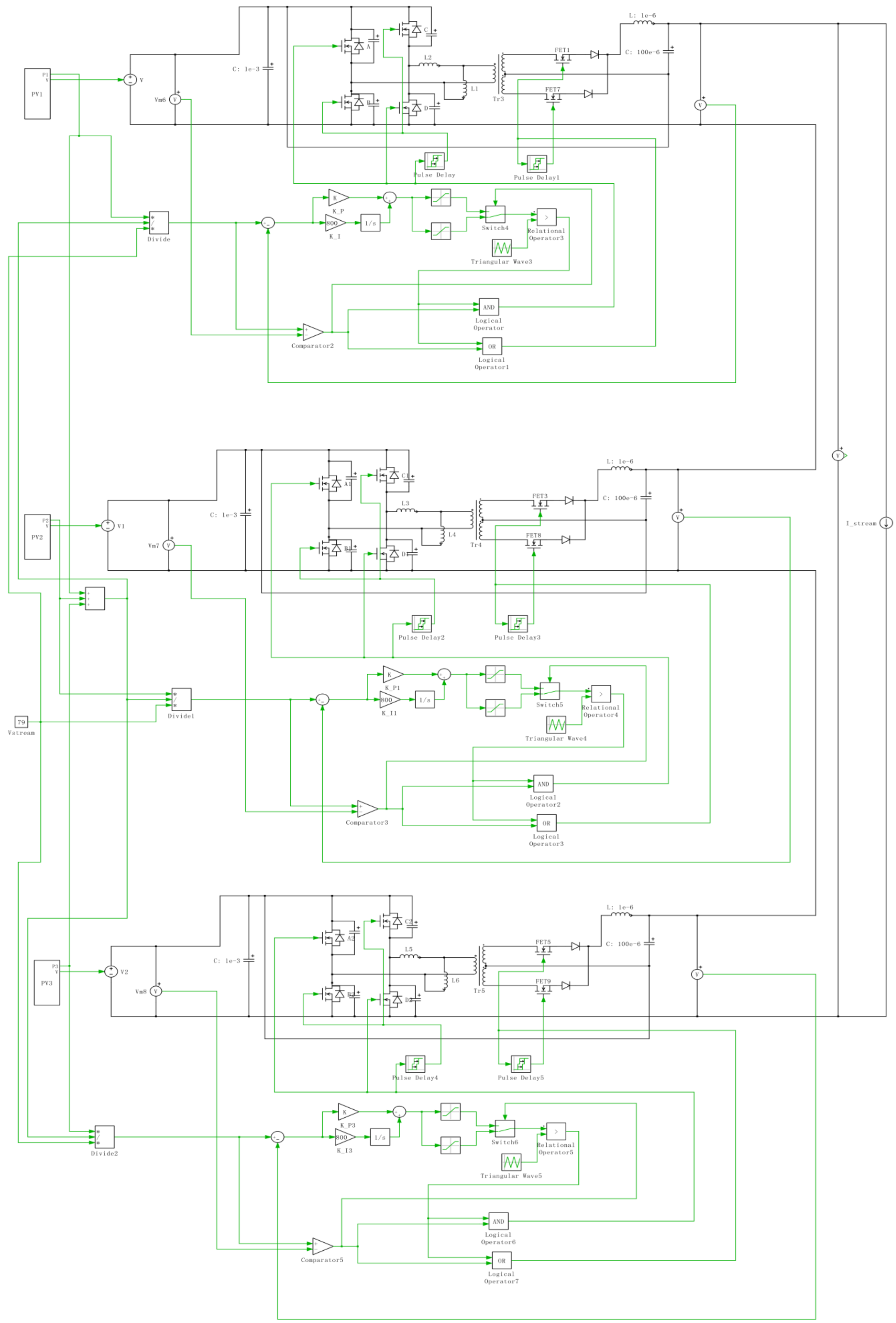

Figure 4.16 Simulation model with 3-module DMPPT PV system in PLECS

Table 4.1 shows the simulation results of the output voltage for each module when the three series connected panels have the same illumination. Notice that the DMPPT blocks are able to successfully track the maximum power point of three interconnected modules while effectively preserving stability. The maximum power produced by all the panels is equal as they are equally illuminated. When they are connected in series, all the panels contribute power to the load. Thus, the output voltage of the module is equal at 26.33V, which means they equally share the string voltage $(26.33 \times 3 \approx 79V)$. When these three panels are not equally illuminated, the power contributed by individual panel will be different, leading to different output voltage of each panel.

Table 4.1 String voltage sharing performance of the three series-connected modules with the same insolation level

The Panel Output Voltage [V]	Voltage
Vdc1	26.33V
Vdc2	26.33V
Vdc3	26.33V
V_{string}	79V

Figure 4.17 shows the characteristics of the DMPPT PV system consisting of three series connected panels where each panel receives different illumination, for example if unshaded Panel-1 receives 100% illumination (operating at a nominal irradiance of 1000 W/m2 and cell temperature = 45 ℃), shaded Panel-2 receives 70% illumination, and Panel-3 receives 50% illumination.

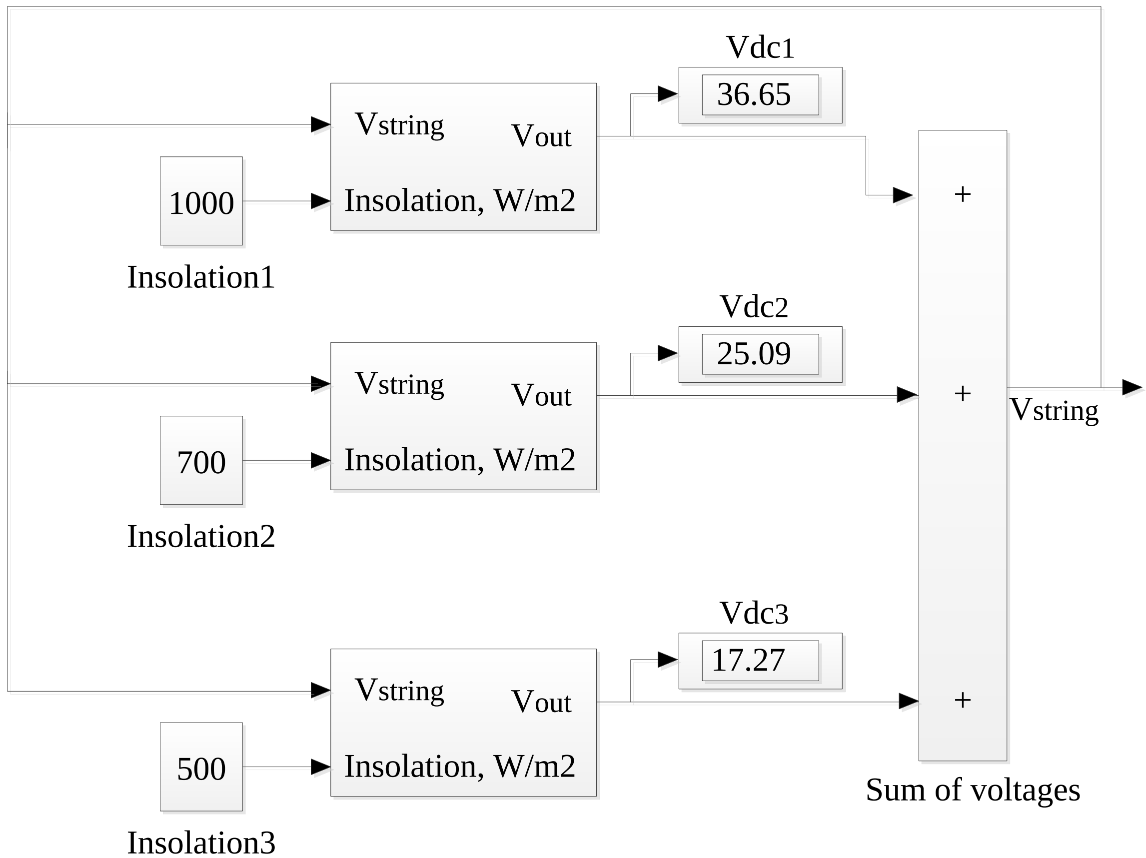

Figure 4.17 Characteristics of the 3-module series connected DMPPT PV system with different illumination

Table 4.2 shows the share of output string voltage of the three modules for shaded conditions, and Table 4.3 shows the corresponding input PV voltage. Each converter in the series string operates with the same current I_{string}, and the converter output voltages automatically adjust according to converter powers. Therefore the output voltage V_{string} can be held constant at the referenced voltage 79V, allowing the downstream inverter to be designed to operate with a regulated dc input voltage.

Table 4.2 String voltage sharing performance of the three series-connected modules with different insolation levels

The Panel Output Voltage [V]	Voltage
Vdc1	36.65V
Vdc2	25.09V
Vdc3	17.27V
V_{string}	79V

Table 4.3 Input PV voltages of the 3 modules at different insolation levels

The Panel Output Voltage [V]	Voltage
Vdc1	36.65V
Vdc2	25.09V
Vdc3	17.27V
V_{string}	79V

The dedicated DC-DC converter of each panel tries to regulate the output voltage according to the maximum input power. The output voltage of Panel1 will increase until it reaches its target voltage. At the same time, the output voltage of Panel2 and Panel3, V_{dc2} and V_{dc3}, will drop because the three converters' output terminals share the string voltage, which remains constant. Finally, the DC string voltage reaches the regulative reference string voltage ($V_{string,ref}=V_{dc1}+V_{dc2}+V_{dc3}=79V$). At the steady-state condition, the three PV modules provide three different maximum output power, and the three distributed converter modules actually share the string voltage according to their power ($V_{dc1}=36.65V$, $V_{dc2}=25.09V$, $V_{dc3}=17.27V$).

This section presented the simulation of string performance of the proposed DC-DC converter. The simulation results further verified the suitability and flexibility of the proposed converter be applied to the series connected DMPPT solar power system. First the converter can function reliably without communications between modules, especial in mismatched conditions. Second, the MPPT algorithms of adjoining modules are effectively decoupled, substantially reducing interactions and stability problems. Third, the autonomous control algorithm naturally allows a central inverter to operate at a fixed voltage, with potential savings in inverter cost and efficiency.

4.6 Summary

Simulation results for the proposed step-up/step-down full-bridge partial power circuit were presented in this chapter. The full-bridge converter with the designed closed-loop controller is the application for PV panel under varying environmental and weather conditions. The PWM controller is used during the power handling stage. The PWM voltage regulation control algorithm is fulfilled by a PI controller. With the proposed control circuit, the circuit is able to perform both step-up and step-down modes. The simulation results clearly demonstrate the operation of the two different modes. The percentage of input power processed by the converter is also calculated and concludes with a curve as a function of input PV voltage. Due to this partial power configuration, the proposed circuit enables a high efficiency for the whole circuit with most of the input power (at least 81.84%) directly feeding forward. Thus, the simulation results which show the maintaining performance of the proposed converter operated at either step up or step down mode means that the proposed converter can fulfill the design objectives of this thesis.

The proposed DC-DC converter was then applied to a 3-module series string simulation for mismatched solar insolation. The performance of the DMPPT PV system, which can compensate for the shading effect and the PV module mismatching as well as to increase the overall output power, was also presented.

Chapter 5: Conclusions and Future Work

5.1 Conclusions

The traditional CMPPT system was introduced in this thesis. However, in case of solar irradiation mismatch, this configuration usually fails to track the absolute maximum power point. Moreover, even when the CMPPT system is able to track the global maximum power of the mismatched PV field, such a power is lower than the sum of the available maximum powers of the mismatched modules. To solve this problem, DMPPT overcomes the drawbacks associated with mismatched solar irradiation and achieves the absolute maximum power output.

In this thesis, series and parallel configurations of distributed PV panel systems were introduced, with the advantages and drawbacks of each system examined in detail. The series connection was selected in this thesis for the DMPPT system, primarily due to the inherently low voltage stress on the converters. Moreover, the concept of partial power processing was presented, including a comparative evaluation of conventional DC-DC converter topologies to be applied in distributed PV plant architectures.

A novel full-bridge DC-DC converter with partial power processing for a PV input voltage range from 25V to 40V was presented that can enable both step-up and step-down functions. The proposed circuit was modified from the standard full-bridge partial power circuit with a newly designed dual-loop control scheme. Due to the partial power configuration, the proposed converter fed forward a minimum of 81.84% of the input power directly to the output side in the worst case when the input PV panel voltage is at 40V.Therefore, only a maximum of 18.16% the input power is processed by the proposed converter. Using previously published work at 95% efficiency for a similar DC-DC converter, with the proposed configuration, when only about 18.16% of the input power is processed by the converter, the overall efficiency can be expected to be above 98%.

A three module series connected DMPPT system with the proposed converter was simulated using PLECS. The simulation can be extended into longer strings of self-controlled PV modules connect in series. They are all commonly connected to the grid-connected inverter with a constant 79V dc-link voltage. Two different conditions were simulated: equal illumination and varied illumination between panels. In both cases, the three PV panel modules shared the 79V output dc-link voltage according to their independent maximum power produced. The newly proposed converter with the flexible voltage range can serve the needs in this series DMPPT PV system where both step-up and step-down modes are required.

5.2 Summary of Contributions

The objective of this thesis is to propose a novel full-bridge step-up/step-down DC-DC converter topology that can be applied to distributed photovoltaic (PV) plant architecture systems, and can minimize the conversion losses to greatly improve the efficiency of solar power systems. Simulation results were presented to prove that the proposed converter circuit meets the design specifications and manages to increase the efficiency of the full-bridge converter for solar power systems. The novel contributions proposed in this thesis are primarily based on the proposed full-bridge buck-boost converter implemented with partial power processing.

A high efficiency step up and step down full-bridge PWM DC-DC converter operated with a MPPT algorithm was first proposed. Based on the standard full-bridge partial power converter, the proposed converter uses two additional MOSFETs in series with a diode in the secondary side of the transformer. The circuit allows a wide input voltage range, while overcoming the disadvantage of the traditional full-bridge implemented in a partial power arrangement, where the output voltage can only be greater than the input. Due to varied solar irradiation, the output power of the PV array can vary and needs to be shared between the DC-DC converters in series. With the proposed control circuit, the converter is able to choose the proper operation mode according to the power portion needing to be shared. Thus, this proposed DC-DC converter can regulate a constant dc-link output voltage under the various operating conditions of a PV panel.

Furthermore, a dual-loop controller using logic and PI control was implemented and applied to the proposed full-bridge step-up/step-down converter in the PV system with MPPT control. The Incremental Conductance method was applied to the converter in order to track the output power of the PV array. The conventional PWM control algorithm is was implemented with a PI controller to achieve a fixed DC bus voltage, therefore simplifying the MPPT implementation. Furthermore, the conversion losses are decreased by having a portion of the input PV power directly fed forward to the output without being processed by the converter. The operation of this converter allows for a simplified maximum power point tracker design using fewer measurements. Thus, these advantages result in the potential improvement of efficiency, size and cost. Finally the proposed converter circuit can be used in cascaded connections in a distributed solar power system. In this case, the voltage change for each converter is narrowed down to near the panel voltage instead of from the panel voltage to directly dc-link voltage, such as 300V.

5.3 Future Work

The following future work is recommended:

1. Hardware implementation

In this thesis, the simulation software PLECS was used to verify the proposed circuit. Although the simulation results prove the feasibility of the circuit and the potential for greatly improved efficiency of the full-bridge buck-boost converter, there may be unexpected problems occurring in the real circuit, requiring modifications to the proposed circuit.

2. Control applications

The proposed control circuit was designed for the two PWM control block at 100 kHz, 28-35V input, 33V output system, which is hard to apply to real hardware applications. It is worth trying to make some adjustments so that the proposed control circuit can be extended to digital applications.

3. Module communication

Usually, 10–20 of the distributed PV modules equipped with the proposed converters simulated in this thesis are connected in series to achieve the desired value of the inverter's DC input voltage. The main causes that limit the efficiency of distributed system are the number of PV modules and dedicated DC-DC converters in a string, the atmospheric operating conditions characterizing each PV module (irradiance and temperature values), the voltage and current ratings of the physical devices the DC-DC converters are made of, and the adopted DC-DC converter topology [97]. The simulation results in the thesis confirm the validity of the proposed DC-DC converter topology. Further work is in progress to identify the remaining factors and also a special control schematic to help balance the DC voltage and the communication between each module.

References

[1] N. Dasgupta, A. Pandey, and A. Mukeziee, "Voltage-sensing based photovoltaic MPPT with improved tracking and drift avoidance capabilities," *Solar Energy Mater. Solar Cells*, vol. 92, no. 12, pp. 1552-1558, Dec. 2008.

[2] O. Lopez Lapena, M. Penella, and M. Gasulla, "A new MPPT method for low-power solar energy harvesting," *IEEE Trans. Ind. Electron*., vol. 57, no. 9, pp. 3129-3138, Sep.2010.

[3] N. Kaushika, N. Gautam, "Energy yield simulations of interconnected PV arrays," *IEEE Trans. Energy Convers*., vol. 18, no. 1, pp. 127–134, May 2003.

[4] N. Femia, G. Lisi, G. Petrone, G. Spagnuolo, and M. Vitteli, "Distributed maximum power point tracking of photovoltaic arrays: Novel approach and system analysis," *IEEE Trans. Ind. Electron*., vol. 55, no. 7, pp. 2610–2621, Jul. 2008.

[5] M. Veerachary, T. Senjyu and K. Uezato, "Maximum power point tracking of coupled inductor interleaved boost converter supplied PV system," *lEEE Proc. -Electr. Power Appl*., vol. 150, no. I, pp. 71-80, January 2003.

[6] Xu Xinyu, Khambadkone A M., Leong T M, and Oruganti R, "A 1 MHz zero-voltage switching asymmetrical half bridge dc/dc converter: analysis and design," *IEEE, Transactions Power Electronics*, 21(1): 105-113, Jan. 2006.

[7] Steigerwald, R. L, "A comparison of half-bridge resonant converter topologies," *IEEE Transactions on Paver Electronics*, 174-1 82, Apr. 1998.

[8] C. Deline, B. Marion, J. Granata, and S. Gonzales, "A performance and economic analysis of distributed power electronics in photovoltaic systems," National Renewable Energy Laboratory, Golden, CO, NREL Tech. Rep. NREL/TP-5200-50003, 2011.

[9] M. F. Ansari, S. Chatterji, and A. Iqbal, "A fuzzy logic control scheme for a solar photovoltaic system for a maximum power point tracker," *Int. J Sustainable Energy*, vol. 29, no.4, pp.245-255, 2010.

[10] S. Brunton, C. Rowley, S. Kulkarni, and C. Clarkson, "Maximum power point tracking for photovoltaic optimization using ripple-based extremum seeking control," *IEEE Trans. Power Electron*., vol. 25, no. 10, pp. 2531-2540, Oct. 2010.

[11] J. M. Carrasco, L. G. Franquelo, J. T. Bialasiewicz, E. Galván, R. C. Portillo Guisado, Ma. Á. Martıacute, n Prats, J. I. León, and N. Moreno-Alfonso, "Power-electronic systems for the grid integration of renewable energy sources: A survey," *IEEE Trans. Power Electron*., vol. 53, no. 4, pp. 1002–1016, Jun. 2006.

[12] B. Kroposki, R. Margolis, and D. Ton, "Harnessing the sun: An overview of solar technologies," *IEEE Power Energy Mag*., vol. 7, no. 3, pp. 22–33, May/Jun. 2009.

[13] D. Abbott, “Keeping the energy debate clean: How do we supply the world’s energy needs?” *Proc. IEEE*, vol. 98, no. 1, pp. 42–66, Jan. 2010.

[14] H. Wilk, D. Ruoss, and P. Toggweiler. (2002) Innovative electrical concepts. International Energy Agency Photovoltaic Power Systems, IEA PVPS 7-07:2002. [Online].Available: www.iea-pvps.org

[15] G Sangmin Jung, Youngsang Bae, Taesik Yu, Sewan Choi, and Hyosung Kim, “A low cost utility interactive inverter for residential fuel cell generation,” *IEEE Trans. Power Electron*, Vol. 22, pp. 2293-2298 Nov. 2007.

[16] L.-R. Chen, C.-H.Tsai, Y.-L.Lin, and Y.-S. Lai, "A biological swarm chasing algorithm for tracking the PV maximum power point," *IEEE Trans. Energy Convers*., vol. 25, no. 2, pp. 484-493, Jun. 2010.

[17] T. M. Razykov, C. S. Ferekides, D. Morel, E. Stefanekos, H. S. Ullal, and H. M. Upadhaya, “Solar photovoltaic electricity: Current status and future prospects,” *Solar Energy*, vol. 85, no. 8, pp. 1580–1608, Aug. 2011.

[18] D. L. King, “Photovoltaic module and array performance characterization methods for all system operating conditions,” in *AIP Conf. Proc*., 1997, pp. 347–368.

[19] A. J. Carr and T. L. Pryor, “A comparison of the performance of different PV module types in temperate climates,” *Solar Energy*, vol. 76, no. 1, pp. 285–294, Jan. 2004.

[20] D. Dondi, D. Brunelli, L. Benini, et al, “Photovoltaic cell modeling for solar energy powered sensor networks in: Advances in Sensors and Interface,” 2007. IWASI 2007. 2nd International Workshop on 26-27 June 2007: 1-6.

[21] Dr. D. Devara Dr. S.Sakthivel Mrs. K.Punitha, “Modeling of Photovoltaic Array and Simulation of Adaptive Hysteresis Current Controlled Inverter for Solar Application,”

[22] D Roche, H Outhred, and RJ Kaye, “Analysis and control of mismatch power loss in photovoltaic arrays,” Progress in Photovoltaics: Research and Applications; 3(2): 115–127, 1995.

[23] G. Lijun, R. Dougal, L. Shengyi & A. Lotova, “Parallel-Connected Solar PV System to Address Partial and Rapidly Fluctuating Shadow Conditions,” *IEEE Trans. on Industrial Electronics*, Vol. 56, No. 5, pp. 1548-1556, May 2009.

[24] H. Patel & V. Agarwal, “MATLAB-Based Modeling to Study the Effects of Partial Shading on PV Array Characteristics,” *IEEE Trans. on Energy Conversion*, Vol. 23, No. 1, March 2008, pp. 302-310.

[25] G. R. Walker and P. C. Sernia, “Cascaded DC–DC converter connection of photovoltaic modules,” *IEEE Trans. Power Electron*., vol. 19, no. 4, pp. 1130–1139, Jul. 2004.

[26] E. Roman, R. Alonso, P. Ibanez, S. Elorduizapatarietxe, and D. Goitia, "Intelligent PV module for grid-connected PV systems," *IEEE Trans. Ind. Electron*., vol. 53, no. 4, pp. 1066–1073, Aug. 2006.

[27] W. Xiao, N. Ozog, and W. G. Dunford, "Topology study of photovoltaic interface for maximum power point tracking," *IEEE Trans. Ind. Electron*., vol. 54, no. 3, pp. 1696–1704, Jun. 2007.

[28] T Zhao, H Wang, X Li, Ju Zhenhe, X Wei, S Zhang, "The distributed maximum power point tracking method and application in the PV grid-connected generation," International Conference on Intelligent System Design and Engineering Application, 2010; 639–642.

[29] A Elasser, M Agamy, J Sabate, R Steigerwald, R Fisher, M Harfman-Todorovic, "A comparative study of central and distributed MPPT architectures for megawatt utility and large scale commercial photovoltaic plants," ECON, 2010; 2753–2758.

[30] Q Li, P Wolfs, "A preliminary study of the distributed maximum power point tracker designs for different types of solar cells in solar and electric vehicle arrays," AUPEC, 2007; 1–6.

[31] Alonso R, Ibáñez P, Martínez1 V, Román E, Sanz A, "Analysis of performance of new distributed MPPT architectures," ISIE, 2010; 3450–3455.

[32] Ahmadi D, Mansouri SA, Wang J, "Circuit topology study for distributed MPPT in very large scale PV power plants," Applied Power Electronics Conference and Exposition (APEC), 2010; 786–791.

[33] Kamnarn U, Yousawat S, Sreeta S, Muangjai W, Somsak T, "Design and implementation of a distributed solar controller using modular buck converter with maximum power point tracking," UPEC, 2010; 1–6.

[34] Chen Y-M, Chen C-W, Chen Y-L, "Development of an autonomous distributed maximum power point tracking PV system," Distributed Energy Conversion Congress and Exposition (ECCE), 2011; 3614–3619.

[35] Poshtkouhi S, Palaniappan V, Fard M, and Trescases O, "A general approach for quantifying the benefit of distributed power electronics for fine grained MPPT in photovoltaic applications using 3D modeling," *IEEE Transactions on Power Electronics*, 2011; 99: 1–26. ISSN: 0885-8993..

[36] Tsao P, Sarhan S, Jorio I, "Distributed maximum power point tracking for photovoltaic arrays," PVSC PV Photovoltaic Specialists Conference, 2009; 2293–2298.

[37] E. Roman, V. Martinez, JC. Jimeno, R. Alonso, P. Ibanez, S. Elorduizapatarietxe, "Experimental results of controlled PV module for building integrated PV systems," Solar Energy, 2008; 82: 471–480.

[38] W. Yao, M. Gao, Z. Ren, M. Chen, Z. Qian, “Improvement of performance and flexibility for photovoltaic module using individual dc/dc converter,” 6th IEEE International Power Electronics and Motion Control Conference - IPEMC, 17–20 May 2009; 441–444.

[39] J. H. R. Enslin, M. S.Wolf, D. B. Snyman, andW. Swiegers, “Integrated photovoltaic maximum power point tracking converter,” *IEEE Trans. Ind. Electron*., vol. 44, pp. 769–773, Dec. 1997.

[40] T. Noguchi, S. Togashi, and R. Nakamoto, “Short-circuit pulse-based maximum-power-point tracking method for multiple photovoltaic- and-converter module system,” *IEEE Trans. Ind. Electron*., vol. 49, pp. 217–223, Feb. 2002.

[41] GarcıaM, Maruri JM, Marroyo L, Lorenzo E, Perez M, “Partial shadowing, MPPT performance and inverter configurations: observations at tracking PV plants,” Progress in Photovoltaics: Research and Applications 2008; 16(6): 529–536.

[42] Sanchis P, Lopez J, Ursua A, Gubıa E,Marroyo L, “On the testing, characterization, and evaluation of PV inverters and dynamic MPPT performance under real varying operating conditions,” Progress in Photovoltaics: Research and Applications 2007; 15(6): 541–556.

[43] Femia N, Petrone G, Spagnuolo G, Vitelli M, “Optimization of perturb and observe maximum power point tracking method,” *IEEE Transactions on Power Electronics*, 2005; 20(4): 963–973.

[44] A. Chouder & S. Silvestre, “Analysis Model of Mismatch Power Losses in PV Systems,” Journal of Solar Engineering, May 2009, Vol. 131.

[45] Germany—BIPV Case Studies, (2007, Mar.), [Online], Available: http://www.cler.org/predac/article.php3?id_article=511

[46] G. Petrone, G. Spagnuolo, and M. Vitelli, “Analytical model of mismatched photovoltaic fields by means of Lambert W-function,” *Sol. Energy Mater. Sol. Cells*, vol. 91, no. 18, pp. 1652–1657, Nov. 2007

[47] H. J. Bergveld, D. B ̈uthker, C. Castello, T. S. Doorn, A. de Jong, R. Van Otten, and K. de Waal, “Module-level dc/dc conversion for photovoltaic systems,” in *Proc. IEEE Int Telecommun Energy Conf*, 2011, pp. 1–9.

[48] J. Imhoff, J. R. Pinheiro, J. L. Russi, D. Brum, R. Gules, and H. L. Hey, “Dc-dc converters in a multi-string configuration for stand-alone photovoltaic systems,” in *Proc. IEEE Power Electron. Spec. Conf*., 1976, pp. 2806–2812

[49] S. Kjaer, J. Pedersen, and F. Blaabjerg, “A review of single-phase grid-connected inverters for photovoltaic modules,” *IEEE Trans. Ind. Electron*., vol. 41, no. 5, pp. 1292–1306, Sep./Oct. 2005.

[50] B. Liu, S. Duan, and T. Cai, "Photovoltaic dc-building-module-based BIPV system—concept and design considerations," *IEEE Trans. Power Electron.*, vol. 26, no. 5, pp. 1418–1429, May 2011.

[51] A. I. Bratcu, I.Munteanu, S. Bacha, D. Picault, and B. Raison, "Cascaded dc-dc converter photovoltaic systems: Power optimization issues," *IEEE Trans, Ind. Electron*, vol. 58, no. 2, pp. 403–411, Feb. 2011.

[52] Photovoltaic Timeline, (2007, Mar.). [Online], Available: http://www. eia.doe.gov/kids/history/timelines/photovoltaics.html

[53] M. R. Patel, "Wind and Solar Power Systems", Boca Raton, FL: CRC Press, 1999.

[54] Li Zhang, Kai Sun, Yan Xing, Lanlan Feng, and Hongjuan GeA, "Modular Grid-Connected Photovoltaic Generation System Based on DC Bus," *IEEE transactions on power electronics,* vol. 26, no. 2, Feb 2011.

[55] N. Hur and N. Kwanghee, "A robust load-sharing control scheme for parallel-connected multisystems," *IEEE Trans. Ind. Electron.*, vol. 47, no. 4, pp. 871–879, Aug. 2000.

[56] J. W. Kim, H. S. Choi, and B. H. Cho, "A novel droop method for converter parallel operation," *IEEE Trans. Power Electron.*, vol. 17, no. 1, pp. 25–32, Jan. 2002.

[57] M. Lopez, L. G. de Vicuna, M. Castilla, P. Gaya, and O. Lopez, "Current distribution control design for paralleled DC/DC converters using sliding mode control," *IEEE Trans. Ind. Electron.*, vol. 51, no. 2, pp. 419–428, Apr. 2004.

[58] M. N. Marwali, J. W. Jung, and A. Keyhani, "Control of distributed generation systems—Part II: Load sharing control," *IEEE Trans. Power Electron.*, vol. 19, no. 6, pp. 1551–1561, Nov. 2004.

[59] K. Siri, V. A. Caliskan, C. Q. Lee, and G. C. Agarwal, "Peak power tracking in parallel connected converters," in *Proc. IEEE Syst., Man, Cybern. Int. Conf.*, 1992, vol. 2, pp. 1401–1406.

[60] K. Siri, V. A. Caliskan, and C. Q. Lee, "Maximum power tracking in parallel connected converters," *IEEE Trans, Aerosp Electron Syst*, vol. 29, no. 3, pp. 935–945, Jul. 1993.

[61] K. Siri, and K. A. Conner, "Parallel-connected converters with maximum power tracking," in *Proc IEE 17th APEC*, vol. 1, pp. 419–425, 2002.

[62] A. Driesse, P. Jain & S. Harrison, "Beyond the Curves: Modeling the Electrical Efficiency of Photovoltaic Inverters," Proceedings of Photovoltaics Specialists Conference (PVSC), pp. 1-6, 2008.

[63] R. Adler, “A New DC/DC switching Regulator Topology Enhances Efficiency and Power Density,” Proceedings of PowerCon, 1984, pp.F1-1-F1-4.

[64] B. Min, J. Lee, J. Kim, T. Kim, D. Yoo & E. Song, “A New Topology With High Efficiency Throughout All Load Range for Photovoltaic PCS,” *IEEE Transactions on Industrial electronics*, Vol. 56, No. 11, Nov. 2009, pp. 4427-4435.

[65] H. Li, H. Chen & L. Chang, “Analysis and Design of a Single-Stage Parallel AC-to-DC Converter,” *IEEE Transactions on Power Electronics*, Vol. 24, No. 12, December 2009, pp. 2989-3002.

[66] M. de Rooij, J. Glaser, and R. Steigerwald, “High efficiency photovoltaic inverter,” U.S. patent application # US2009/0323379A1.

[67] J. Lee, B. Min, T. Kim, D. Yoo, and J. Yoo, “High efficient interleaved input-series-output-parallel-connected DC/DC converter for photovoltaic power conditioning system,” inProc. Energy Convers. Conf. Expo., 2009, pp. 327–329.

[68] Agamy, M.S., “An Efficient Partial Power Processing DC/DC Converter for Distributed PV Architectures,” Power Electronics, IEEE Transactions, 29: 674–686, 2014.

[69] Agamy M.S, “DC-DC Converter Topology Assessment for Large Scale Distributed Photovoltaic Plant,” *IEEE Transactions*, 11: 764-769, 2011.

[70] M. Kazimierczuk & D. Czarkowski, “Resonant Power Converters,” 1995. John Wiley & Sons, INC.

[71] Steigerwald, R. L, “High frequency resonant transistor dc-dc converters,” *IEEE Transactions on Power Electronics*, 174-182, Apr. 1988.

[72] Mario Cacciato, Alfio Consoli, Rosario Attanasio, and Francesco Gennaro, "Soft switching Converter with HF Transformer for Grid Connected Photovoltaic Systems," *IEEE ind. Electron*., vol. 57, May 2010, pp. 1678 -1686.

[73] Mario Cacciato, Alfio Consoli, Rosario Attanasio, and Francesco Gennaro, "A Digitally Controlled Double Stage Soft-switching Converter for Grid Connected Photovoltaic Applications," *IEEE APEC*', 08, 24 - 28, Feb. 2008, pp.I4I-I47.

[74] Deline C, Marion B (National Renewable Energy Laboratory), Granata J, Gonzalez S (Sandia National Laboratories), “A performance and economic analysis of distributed power electronics in photovoltaic systems,” Technical Report NREL/TP-5200-50003, January 2011.

[75] V. Salas, E. Olıacute;as, A. Barrado, and A. Lázaro, “Review of the maximum power point tracking algorithms for stand-alone photovoltaic systems,” Sol. Energy Mater. Sol. Cells, vol. 90, no. 11, pp. 1555–1578, Jul. 2006.

[76] E. Koutroulis, K. Kalaitzakis, N. C. Voulgaris, "Development of a microcontroller-based, photovoltaic MPPT control system," *IEEE Transactions on Power Electronics*, vol. 16, no. 1, pp. 46-54, 2001.

[77] P. Huynh and B. H. Cho, "Design and analysis of a microprocessor-controlled peak power tracking system," *IEEE Trans. Aerosp. Electron. Syst*., vol. 32, pp. 182–189, Jan. 1996.

[78] D. B. Snyman and J. H. R. Enslin, "An experimental evaluation of MPPT converter topologies for PV installations," in Proc. Renewable Energy, vol. 3, no. 8, pp. 841–848, 1993.

[79] M. A. El-Shibini, and H. H. Rakha, "Maximum power point tracking technique," in Proc. of Integrating Research, Industry and Education in Energy and Communication Engineering (MELECON), pp. 21-24, 11-13 April, 1989.

[80] V. Arcidiacono, S. Corsi, L. Lambri, "Maximum power tracker for photovoltaic power plants," IEEE PESC Conf. Rec., pp. 507-512, 1982.

[81] W. Xiao, M. G. J. Lind, W. G. Dunford, and A. Capel, "Real-time identification of optimal operating points in photovoltaic power systems," *IEEE Trans. Ind. Electron*., vol. 53, no. 4, pp. 1017–1026, Jun. 2006.

[82] I.-S. Kim, M.-B. Kim, and M.-J. Youn, "New maximum power point tracker using sliding-mode observer for estimation of solar array current in the grid-connected photovoltaic system," *IEEE Trans. Ind. Electron*., vol. 53, no. 4, pp. 1027–1035, Aug. 2006.

[83] J.-M. Kwon, K.-H. Nam, and B.-H. Kwon, "Photovoltaic power conditioning system with line connection," *IEEE Trans. Ind. Electron*., vol. 53, no. 4, pp. 1048–1054, Jun. 2006.

[84] N. Mutoh, M. Ohno, and T. Inoue, "A method for MPPT control while searching for parameters corresponding to weather conditions for PV generation systems," *IEEE Trans. Ind. Electron*., vol. 53, no. 4, pp. 1055–1065, Jun. 2006.

[85] N. Mutoh and T. Inoue, "A control method to charge series-connected ultra-electric double-layer capacitors suitable for photovoltaic generation systems combining MPPT control method," *IEEE Trans. Ind. Electron*., vol. 54, no. 1, pp. 374–383, Feb. 2007.

[86] K. Kobayashi, H. Matsuo, and Y. Sekine, "An excellent operating point tracker of the solar-cell power supply system," *IEEE Trans. Ind. Electron*., vol. 53, no. 2, pp. 495–499, Apr. 2006.

[87] J.-H. Park, J.-Y. Ahn, B.-H. Cho, and G.-J. Yu, "Dual-module-based maximum power point tracking control of photovoltaic systems," *IEEE Trans. Ind. Electron*., vol. 53, no. 4, pp. 1036–1047, Jun. 2006.

[88] D. Sera, R. Teodorescu, J. Hantschel, and M. Knoll, "Optimized maximum power point tracker for fast-changing environmental conditions," *IEEE Trans. Ind. Electron.*, vol. 55, no. 7, pp. 2629–2637, Jul. 2008.

[89] K.H Hussein, I.Muta, T.Hoshino, et al, "Maximum Photovoltaic Power Tracking, An Algorithm for Rapidly Changing Atmospheric Conditions", in *IEEE Proc. Gener. Transm .Distrlb,* vol. 142, vol. 1, pp. 59-64, 1995.

[90] S. Mekhilef and M. N. Abdul Kadir, "Novel Vector Control Method for Three-Stage Hybrid Cascaded Multilevel Inverter," *IEEE Transactions on Industrial Electronics,* Vol. 58, Issue 4, pp. 1339-1349, 2011.

[91] Bangyin Liu, Shanxu Duan, Fei Liu, and Pengwei Xu, "Analysis and improvement of maximum power point tracking algorithm based on incremental conductance method for photovoltaic array," pp.637~641, PEDS IEEE 2007.

[92] Vikrant.a.chaudhari, "Automatic peak power tracker for solar PV modules using dSpace software," Thesis, Energy centre Maulana Azad national institute of technology July 2005.

[93] O. Wasynczuk, "Dynamic behavior of a class of photovoltaic power systems," IEEE Trans. Power App. Syst., vol. 102, no. 9, pp. 3031–3037, Sep. 1983.

[94] A. F. Boehringer, "Self-adapting dc converter for solar spacecraft power supply," IEEE Trans. Aerosp. Electron. Syst., vol. AES-4, no. 1, pp. 102– 111, Jan. 1968.

[95] E. N. Costogue and S. Lindena, "Comparison of candidate solar array maximum power utilization approaches," in Intersociety Energy Conversion Eng. Conf., 1976, pp. 1449–1456.

[96] Si1555DL Complementary Low-Threshold MOSFET Pair Data Sheet, Vishay Siliconix, Shelton, CT, May 2010.

[97] M. Vitelli: "On the necessity of joint adoption of both Distributed Maximum Power Point Tracking and Central MCL'Cimum Power Point Tracking in PV systems," Progress. In Photovoltaics: Research and Applications (2012), 001: 10.1002/pip.2256.

Appendix A: E24

E24 is one of the standard ranges set by Electronic Industries Association (EIA) with a tolerance of 5% for passive component values. The numbers in the table are the available values for each decade.

Table A.1 Preferred values for passive circuit components

E24 (5%)							
10	11	12	13	15	16	18	20
22	24	27	30	33	36	39	43
47	51	56	62	68	75	82	91